The development of an active implantable neural probe system for chronic use

A thesis submitted to the University of Dublin, Trinity College

In partial fulfilment of the requirements for the degree of Doctor of Philosophy

Laura Constance Frey

Supervised by Dr. Kevin O'Kelly

Trinity College Dublin, May 2017

Department of Mechanical Engineering, Trinity Centre for Bioengineering

Declaration

I declare that this thesis has not been submitted as an exercise for a degree at this or any other university and it is entirely my own work.

I agree to deposit this thesis in the University's open access institutional repository or allow the library to do so on my behalf, subject to Irish Copyright Legislation and Trinity College Library conditions of use and acknowledgement.

Signed,

Laura Frey

May, 2017

Abstract

The alleviation of symptoms of debilitating neural conditions via neural probes is an increasingly important area of research. However, the effectiveness of these probes decreases over time due to the formation of a glial scar around them. In order to design probes that can function long-term, this research study developed two main approaches to reduce the inflammatory response: one focusing on reducing the inflammatory response around the probe via a coating with controllable surface topography and drug delivery capabilities and the other on designing a neural probe utilising cooling as an alternative therapy to electrical stimulation to reduce the inflammatory response at the functioning tip.

In order to assess material topographical effects *in vitro*, PC12 cells, primary neuronal cells from rats and human astrocytes were plated onto hydroxyapatite (HA) discs of various degrees of roughness. A method of encapsulating astrocytes in a gelatin methacryloyl (GelMA) hydrogel was also devised in order to allow studies of over a week to be carried out. HA was found to be non-cytotoxic, with PC12 and primary neuronal cells surviving and attaching to the moderately rough surface best, implying there is an optimum roughness to promote neuronal survival. This was further corroborated by astrocytes, as they exhibited the highest expression of inflammatory cytokines TNF-α and IL-6 when plated on the very rough surfaces.

As topographical control alone was found to be insufficient to significantly reduce the inflammatory response, a drug eluting coating was also developed. This consisted of a dual layered microfluidic system capable of delivering multiple anti-inflammatory

factors to brain tissue long term. This system offered the added benefit of being able to be inserted in its thin dry state before reswelling to provide anchorage against micromotion. Diffusion tests showed the system could release cytokines over a 4 day period from one infusion and could release small drugs with minimal burst release. Repeated infusions of IL-4 upregulated anti-inflammatory M2 phenotype macrophages and downregulated the expression of pro-inflammatory markers in astrocytes over a 3 week period.

An experimentally validated thermal model was created in Comsol® to assess temperature profiles around a cooling probe in the human brain. This was linked with a Peltier chip and heat sink model in order to create a tool allowing for the prediction of Peltier and heat sink settings required to deliver a desired temperature at the probe tip. A 4mm probe consisting of silver core coated with HA was suggested as the current best method of ensuring therapeutic temperatures at the tip. This probe would also offer mild cooling along the probe length to reduce glial activation and therefore the formation of a glial scar.

These two strategies were initially proposed as complementary ideas, however, the results of the investigations indicated that the cooling along the length of the cooling probe and the potential to release anti-inflammatory factors preferentially at the functioning tip of the probe resulted in an overlap in function between the two strategies. They are therefore presented as two separate solutions – a novel cooling probe or alternatively a coating system to increase the efficacy of current electrodes. With further work, both of these probe designs have the potential in the future to be clinically relevant and improve the lives of patients with neurological conditions.

Acknowledgements

Firstly, a huge thank you to my supervisor Dr. Kevin O'Kelly for giving me this opportunity. His guidance and support has been invaluable and I thank him for all the time invested in helping me improve and advance my project and research skills.

I would also like to thank Prof. Ali Khademhosseini for hosting me in Harvard and for his advice and support at all stages of the project. A special mention must go to my inspirational mentor Dr. SuRyon Shin for her unwavering encouragement and guidance and the drive and belief she instilled in me. A further thank you to Fulbright Ireland for facilitating my time abroad and making sure my experience was the best it could be.

For their generous consultancy, thanks to Prof. Shane O'Mara and Prof. Kumlesh Dev for teaching me about all things brain and Dr. Tony Robinson for his help, enthusiasm and encouragement in heat transfer. The help I received in both universities was wide and varied and I thank every team member, technician, collaborator and friend I met along the way. To my friends in TCBE and the Khademhosseini lab, thank you for your kindness and camaraderie – particularly to Jacob Mealy my partner in crime in Trinity and Julio Aleman at Harvard, part time advice giver and counsellor, full time friend. A special mention must also go to DUHAC for enriching my university experience, giving me some of my best friends and saving my sanity at the track, particularly in final year.

Finally, my parents, my grandparents and my sister Alana, thank you for your unwavering support and belief in me, not just in the past 4 years but in all 27. I wouldn't be where I am today without the love and guidance you give me and your patience and encouragement particularly in the final stages has been overwhelming.

"Two roads diverged in a wood,

And I – I took the one less traveled by,

And that has made all the difference."

Robert Frost

Contents

List of Figures

List of Tables

List of Abbreviations

Ara-C	Cytosine beta-D-arbinofuranoside
BBB	Blood Brain Barrier
BSA	Bovine Serum Albumin
ClO_4	Perchlorate
CNS	Central Nervous System
CSF	Cerebrospinal Fluid
DAPI	4, 6-diamidino-2-phenylindole
DBS	Deep Brain Stimulation
DEX	Dexamethasone
DI	De-ionised
DMEM	Dulbecco's Modified Eagle Medium
ECM	Extracellular Matrix
ECD	Electrochemical Deposition
EPD	Electrophoretic Deposition
FBS	Fetal Bovine Serum
FDA	Food Drug Administration
FEM	Finite Element Method
FITC	Fluorescein isothiocyanate
GelMA	Gelatin methacryloyl
GFAP	Glial Fibrillary Acidic Protein
HA	Hydroxyapatite
IL-X	Interleukin-X
MW	Molecular Weight
NGF	Nerve Growth Factor
PAA	Polyacrylic acid
PBS	Phosphate Buffered Saline
PDMS	Polydimethylsiloxane
PEDOT	Poly(ethylenedioxythiophene)
PEG	Polyethylene Glycol
PEG-PLA	Polyethylene Glycol-Polylacticacid
PFA	Paraformaldehyde
PI	Photoinitiator
PLA	Polylactic Acid
PLD	Pulsed Laser Deposition
PLGA	Poly(lactic-co-glycolic) acid
PMMA	Poly(methyl methacrylate)
PNS	Peripheral Nervous System
Ppy	Polypyrole
pSS	Polystyrene sulfonate
pTS	p-toluene sulfonate
PU	Polyurethane
PVA	Polyvinyl acid
RPMI	Roswell Park Memorial Institute
SD	Standard Deviation
SEM	Scanning Electron Microscopy
TNF-α	Tumor Necrosis Factor alpha
UV	Ultraviolet
α-MSH	alpha Melanocyte Stimulating Hormone
α-TCP	alpha-Tricalcium Phosphate

Presentations and Publications arising from this Study

Presentations:

Bioengineering in Ireland (BINI) January 2013, Meath – **Poster Presentation** PC12 neural cell response to surface composition and topology of insulating materials for neural probes

European Society for Biomaterials (ESB) September 2013, Madrid - **Oral Presentation** PC12 Cell and Primary Cortical Neuronal Response to Surface Composition and Topology of Insulating Materials for Neural Electrodes

Bioengineering in Ireland (BINI) January 2014, Limerick – **Oral Presentation** Primary Cortical Neuronal response to Surface Composition and Topography of Insulating Materials for Neural Electrodes

European Society for Biomaterials (ESB) September 2015, Krakow - **Oral Presentation** A Dual-layered Microfluidic System for the Controlled In Situ Delivery of Anti-inflammatory Factors in Chronic Neural Implants

Bioengineering in Ireland (BINI) January 2016, Galway – **Oral Presentation** Increasing the lifetime of neural probes via cooling technology and long-term drug-eluting coatings to allow their utilisation as a chronic therapy

World Congress of Biomaterials (WCB) May 2016, Montreal – **Oral Presentation** Design of a neural probe using localised cooling and long term delivery of anti-inflammatory factors to reduce glial scar formation and improve the chronic efficacy of therapeutic probes

Publications:

A Dual-layered Microfluidic Chip for Long-term Controlled In Situ Delivery of Multiple Anti-inflammatory Factors for Chronic Neural Applications. Laura Frey, Su Ryon Shin, Praveen Bandaru, Yu Shrike Zhang, Kevin O'Kelly, Ali Khademhosseini. Invited Full Paper, submitted Apr 1st 2017, **Advanced Functional Materials.**

PC12, Primary Cortical Neuronal and Astrocyte Response to Surface Composition and Topography of Insulating Materials for Neural Probes. Laura Frey, Kevin O'Kelly. Full Paper, to be submitted May 2017.

An experimentally validated thermal Model for a therapeutic focal Cooling Probe for use in Humans as an Alternative to Deep Brain Stimulation. Laura Frey, Tony Robinson, Kevin O'Kelly. In Draft.

1 Introduction

Neurological disorders are becoming more prevalent as advanced economies generally experience a steady aging of their population profiles. In the UK alone, almost 500,000 people suffer from epilepsy[6] and 127,000 from Parkinson's disease[7], with other debilitating neural conditions such as motor neurone disease, dystonia, paralysis and depression also requiring huge investments in research for therapeutic solutions.

Some patients will respond well to treatment via medication where available, but others do not and have to cope with their symptoms on a daily basis. In recent decades, this has led to an increasing emphasis on the search for alternative solutions. One of the most promising areas of research has involved physically disrupting the signals in the problematic area of the brain. This can be done either via electrical stimulation or localised cooling of the target region. Over the years, the more prevalent of these two methods has become that of electrical stimulation in the form of Deep Brain Stimulation (DBS). DBS has shown very promising results *in vivo*, in clinical trials and in patients, resulting in Food Drug and Administration (FDA) approval for its use as treatment in the United States for dystonia, Parkinson's disease and essential tremor.

However, despite appearing to be effective in the early stages of treatment, DBS has failed to offer a long term solution to these conditions. Although significant reductions in the symptoms associated with these conditions – such as the seizures that occur during an epileptic fit – are evident in the first few months, as time goes on the electrodes' therapeutic effects become less and less effective, which can leave a patient more distressed than before. This reduction in effectiveness is normally attributed to

the encapsulation of the electrode in scar tissue over time as the result of one or more of the following: the initial insertion-associated injury (acute response); the presence of a foreign material (chronic response); the damage caused by micro-motion of the inserted electrode; the repeated electrical over-stimulation of the tissue.

In order to address this loss of effectiveness, research has focused on a number of research areas, including making the probes smaller and designing biomimetic coatings with properties close to that of native brain tissue to reduce the brain's inflammatory response to the probes or utilising adaptable surface topography to promote neuronal cell survival alongside the implant. The inclusion of anti-inflammatory factors or drugs into the probes' coating is also a promising area of research, as these can be used to target precise timepoints in the process of inflammation of the brain tissue and prevent the formation of this inhibitory glial scar. Many studies have shown this can be effective in its short term effects by reducing the acute inflammatory response, however, there is limited success reported in maintaining these reductions in inflammation long-term.

Furthermore, as well as improving current electrode designs and strategies, investigation into an alternative therapeutic mechanism of the probe itself may also be advantageous. Although electrical stimulation has been the favoured method thus far, some research has indicated that repeated electrical over-stimulation of the tissue is further aggravating the problem. For this reason, a return to researching focal cooling probes could result in more positive outcomes, as they have been shown to interrupt brain signals in a reversible way with no long-lasting damage. As well as this, the focal cooling may be able to reduce inflammation *in situ* and therefore the encapsulation of the functioning tip by the glial scar. The design of cooling probes introduces several new

challenges as coating materials need to be thermally insulating and the probe will by nature need to be thicker in order to cool tissue deep in the brain as, unlike electrical conductivity, thermal conductivity is dependent on thickness. While many biomimetic polymers currently utilised as probe coatings are not sufficiently thermally insulating, there are several potential options for multifunctional thermally insulating coatings. Ceramic materials traditionally used in orthopaedic implants such as hydroxyapatite (HA) are widely regarded as being highly biocompatible and providing good thermal insulation. It is also possible to incorporate porosity into their structure which could be used to release anti-inflammatory drugs to reduce the brain's immune response to the probes. Alternatively, thermally insulating polymers could also offer sufficient insulation while allowing the introduction of microfluidic systems for sustained drug delivery within their structure. The optimisation of the materials used to fabricate such a probe are important to minimise the total size and therefore injury of a probe capable of delivering therapeutic temperatures to the depth required for human applications.

This outline of the ongoing challenges faced by researchers attempting to develop new, more successful interventions to mitigate neurological disorders provides the context for this research study. In turn, the rationale for the study emerges from this context, a context which has highlighted the need for further more specific research that builds on previous advances and offers the possibility of significant improvements in the long-term outcomes for patients with debilitating neurological disorders who opt to use Deep Brain Stimulation as a treatment method to control their symptoms. Any significant advances in this field would result not only in an improved quality of life for these patients over a longer time period, but also facilitate a higher degree of independent

living for older people as well as an associated reduction in medical and welfare costs for Government.

The overall aim of this study is to develop a functional neural probe with additional potential to reduce inflammation of brain tissue upon insertion into the brain, a probe that will thus limit the development of a surrounding glial scar, allowing it to function as required for extended periods of time.

This aim encompasses two broad objectives representing two separate strands of research, which, if both are successfully achieved, have the potential to mutually reinforce the effectiveness of the treatment:

1. *To design a clinically viable cooling probe capable of delivering 10°C of cooling to brain tissue up to depths of 10cm in order to eradicate the need for electrical stimulation during treatment.*
2. *To design a probe coating capable of mitigating the chronic inflammatory response of brain tissue as well as the acute response.*

With these objectives in mind, Chapter 2 will provide a wide-ranging literature review that examines and evaluates the significant previous studies carried out in these two areas of research. This will in turn help highlight any knowledge gaps and form the basis for the specific research questions to be addressed and hypotheses to be tested in the subsequent experiment-focused chapters. The discussion of the experimental results and their findings and limitations will allow conclusions to be drawn and aligned with the overall aim and objectives.

2 Literature Review

2.1 Introduction

The field of neural engineering is becoming increasingly significant within the bioengineering research community. Considerable advances have been made in recent years, regarding the use of neural electrodes to not only measure and record brain functionality, but to suppress or stimulate different areas of the brain in order to treat a variety of conditions. There has been successful employment of these electrodes to minimise the effects of motor neurone disease[5,8], Parkinson's disease[9–12], epilepsy[8,9,11,13] and to overcome the effects of paralysis[2,14]. As well as this, advancements are being made in the use of electrodes to combat deafness and blindness through cochlear[10,11,15] and retinal implants[9,11] and to reduce the effects of mood disorders by deep brain stimulation (DBS)[11,13].

2.2 Neurobiology[16]

In order to begin understanding and treating neural conditions, we first need to understand the physiology of the brain. The brain is the body's central control system; it receives signals from nerves throughout the body and responds to them based on its interpretation of these signals. The brain itself and the spinal cord make up the central nervous system (CNS) and works in conjunction with nerves throughout the body which are known collectively as the peripheral nervous system (PNS).

The brain is made up of three main areas: cerebrum, cerebellum and brain stem. The cerebrum is divided into two halves, the left and right cerebral hemispheres and further

divided into four lobes (Fig. 2.1). The left and right hemispheres control the right and left hand side of the body respectively and are connected by a bridge of fibrous neural tissue. The outer surface of the cerebrum is called the cortex and is where nerve cells make connections (synapses) that control brain activity. It is also sometimes referred to as “grey matter” as it contrasts in colour to the “white matter” underneath. This colour of the inner area of the cerebrum comes from the myelinated sheaths of axons – the insulated parts of the neural cells which act as messengers between the brain and the spinal cord. The cerebrum as a whole controls movements, speech, hearing, vision, emotions and intellectual functioning. The next largest section of the brain is the cerebellum which is located at the back of the brain underneath the cerebrum. It also consists of white and grey matter and controls complex actions such as walking by co-ordinating actions and also controls reflexes and collecting sensory information from the body. Finally, the brain stem is a bundle of nerve tissue connecting the brain to the spinal cord and transmitting messages between the two. It also has an important role in respiratory and circulatory function and regulates the CNS to control consciousness and create a sleep cycle.

As well as these 3 main areas of the brain and a few smaller sections, there are other constituents of brain tissue that serve important purposes. The brain contains cerebrospinal fluid (CSF) that surrounds protects the brain from damage and delivers nutrients to and removes waste products from the brain. The blood brain barrier (BBB) is a specialised system of capillaries throughout the brain that help maintain a constant environment for the brain and protects it against chemicals or toxics produced by bacteria via enzymes.

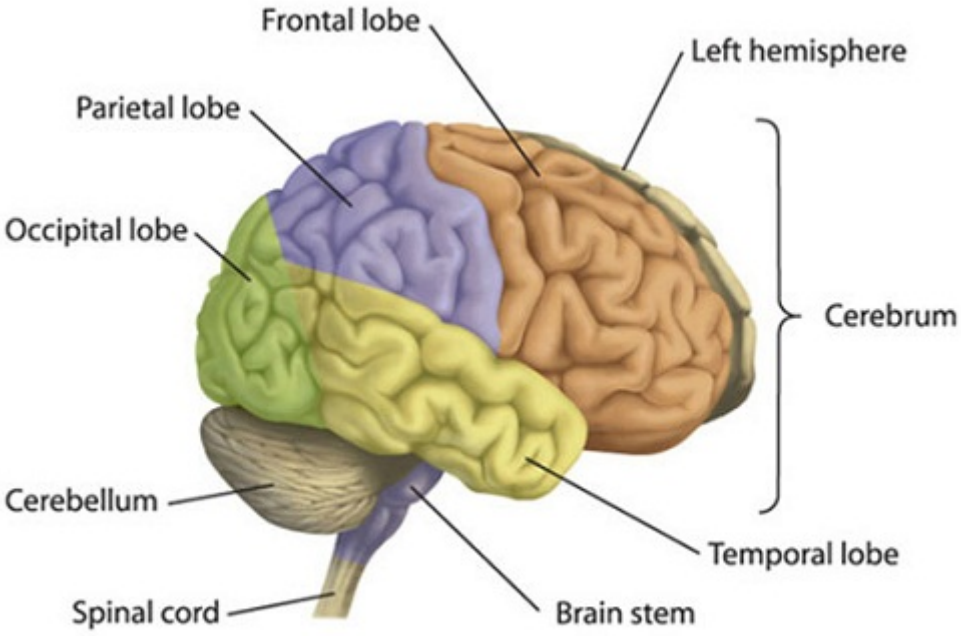

Figure 2.1. Diagram of the human brain[1]

2.3 Brain Cell Types and Functions

Within every section of the brain, there are different cells with different roles and neurological disorders are a result of these not functioning correctly. Neurons are generally considered the most important cell in the brain as these are the cells that send signals to specific target cells. These cells are made up of a cell body, dendrites and axons which are long protrusions that vary hugely in length depending on the location of the cell they are trying to reach. They transmit signals via synapses which are the junctions between cells. Signals travel through cells as electrochemical pulses which cause neurotransmitters to be released at a synapse. These chemicals are detected by the receiving cell, converted back into neurotransmitters and the message is passed on.

As well as neuronal cells, there are also glial cells in the brain. These are broken up into three predominant categories: microglia, astrocytes and oligodendrocytes[17]. These cells serve to protect the neurons via insulation and ensure they get enough nutrients as well as killing pathogens and removing dead cells from the brain when necessary. They also enable the formation and maintenance of synapses between cells[18]. The glial cells are set apart from neurons by their lack of axons, inability to form action potentials and ability to readily proliferate. In the CNS, one key feature of the glial cells is their reaction to cell damage – microglia are the first line of defence and will infiltrate the injured area within hours and release signals to astrocytes causing them to enlarge and proliferate to form a scar and contain the damage[17–19]. Microglia are the resident macrophages of the brain: they engulf and destroy infectious agents and decrease initial inflammation at the site of injury or infection and make up 10-20% of glial cells[19]. They can also release cytotoxic materials in order to destroy infections. This can result in large scale neural damage if chronic inflammation occurs as the microglia repeatedly try to eliminate the cause and destroy healthy cells at the same time[18]. In this state they are described as being activated[2] (Fig. 2.2). Astrocytes are the most prevalent cell in the brain and form scar tissue by filling the area left behind by dead cells and also enter an activated state during brain injury[17,19] (Fig. 2.3). They also promote the myelination of oligodendrocytes which is their main role – to support and insulate axons; oligodendrocytes do not play a major role in the brain's response to injury[2,17].

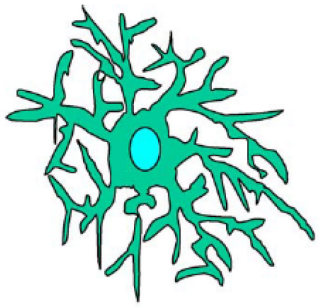

Resting or Ramified Microglia

- No Fc receptors, no macrophage specific receptors
- Large, dense chromatin masses in small flattened nucleus
- 5-10% of glial population
- Many long, thin processes

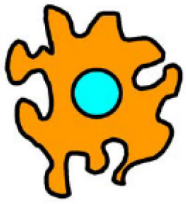

Activated or Amoeboid Microglia

- Upregulation of lytic enzymes
- Retraction of cytoplasmic processes to stouter, thicker pseudopodia
- Accumulation of phagocytosed material and lipid droplets
- Ameboid and motile abilities
- Release of inflammatory factors MHC I, II expression
- Active Proliferation

Figure 2.2. The differences between resting and activated microglia in the brain[2].

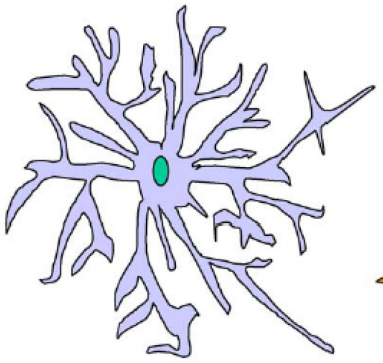

Normal Astrocyte

- 8-10 nm diameter GFAP filaments
- Round nucleus
- 10-40 nm glycogen particles
- Large mitochondria
- Gap junctions with other astrocytes
- Maintain proper neuronal environment
- 30-65% of glial population

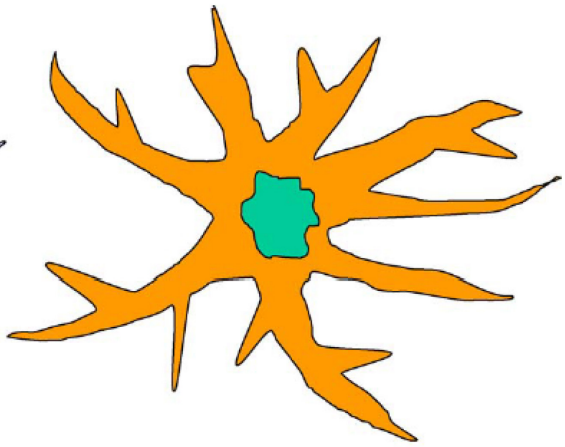

Reactive Astrocyte

- Large increase in GFAP filaments, glycogen deposits
- Irregular nucleus
- Increase in mitochondria and multiple Golgi complexes
- Hypertrophy
- Phagocytosis
- Proliferation
- Migration
- Extracellular matrix production
- Production of neurotrophic and inflammatory factors

Figure 2.3. The differences between resting and activated astrocytes in the brain[2].

2.4 Electrode Design and Functionality

2.4.1 History of DBS

The utilisation of electrical stimulation on brain tissue dates as far back as the first century whereby a physician to the Roman emperor Claudius prescribed the use of an electric ray to alleviate headaches[20,21]. It was not until the 19th century that experimentation seriously began, with tests being carried out on the cortex of recently deceased prisoners and animals in order to ascertain which areas of the brain corresponded with which functions[20]. The first instance of modern therapeutic brain stimulation was that of electroshock therapy for the treatment of psychosis devised by Ugo Cerletti in 1938[22], however, the first reported instance of chronic Deep Brain Stimulation for the treatment of movement disorders came from the University Hospital of Grenoble, France[23–25]. The interest in these results led the medical device industry developing a specific neurostimulation device, with Medtronic being the first in 1968, followed by Avery Laboratories in 1982[24]. Medtronic went on to collaborate heavily with the Grenoble group and a consortium of experts known as the Movement Disorder Society who developed the Unified Parkinson's Disease Rating Scale (UPDRS)[24]. This led to the presentation of clinical trial results to the FDA in 1997, with DBS being an approved therapy for the suppression of tremors due to essential tremor or Parkinson's Disease in the same year[20,23–25]. The FDA would go on to approve the use of DBS for control of the symptoms of both dystonia and OCD in 2003 and 2009 respectively via the Humanitarian Device Exemption method[23]. Medtronic were consistently the first company to receive FDA approval for DBS devices for various applications but are currently joined on the market by St. Jude Medical and Boston Scientific, with their current technologies to be discussed in the next section.

2.4.2 Current Electrode Design

DBS is already a Food and Drug Administration (FDA) approved treatment for controlling tremors during Parkinson's disease and dystonia in the US, whereas effects on other conditions are still at the testing stage[26]. The precise mechanisms of how DBS counteracts these tremors is still not fully clear, but it is thought that passing an electrical current through the affected area of the brain either interrupts the mis-functioning signals or induces the correction of these signals, much like a pacemaker does in the heart[26]. In order to develop ways to improve the efficacy of therapeutic probes, a review of current clinically relevant electrodes is necessary. The current industrial design of these electrodes consists of a lead with 4 electrode tips that can be inserted into the brain and connected to a neurostimulator which generates a current and is normally implanted under the skin on the chest. Medtronic is the world's largest medical technology company and is a key market shareholder in DBS electrodes[27]. As such, key features of its most commonly implanted electrode are outlined below as an example of a typical electrode on the market. Medtronic designs all of its leads to be 40cm in length so they can be inserted to any depth. The electrode itself has 4 electrode tips spaced 0.5mm apart along the length which can be activated all at once or individually when required (Fig. 2.4). This is to give doctors some flexibility with positioning the electrode in the precise area to be stimulated. This results in a device being inserted into the brain that is 1.27mm wide with the electrodes for stimulation being 1.5mm in length each. Although 0.5mm is Medtronic's standard electrode spacing, they also produce electrodes with 1.5mm spacings[27]. These electrodes are inserted in the subthalamic nucleus for most current treatments[28,29] (Fig. 2.5).

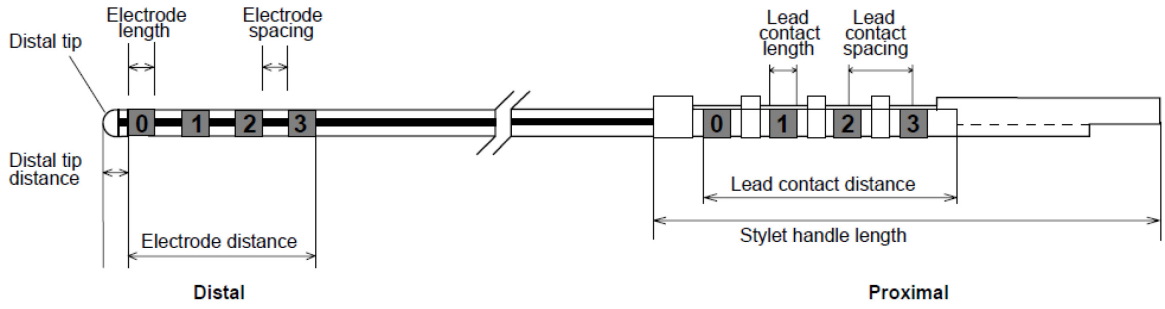

Figure 2.4. Medtronic DBS electrode design[3].

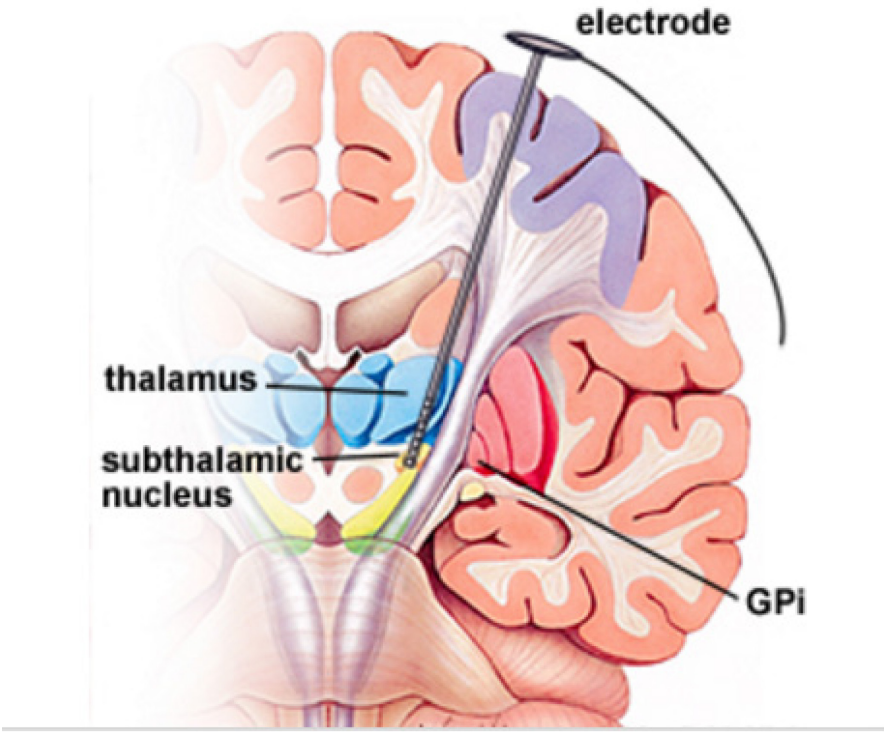

Figure 2.5. Cross-section of the brain showing DBS electrode placement in the sub thalamic nucleus[4].

The electrodes currently on the market from St. Jude's Medical consist of a similar set up to those of Medtronic, however, they offer a baseline electrode with a diameter of 1.27mm and 1.5mm height or a larger cylindrical electrode with a diameter of 1.41mm and a height of 1.5mm or 3mm[30] with each lead having 4 electrode contact points[30].

Boston Scientific's Vercise® DBS system was approved by the FDA for Parkinson's, dystonia and essential tremor in 2015 and is marketed as the first commercially available eight contacted lead system[31]. These 1.3mm diameter leads can be purchased in 30 or 45cm configurations, with electrode contacts of 2mm in length with 1.5mm spacings[31].

2.4.3 Ideal Electrode User Requirements

Ideal User Requirements are regularly devised during the development of medical devices in order to improve the safety and usability of the devices, therefore reducing the recall of devices and improving patient outcomes and satisfaction[32]. The principle user requirement for a DBS device is that it reduces or eradicates the symptoms of the relevant neurological condition – it needs to help the patient manage their symptoms. It should also be minimally invasive in order to cause as little damage upon initial implantation as possible. Furthermore, the device should have multiple electrodes along the length of the lead, that can be activated or deactivated by a controller outside the brain region as required if a larger volume of tissue or a slightly different area needs targeted. It should remain in place for a number of years and maintain function through that time period, without any adverse side effects. The device itself should also be fully implantable in order to reduce the risk of complications via infection, particularly upon initial implantation. For a cooling probe there are several additional user requirements. Firstly, the probe should reduce the temperature of the target brain area by 10°C at a depth of 10cm. It should only interrupt the function of the brain via cooling at the tip of the probe, therefore it should be sufficiently insulated. It should also reach this temperature very quickly in case it can be linked to a feedback loop for pre fit warnings for epilepsy.

2.4.4 Current Electrode Limitations

All neurological disorders that are suitable for DBS treatment require on-going intervention and so an electrode must be chronically implanted in the brain for long-term benefits. Maintaining the effectiveness of these electrodes has proved difficult long-term which has been reported in clinical follow ups and *in vivo* studies. A follow up study on 27 patients who had a total of 31 electrodes implanted to control symptoms of essential tremor found that 4 electrodes had lost their stimulation effects entirely by an average of 39 months[33]. As well as this, at an average of 40 months follow up, 10 electrodes required a voltage supplied to the electrode of over 3.6V compared to a starting voltage of 2.2V. This increased voltage to have an effect on tremor reduction is described as an unsatisfactory result and at higher voltages more adverse side effects occur[33]. Pelitsis *et al* (2008) also compiled and summarised similar data from other papers, showing that 13-40% of patients experienced tremor worsening after a minimum of a year's implantation though it highlights some of these failures may have been due to suboptimal placement of the electrode[33]. A follow-up of up to 7 years (an average of 56.9 months) after DBS surgery for essential tremor in 22 patients assessed the electrodes success via Fahn-Tolosa-Marin tremor scores, whereby the lower the number, the less severe the tremor is. Scores over a two year period increased from 0.33±0.49 to 0.67±0.72[34]. The difference was not statistically significant and was still an improvement from zero stimulation scores of 3.27±0.87 but the mean voltage to achieve these scores was also steadily increasing and 2 patients ceased to use the system due to persistent paraesthesias - tingling or burning sensations under the skin[34].

These reductions in the effectiveness of probes have also been shown in *in vivo* studies. Two separate studies in cats have shown that *in vivo* cortical cell responses to

stimulation degrade after 100 days[35] and that recordings from the sciatic nerve last for a maximum of 7 months[36]. Microelectrode arrays suffer similar loss of function with arrays implanted in macaque monkeys reporting a 35% loss in function over 18 months[37] and in a study using cats, after 6 months only an average of 60% of original microelectrodes could still record signals[38].

2.5 Problems with Design

In order to obtain a viable chronically implantable working probe, it is important to understand why so many systems fail over time and many investigations have focused on identifying the problem. Most studies attribute the failure of electrodes to the formation of an inhibitory glial scar around the electrode (Fig. 2.6), either due to the insertion-associated injury (acute response), presence of a foreign material (chronic response) or damage caused by micro-motion of the inserted electrode[2,10,39,40] with intensity of electrical stimulation also included as a factor[41,42]. However, some studies have indicated that although there is a change in impedance due to the scar, it does not significantly affect an electrode's ability to record[43]. They instead suggested that chronic local inflammation of the tissue occurs due to the continued presence of the electrodes, which correlates with local neurodegeneration resulting in neuronal loss, dendritic loss and taupathy[43]. All of these theories are centralised around the inflammatory reaction of brain tissue and therefore current research is heavily focused on reducing this inflammatory response *in vivo.*

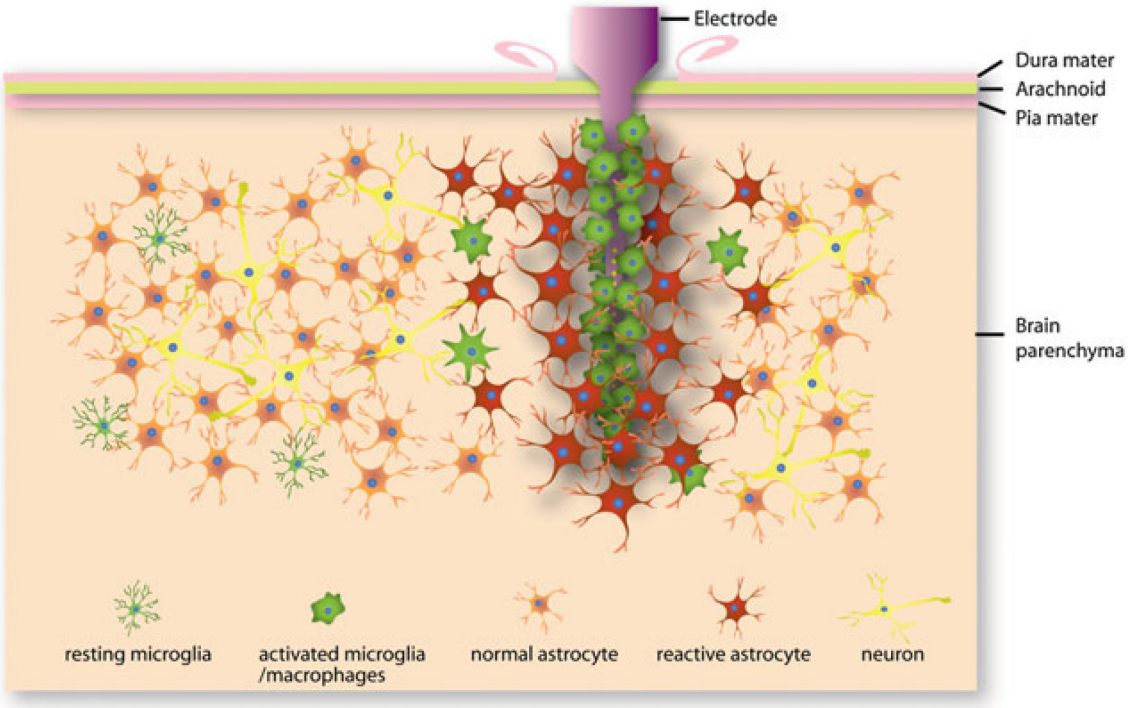

Figure 2.6. Schematic of cellular changes induced by electrode insertion into the brain, resulting in glial scar formation and encapsulation of the electrode[5].

2.6 Strategies to reduce Inflammatory Response

Regardless of therapeutic strategy or probe function, reduction of the brain's inflammatory response to the implant is crucial to maintaining its function long-term. In order to achieve this, a number of key strategies for optimisation of probes, electrodes and microelectrodes have been investigated. These include looking at the probe material, the probe shape, the coating and incorporating anti-inflammatory drugs into the design. The progress and unanswered questions from these investigations are outlined below in order to develop further areas or strategies for investigation.

2.6.1 Coating Material

Probes may be coated with a material to ensure insulation of the brain tissue from the probe function for everywhere except the probe tip or to reduce the inflammatory

response to the probe or for a combination of the two. Biomimetic coatings are designed to mimic brain tissue as closely as possible to assist with tissue integration and prevent an immune response. As such, many of the investigated coatings are derived from natural materials such as collagen and laminin[10]. Both of these materials are found in the human body as part of the extra cellular matrix (ECM) – the support structure for the cells in the body, which also carries out other duties such as storing chemical growth factors and aiding wound healing. Collagen is the predominant protein within the ECM and laminin is often present to assist with adhesion and keep the tissue connected, making these materials of significant interest[44].

Large scale isolation of ECM proteins can be challenging and the use of such bulky structures can also result in steric issues as the large polymers get in the way of each other. Another approach is to look at the integrins – the trans-membrane receptors that bind a cell to the ECM, providing it with stability and passing messages both ways. It has been shown that integrin binding to ECM proteins actually relies on short peptide motifs – the sequences of amino acids that determine the properties and identify individual peptides. The sequence known as the trimer RGD peptide sequence is the most effective and most utilised sequence to enhance cell adhesion onto synthetic surfaces[45]. It is found throughout the body and can address more than one cell receptor. When looking specifically at neural cells, research has indicated that other sequences such as IKVAV and YIGSR, present in laminin, may be the most effective at increasing neuronal adhesion[46]. One study concluded that RGD peptide grafted substances promoted fibroblast and glial cell adhesion which implied that it would be useful where tissue anchorage is required to prevent micromotion[39]. In contrast, the IKVAV peptide grafted

substances promoted substantial neuron cell adhesion and neurite growth and minimised fibroblast and glial cell adhesion, indicating potential to promote signal transfer between neurons and implants[39]. These sequences can also be incorporated as part of a longer structure such as DCDPGYIGSR. *In vivo* studies of this peptide co-deposited with the conducting polymer polypyrole on neural electrodes were carried out on guinea pigs. The tissue was analysed at 1, 2 and 3 weeks and it was found that glial scarring was not prevented but that neuron attachment was promoted and strong connections with the neural tissue occurred[47]. Polypyrole coatings alone have also been investigated as a method of integrating electrodes, without affecting electrical transmission of stimuli, another important consideration of any coating. It was ascertained that if polypyrole was grown up through a layer of hydrogel rather than used as a film, the electrical impedance could be reduced from 100kΩ to 7kΩ[48]. Polypyrole's advantageous properties are also used in the integration of cochlear implants to promote neuronal cell adhesion[15].

Another conducting polymer that can be utilised in neural electrode coatings is poly(ethylenedioxythiophene) (PEDOT) which outperformed polypyrole in terms of rate capability and stability at higher charge rates[49]. PEDOT's electronic and ionic conductivity makes it a good alternative and anion doping (PEDOT+A- formation) results in the high electronic conductivity that is required for low impedance recordings[49]. Ludwig *et al* (2006) investigated a PEDOT film covered electrode system and found it had an improved signal to noise ratio and that over 6 weeks implantation in rats, the mean impedance at day 40 was 30 times less than the non-coated electrodes[50]. As well as this, 58% of the covered electrodes after 6 weeks were still producing quality

recordings versus only 41% of non-coated electrodes[50]. The effects of the improved impedance were thought to have been lessened by the remaining persistent glial scarring caused by the immune response. A study by Green *et al (2009)* investigated the use of large synthetic laminin molecules as anionic dopants and ascertained that although impedance was improved, there was a reduced electrochemical stability and film adherence to the electrode[51]. They concluded that a smaller molecule would be preferable. As part of more recent work they tested a variety of different smaller dopants including p-toluene sulfonate (pTS), polystyrene sulfonate (PSS) and perchlorate (ClO_4). PEDOT/pTS and PEDOT/$Cl0_4$ performed best and showed promise as a potential chronic implant coating whereas PSS was likely to delaminate with time[52]. Another study also showed doping PEDOT with carbon nanotubes improved the impedance and stability of uncoated electrodes and resulted in a 10 times higher charge storage capacity than versus PEDOT/PSS films, though no comparison with pTS was carried out[53].

Many of the coatings that are investigated are hydrogels or are incorporated into a hydrogel. This is because hydrogels possess a structure very similar to most tissues – they consist of a network of polymer chains which are water insoluble and super absorbent. Their ability to swell is thought to anchor implants in the tissue into which they are inserted and improve integration[48]. One study used a combination of polyvinylalcohol (PVA) and polyacrylicacid (PAA) to improve the electrode/neural tissue interface and found that the coated electrodes had a good electrochemical performance with a good bulk ionic conductivity and proper swelling ratio[9]. The gel discouraged non-specific protein absorption and therefore promoted nerve cell attachment. In order to

monitor glial scarring, glial fibrillary acidic protein (GFAP) staining was carried out in rats implanted with coated and uncoated electrodes for 6 weeks and scarring was shown to be significantly less ($p<0.05$) in the coated electrodes with a GFAP zone of only 50-100µm around the insertion site[9]. However, the study also acknowledged that this could have been partly attributed to the hydrogel causing a smoother insertion phase and less acute trauma rather than a better chronic response[9].

Another study tested a polyethylene glycol (PEG) containing polyurethane (PU) hydrogel coating which resulted in a 93% decrease in protein absorbance[10]. The GFAP scarring in rats after 6 weeks was also significantly lower in the coated group, with the glial scar measuring 22µm versus 35µm on the uncoated electrodes[10].

2.6.2 Flexible Probes

Micro-motion is also thought to be a contributing factor to glial scarring. Insufficient anchorage means electrodes can shift position as the subject moves, causing tearing and irritation of the surrounding tissue. As brain tissue is soft, it has been predicted that small flexible wires will result in a reduction of this problem – a study by Lee *et al* (2004) achieved this by using thin wires with a silicon backbone in order to retain enough stiffness for easy insertion[54]. As well as utilising polymers to ensure the coating of a probe has similar mechanical properties to brain tissue, there is increasing work to construct entirely flexible probes for better integration into the neural tissue. One study investigated the use of parylene-C coated with PEDOT as a flexible material for microelectrodes, however, it focused on *in vitro* recording quality of electrodes rather than confirming its mechanical properties or the brain's immune reaction to such an implant[55]. Probes made of sputtercoated aluminium covered in epoxy resin have also

been designed and tested mechanically in an agar gel brain model and cadaveric porcine tissue. Although still significantly mechanically stiffer than brain tissue, compared to silicon probes these arrays had a much lower Young's modulus and compressive strength as well as bending up to 0.8mm before breaking under tension[56]. No cellular testing was undertaken so it remains to be seen if these reductions in mismatch in mechanical properties reduce the inflammatory response to implants. SU-8 has also been investigated as a flexible probe material with mechanical tests showing sufficient strength for insertion into an agar brain phantom or a rat's brain and bending flexibility of up to 60° before probe failure occurred. Primary cortical neurons survived on the probes surface comparably to the positive control and when implanted *in vivo*, astrocytic aggregation around the lesion site occurred no glial sheath formed[57]. All of these studies stress the importance of having a probe with enough mechanical strength for insertion into the brain without dimpling but having improved flexibility post insertion to reduce damage due to mechanical mismatch and micromotion. One approach that could be applied from another area of bioengineering involves the utilisation of a swellable polymer polacrylic acid (PAA) in microneedles to ensure easy insertion followed by mechanical interlocking to reduce micromotion[58]. This approach was designed following the study of a parasitic worm that uses a similar method to attach to its host's intenstinal wall and could prove useful in a neural probe.

2.6.3 Topographical Control of Coating Surface

As well as the composition of the surface itself, the texture of the surface can also have an effect on tissue response. It is thought that manipulation of the surface can result in a surface that neural cells are more likely to adhere to, reducing the glial response and

improving anchorage of the electrode. Several studies have been undertaken to show how roughening the surface affects neural cells. Green *et al* (2012) found that laser roughening of an electrode's surface pre-polymer coating resulted in a roughened polymer surface[52]. This not only reduced the likelihood of the coating delaminating from the electrode surface but was found to elicit improved cell response and neurite outgrowth in PC12 cells (a cell line developed from rat's adrenal glands that behave similarly to neural cells when treated with nerve growth factor(NGF))[52]. As well as "random" roughness, precise nano-engineering of surfaces has been investigated. Parallel grooves have been added to materials at the micro and nano scale in order to analyse the effects on cell attachment.

Ereifej *et al* (2013) used nano-imprint technology to create grooves of 120nm width of electrode pin coatings and insert them into "living" brain tissue culture slices[59]. It was shown that the neural cells grew in an aligned manner on the patterned pins but that cell number and distribution were not significantly different between patterned and smooth surfaces[59]. However, the expression of inflammatory markers such as GFAP and tumor necrosis factor(TNF)-α did significantly decrease on the patterned pins, suggesting that there was less inflammation of the tissue which could potentially lead to a reduction in scar tissue formation[59]. It has also been shown that mouse axons tend to adhere along ridges and elevations rather than the grooves of a channel and that if microchannels are over 40μm wide, the neurites will extend horizontally across grooves rather than along them[46].

Chen *et al (*2010) used surface lithography to create grooves in polymer surfaces ranging from 250nm to 2mm in width and compared how macrophages attached to their surface[60]. Results showed that the macrophages elongated in line with the grooves and had significantly more attachment to the rough surfaces than the smooth[60]. Microglia are the brain's resident macrophages and form the first initial response of scar tissue in the brain, so this improved attachment could be an undesirable property[60]. The idea of guiding the growth and attachment of neurons can also include the addition of mechanical or chemical cues near the electrode surface, to encourage axon growth towards it[61].

2.6.4 Size, Shape and Insertion

Another important consideration is the shape and size of the probe. These properties can have a large effect in terms of reducing the initial insertion trauma, one of the key causes of inflammation, although very small probes may require a novel insertion method[62]. An increasing number of electrode array systems use microwires to try to limit the scarring but research by Polikov *et al* (2009) indicates that microwires of 50µm thickness still result in a scar index (based on their new measuring protocol) of 7.6±0.66 – significantly higher than the suggested upper limit of "minor scarring" of 4[63]. A study by Szarowski *et al* (2003) investigated the shape and size of electrodes using two basic shapes, a chisel shape with sharp corners and a smooth round tipped one with diameters varying from 50 to 140µm in rats over a 12 week period[40]. The results showed that although the small rounded tips showed the best initial response with a smaller amount of reactive tissue generated, at the end of the 12 week period all devices had similar compact glial sheaths surrounding them[40]. A better initial response is an improvement,

however, the study indicates that for chronic use, another method of reducing scarring tissue other than size or shape needs to be utilised. A study carried out by Karumbiahi *et al* (2013) compared the acute (3 day) and chronic (12 week) responses of several electrodes currently available on the market[64]. The smaller diameter M15 (15µm diameter) Michigan probes elicited a smaller glial scar and resulted in reduced neuronal death than the larger diameter M50 probes. Cylindrically shaped microwire electrodes also performed much better than the M50 probes chronically. This was attributed to the reduction in the breach of the blood brain barrier improving survival rate of neurons and therefore reducing glial scarring[64]. The probes tested also included both tethered and untethered probes and the study concluded that chronic glial scarring was reduced in untethered probes as there was a reduction in tether included micromotion of the electrode. This corroborated work carried out by Biran *et al* (2007) investigating the effect of tethering on the brain's foreign body response to electrodes whereby increased levels of ED-1+ and GFAP+, antibody markers for glial cells, were present and reduced levels of NeuN neuronal markers were apparent with the tethered implants[65].

The size of the electrode also affects the method of insertion into the brain which can in turn affect acute damage. A study by Bjornsson *et al (2006)* investigated different tip shapes and speeds of insertion to determine the optimum conditions. They found that a lower insertion speed resulted in increased vascular damage and came to the conclusion that a sharper tip inserted quickly produced the lowest mean effective strain[62].

As well as insertion speeds, different methods of insertion have also been investigated. This can become a problem with smaller electrodes as traditional methods can result in buckling. A study by Rennaker *et al (2005)* compared the mechanical insertion of an electrode array with manual insertion. Mechanical insertion resulted in no brain compression and 60% of the electrodes were still recording after 6 weeks, whereas manual insertion compressed the brain and no electrodes were functional after 3 weeks[66]. Another array used electrodes of staggered lengths (5-6mm) to prevent dimpling of the brain during insertion[67]. Jaroch *et al* (2009) innovated a new magnetic insertion system in order to allow soft flexible thin probes to be used. The system used tension based propulsion by accelerating a ferromagnetic tip within a pulsed magnetic field. The probe tip, attached to a conductive tether, held the tether in tension due to its pulling force during acceleration[68]. All electrodes were thinner than 0.6mm and could be inserted to depths of at least 4mm[68]. This could also be an interesting insertion method as it could be combined with the neuroprotective effects of low intensity static magnetic fields against apoptosis in primary neuronal cell cultures[69]. One insertion methodology demonstrated by Eliades *et al* (2008) in monkeys, involved first attaching a head cap to the brain, following the removal of a section of skull and the underlying muscle. The electrodes can then be fitted into guide tubes, where a bent end holds them in place and allows deeper electrode placement if required[70]. This ability to move improves the chances of finding the best signal along a channel and the subtle movement is thought to prevent scarring to an extent[70]. The removable pushing devices also reduce the weight on the head but mean that electrodes can only be placed further into the skull, not then withdrawn[70].

2.6.5 Drug Delivery

The concept that glial scarring occurs due to the brain tissue rejecting the probe as a foreign body is a common one. As such, a method to inhibit this response using anti-inflammatory drugs could prevent or significantly reduce the scarring and allow an electrode system to reliably record or stimulate the brain long term. Several problems exist with this hypothesis; firstly, it is generally not considered to be practical to administer drugs as a long term solution[2] and secondly, there is a higher chance of infection as the brain's immune system is effectively weakened. However, particularly when reducing the brain's acute response to injury, it could have a significant positive effect. *In situ* drug delivery is also preferred as it allows localised reduced dosages, particularly important in the case of strong corticosteroids such as dexamethasone (DEX). Systemic doses of drugs can cause problems in other parts of the body including the kidneys and liver as well as requiring higher dosages so that enough of the drug reaches the required area[71]. Although there have been advances in manufacture of drug delivery particles that can traverse the blood brain barrier including magnetic nano particles that can be conjugated with peptides and antibodies for further treatments[13], this review will focus on the *in situ* deliveries.

2.6.5.1 Scaffold Degradation

Firstly, drugs may be delivered by the progressive degradation of a scaffold or by diffusion[13]. The regulation of dosage is controlled by the correct ratio of drug to scaffold material and a precise scaffold porosity and density[13]. A review by Willerth *et al* (2007) highlighted many of the key studies focusing on scaffold based drug deliveries in the neural region[72]. Some of the successes include a study whereby ECM molecule LN-1 was coupled with NGF and incorporated into an agarose scaffold which was predicted to

release the molecules for up to 42 days[73]. This mathematically modelled release was not confirmed experimentally but scaffolds eluting this combination of molecules into 10mm defects in rats' spines were the only scaffolds that showed a comparable growth of myelinated axons to autografts – the current clinical "gold standard" – after two months *in vivo* implantation[73]. As well as this, neurotrophins were successfully encapsulated in a polyethylene glycol (PEG)-based hydrogel and released via degradation for up to 3 weeks, although there was a significant initial burst release[74]. The release of these neurotrophins, despite the presence of the hydrogel breakdown products, stimulated proliferation of a TF-1 cell line and increased neurite outgrowth in retinal explants versus the controls over a week of culture[74]. This effect was further investigated using a polyethylene glycol-polylactic acid (PEG-PLA) hydrogel coating on a multi-electrode array which was tested *in vitro*. These coatings could release neurotrophins for up to a week with increased neurite outgrowth from PC12 cells as a result, though it was noted coatings broke down more quickly than anticipated once cells were added to the environment[75]. Another study looked at the effects of releasing the anti-oxidant curcumin from a polyvinyl alcohol (PVA) film coating on an intra-cortical implant in rats up to 12 weeks. Interestingly, although the curcumin releasing implants showed improved neuronal survival at 4 weeks despite only releasing the anti-oxidant for 48hrs, this improvement could not be seen at 12 weeks[76]. This supports the hypothesis that a mechanism to increase the expression of an anti-inflammatory factor long term is required to ensure probes can function in chronic applications.

2.6.5.2 Liposomes and microspheres

Liposomes are microscopic vesicles with phospholipid bilayers and are a common drug delivery mechanism as they can improve drug loading efficiencies and prolong the

activity of active drugs *in vivo*[77]. These particles have successfully been utilised to transport DEX to injured liver models in mice and reduce the expression of inflammatory cytokines IL-1β and IL-6 as and reduce the advancement of necrotic tissue over a period of 4 weeks[78]. This encapsulation and delivery method can also be used to transport NGF. One study determined NGF to be present in the striatum, hippocampus and cortex post intravenous injection of NGF encapsulated liposomes *in vivo,* highlighting the success of the liposomes in helping the NGF traverse the BBB[79]. However, when looking at glial scarring, as discussed previously, a more localised delivery would be advantageous[80]. Microspheres and nanoparticles can be polymeric and proteinaceous in nature and are also investigated as encapsulation methods to increase the efficacy and duration of drug release[77]. They can also have the advantage of allowing the administration of multiple drugs with individual release profiles as shown by the extended delivery of multiple neurotrophins from poly(lactic-co-glycolic acid) (PLGA) microspheres *in vitro* with further work to be done to confirm the positive effects of this[74]. Anti-inflammatory cytokines such as IL-1α have also been encapsulated into PLGA microspheres, resulting in increased survival rates in mice at days 7 and 12 after tumour cell inoculation[81]. The release of the cytokines *in vitro* was measured up until 20 days, however, this came with a reduction in bioactivity to 11.2% but this may not be reflective of what occurs *in vivo* as breakdown products of microspheres would be removed in this case[81]. For example, an *in vivo* study in guinea pigs whereby DEX was encapsulated in PLGA nanoparticles and released from alginate gels for up to two weeks, showed that the electrical impedance of a conducting electrode due to the formation of the glial scar was unchanged in the 3 week period, whereas the impedance of the non-eluting control had tripled by 2

weeks[82]. In order to address the issue of sustained release, one study suggested a method of predegrading PLGA microspheres with encapsulated DEX for one and two week periods and then mixing these with undegraded microspheres[83]. This mix of microspheres was then able to release DEX for up to a month *in vitro* and it was suggested that the addition of 10% PEG to the microspheres could further extend this release by up to 10 days. However, it was noted that the effectiveness of DEX was reduced over time and that cell studies would have to be carried out to assess the effect these microspheres could have on reducing inflammatory response long term[83].

2.6.5.3 Surface Coating

Simple surface coatings are another method of delivering drugs *in vivo.* One study showed clearly how surface coatings of alpha melanocyte stimulating hormone (α-MSH), an anti-inflammatory peptide, reduced the expression of inflammatory cytokines IL-1 and TNF-α and consequently reduced the glial response[13]. Another study showed that immobilising alpha-MSH to the electrode surface could significantly attenuate the glial response to implants in rats over a 4 week period[8] after confirming that the molecule being released would still be bioactive after 21 days and would be released steadily[84]. A review by Bridges *et al* (2005) discussed a variety of *in-situ* drug delivery methods. Firstly, the anti-inflammatory agents can be immobilised onto non fouling polymeric surfaces or delivered in soluble form from a surface[80]. This release can be achieved by a number of mechanisms including diffusion, biodegradable coatings, swelling coatings and enzyme degradable linkages[80]. The bio active electrode coatings used for retention and release of these drugs can be basic polymers such as nitrocellulose[11] or more commonly hydrogels such as polyethylene glycol-polylactic acid (PEG-PLA)[75].

2.6.5.4 Microfluidics

The neural probes can also incorporate microfluidic channels in order to deliver molecules *in situ*[11]. These channels result in a more flexible system with more precise control over quantity and delivery area, but result in a much more complicated device that could fail more easily[11]. One design involved the centre of the probe being hollow in order to allow administration of drugs through this channel. Dielectric shutters allowed some control of release of anti-inflammatory compounds with a 25 fold improvement versus an open orifice but there was still a lack of precision with the dosages varying by up to 10%[85]. A further study involved the integration of polydimethylsiloxane (PDMS) microchannels of 50µm by 200µm onto microelectrodes and studied the release of Rhodamine B as a drug model into an aqueous environment and an agarose gel as a brain model[86]. It found that drugs could be released at 20% of their total amount for the first two days and 4% in each of the next 10 days which, although not be long enough to reduce inflammatory response long term as the channels are not refillable once implanted, could be optimised further by adapting the geometry of the microchannels and the initial drug loading to extend drug release time[86].

2.6.5.5 Encapsulation in Ceramic Coatings

A limited number of studies have also investigated the release of drugs from ceramic or ceramic polymer compounds. Ceramics such as hydroxyapatite (HA) are traditionally cheap to make, biocompatible and their porosity is easily controllable by a variety of techniques such as: gel-casting, the use of hollow spheres or surfactant foaming[87,88]. These porosity inducing techniques are also very versatile as they can be used on a wide range of ceramics including zirconia and alumina. Netz *et al* (2001) used a gel casting

technique to create a porous HA structure with open micropores and closed macropores ranging in size from 15-34μm[87]. By creating a cylindrical gap in the samples, filling this with cisplatin (a compound for treating tumour cells) and sealing the gap with photoresin, a particle with drug delivery potential was created[87]. Over a 7.5hr period 20-40% of this cisplatin was released into the test medium, with samples with larger pores resulting in a higher but more irregular release profile[87]. A similar study was also conducted whereby microparticles of different commercially available forms of HA were vacuum loaded with different acidic solutions including benzoic acid and hydrochloric acid. It was discovered that there was an initial burst release of chemicals attributed to the particles lying on the HA surface, followed by a period of sustained release[89]. It also confirmed the idea that finer pores result in a slower release profile in general but that solution concentration and the ceramic's bulk density also has an effect[89].

Although ceramics have many desirable properties, they are non-biodegradable which limits their ability to retain drugs and release them over sustained periods of time[88]. The inclusion of biodegradable polymers within their structure increases their potential to elute drugs more slowly and this biodegradability can be controlled in order to release drugs at an optimum rate[88]. The introduction of polymers also reduces the brittleness of these ceramic materials[88]. There are a range of categories of polymers that have been tried and tested as bioceramic compounds, including those that are based on PLA and PLGA[88]. These compounds with an ester backbone can be altered via their L:G ratio and molecular weight to manipulate degradation rate. However, some of the faster degrading compounds such as PLGA have been shown to have cytotoxic effects *in vivo*[88]. Protein based biopolymers such as collagen and gelatin have great potential as they

have a similar structure to the natural human tissue. For these molecules, degradation rate is altered by precise chemical crosslinking as these crosslinks reduce the number of sites available for proteolytic degradation[88]. Crosslinking was also found to reduce the quantity of drugs released during the initial burst phase when using carbohydrate based polymers such as chitosan and cellulose[88]. However, bone cements were found to have better release profiles than bioceramic compounds as they did not exhibit this initial burst release and resulted in a more sustained and steady release profile[88].

These methods can prove complicated as it is necessary to design for the correct release profile, ensure the anti-inflammatory agent functions for the required duration and ensure sterilisation does not affect the activity of the drug[80].

2.6.5.6 Drug Choice and Effectiveness

The choice of anti-inflammatory drug or factor itself is another important consideration. Heparin, often used as an anti-coagulant, can reduce protein absorption and bind cytokines[61,80]. Alpha-MSH was shown to significantly reduce levels of pro-inflammatory TNF-α, increase those of anti-inflammatory IL-10 in stimulated human monocytes and reduce the electrodes electrical impedance[80]. It also inhibits neurotoxic NO production by microglia[8]. A study by He *et al* (2007) used a hetero bi-functional crosslinker to couple the α-MSH to the silicon surface and reduced the NO production by nearly 50% versus the control setup[8] and TNF-α expression was downregulated. Tissue response at 1 and 4 weeks was also measured by monitoring the level of ED-1 positive cells. The ED-1 immunoreactivity around the implant was measured as 67% less than that of implants without the α-MSH coating and the anti-inflammatory effect was still functioning after 4 weeks of tethering[8]. Microglial response monitored by GFAP was also statistically

significantly reduced after 4 weeks, as the α-MSH modulated the expression of inflammatory cytokines[8].

DEX is a strong corticosteroid which is regularly used to reduce inflammation in a variety of situations around the body. Increasingly it is being released from photocrosslinkable hydrogels in order to control the speed of release and aid the biocompatibility of the healing matrix[90]. For example, DEX was successfully incorporated into a photocrosslinkable hyaluronic acid which degraded in media. This degradation and release was tested on mouse macrophages was and shown to reduce levels of inflammatory markers TNF-α and IL-6[90]. This reduction in inflammation with DEX has also been shown in neural probe applications. A study by Zhong *et al* (2007) used a nitrocellulose based coating on silicon probes to deliver DEX and tested it on rat brains at 1 and 4 weeks[91]. It found that this attenuated the astroglial response and reduced neuronal loss but that EDI staining at 4 weeks was not statistically different, suggesting a stabilised inflammatory response by then[91]. It also ascertained that the drug could be released steadily for 16 days but could not determine the necessary duration for an effective treatment[91]. DEX loaded silicone microelectrodes were also shown to reduce insertion associated trauma in cochlear implanted after 3 months[92].

As well as strong nonsteroidal anti-inflammatory drugs, there is also increasing interest in releasing anti-inflammatory cytokines *in situ*. There has been a great deal of research into macrophages and their ability to polarise into anti-inflammatory M2 type macrophages or pro-inflammatory M1 macrophages, as well a range of other polarisations[93–95]. Microglia are widely viewed as the macrophages of the brain and as

such, several studies have also investigated and confirmed the similar polarising potential of microglia[18,96]. Primarily the positively polarising effects of cytokines has been studied on monocytes and macrophages, with IL-4 improving ratios of M2:M1 polarisation versus the negative control in a number of cases[97–99]. This implies that it has the potential to do the same with microglia but has yet to be extensively tested *in vitro* or *in vivo*.

2.6.6 Neuronal Cell Regeneration

It is well documented that neuronal cells do not regenerate readily like most other cell types. For this reason a lot of research focuses on preventing or limiting neuronal cell death rather than trying to regenerate neurons. However, a number of studies have investigated the possibility of using stem cells to regenerate neuronal networks when they have been affected by some sort of trauma. Jurga *et al* (2011) designed a laminin containing cryogel scaffold seeded with undifferentiated human blood cord derived stem cells which was implanted into Wistar rats[100]. These stem cells differentiated into full 3D neural networks consisting of both neuronal and glial cells[100]. They concluded that the optimum pore size was 80-100µm for neural tissue engineering as it gave enough space for cell expansion and network formation without being too large to make the necessary connections between cells[100]. The speed of degradation of the scaffold was also examined and it was found that a 10 fold increase in the crosslinking of the cryogels resulted in a roughly 80 fold decrease in degradation rate[100]. Although biodegradability of the scaffold is important, if it happens too quickly the breakdown products can be cytotoxic and the neural cells can lose their structural support for growth before they are well developed. In light of this, 0.3-0.5% crosslinking was recommended[100]. The laminin based cryogel scaffold was also found to elicit a very

limited glial response once implanted, limit scar tissue formation and actually attract neuroblasts which indicates good neuroregeneration[100]. However, it is important to note that these experiments were only carried out over 7 days, so any chronic immune response if these principles were applied to an electrode system could not be observed during these tests. A study by Koutsopolous *et al* (2013) compared the performance of neural stem cells (mouse-derived) depending on what they were encapsulated in. They found that their designer self-assembling peptide hydrogel scaffolds not only allowed the stems cells to differentiate into progenitor neural cells, neurons, astrocytes, and oligodendrocytes but also exhibited improved cell survival rates after 5 months versus encapsulation in matrigel or collagen (despite matrigel's improved performance over the first two weeks)[101]. They also highlighted that including the RGDS sequence in their hydrogels (a sequence thought to improve cell adhesion) did not have any significant effect on improving cell viability but did not do any statistics on whether they did indeed have a higher number of cells attached[101]. Although the chronic element of these experiments make them interesting, no tests have been carried out *in vivo* as of yet.

In conclusion, there are several key strategies being employed to reduce inflammation caused by current neural probes and electrodes. These include minimising the size of the probes to prevent acute inflammation, increasing the flexibility of the probe and using biomimetic coatings to reduce chronic inflammation of the tissue and to reduce damage due to micromotion. Incorporating drugs and anti-inflammatory factors into the coatings is also a promising area of research, with significant progress in reducing the acute inflammatory response but reductions in chronic inflammation are proving more

difficult. Based on this review, a section of this work will focus on the design of coating materials with adaptable topography and the potential for incorporated chronic drug delivery strategies.

2.7 Alternative Therapeutic Strategies

As well as working to reduce the brain's inflammatory reaction to current probes, investigating a different form of therapeutic probe that may elicit a reduced immune-response at the functioning tip may be advantageous. By utilising cooling rather than electrical stimulation to interrupt signals in the desired area of the brain, the formation of a glial scar could be reduced, allowing probes to function better long-term. Not only has electrical over-stimulation itself been highlighted as a potential cause of glial scarring[41], but the cooling effects of the therapy may also translate to less activation of glial cells around the functioning tip, allowing probes to be active for a longer period of time[102–105]. It has also been indicated that the severity of epileptic episodes could be connected to an increase in temperature in the brain, for which focal cooling would therefore provide additional benefits[106]. Induced epileptic activity in rats resulted in an increase of 0.65±0.22°C and a further 0.26±0.22°C when the level of anaesthesia was reduced.

2.7.1 Cooling Strategies

Vernon B Brooks was one of the first people to see the huge potential in cooling therapy electrodes and compiled a 109 page report detailing all previous experimental work that had been done, the history of cooling, the mechanisms of cooling and the potential applications[107]. He highlighted that the major advantage of any cooling therapy is that short term treatments are reversible and therefore it has no long-lasting ill effects on the brain tissue and that the major disadvantage is that it is hard to target one area without affecting the surrounding tissue too, however, this is also an issue with stimulating electrodes[107].

2.7.1.1 Surface and Cortex Cooling of the Brain

A study by Lomber *et al* (1999) investigated the usage of a cryoloop to deactivate brain function in cats and monkeys[108]. The loop functioned by delivering cooling via a methanol coolant and a double tubed structure so as only to cool the desired area. They found that it cooled brain tissue successfully to 20°C up to 2.5mm away from the loop and these devices were able to be implanted chronically and anchored using quick setting acrylic[108]. Whether the cooling was suppressing brain activity or not was measured by turning the cryoloops on and off and running a number of tests with the animals. Both monkeys and cats were unable to detect and orient towards a stimulus while the loops were activated and these results were found to be consistently reproducible up to 2.75 years after implantation[108]. However, the deepest tissue reached using these cryoloops was 2.5mm, still within the cortex, which would not suit the purposes of deep brain stimulation. Cerebral cortex cooling has also been tested in human trials and found to be safe and effective. Bakken *et al* (1999) found that cooling, using a cold saline input, could disrupt speech activity but that speech quickly returned once the cooling mechanism was removed[109]. They stated that the temperature needed to be reduced below 20°C to do so and this was achieved by keeping the saline below 3°C. In line with other studies they discussed the difficulty in cooling a region more than 4mm away from the probe and attributed the steep temperature gradient to the efficiency of the brains blood vessel system[109]. The study also highlighted that further work needed to be done to assess the difference between synaptic interruption using this method and the electrical stimulation method in order to ascertain whether they could be used interchangeably or not[109].It is also important to note that temperatures reported on the cortical surface are lower than those resulting in the brain, with

temperature increases of approximately 5°C below the superficial layers of the cortex[110]. A further study outlined the successful control of seizures in rat hippocampal brain slices with a temperature of 26°C.

More recently, cooling of the neocortex has been carried out in a range of animals from rodents to primates via a PDMS "cooling chip" with chilled ethanol circulating through silicone tubing[111]. They found they could drop the temperature in the brain by 17°C within 3min and control the temperature within 0.3°C using an implanted microthermocouple providing feedback. This temperature drop completely stopped neuronal function, which then returned once the cooling was removing, again demonstrating the reversible effects of this methodology. The chip was active in the animals for a 12 week period with no reduction in effectiveness over this time and the advantages in the small and lightweight nature of the chip was highlighted, however, the chilled ethanol needed connected to two reservoirs and passed through a dry ice bath which limited the movement potential of the animals[111].

A review by Rothman *et al* (2003) discussed the usage of focal cooling for neo-cortical epilepsy and explained that surgery often yields unsatisfactory results[112]. Tests have shown that focal cooling when applied immediately during a seizure in brain slice studies could reduce the seizure duration from 40s to below 10s and if such a system was coupled to a seizure detector it could potentially prevent seizures entirely, particularly important in areas of the neocortex that are viewed as essential whereby surgery would reduce patients' ability to function in some way[112]. Instead of using a coolant filled device like previous methods, the idea of a thermoelectric cooler (TEC) Peltier chip was

discussed as a viable option. These devices consist of two plates: one rapidly cooling and one rapidly heating once a current is applied, however, they require a heat sink attached to the hot plate to minimise the heating up of the cold plate. This could be problematic as extra hardware may be required but the idea of using the brains own blood system as a heat sink has been discussed[112]. In this solution, temperatures between 20 and 26°C were found to suffice to control seizures effectively, but had not been tested *in vivo*[112].

A further study used a Peltier chip with a 37°C liquid controlled heat sink attached to the hot side of the Peltier and it was able to reduce induced epileptic seizures in rats by reaching temperatures of 30°C 2mm into cortex and eradicate them entirely below 25°C[113]. It was noted that epileptic seizures actually limited the minimum temperature of the cortical surface to 23°C rather than 15°C as seizures increase the blood flow and the relatively high temperature of the cooling liquid through the heat sink was justified by planning to use cerebrospinal fluid to make the entire device implantable in the future, however, potential contact with a 60°C hot side plate would have to be carefully avoided[114].

2.7.1.2 Deep Cooling of the Brain

The same laboratory that carried out the cortical cooling of the rats brains[114] built upon this research by progressing to reducing hippocampal seizures using a silicone coated copper probe attached to a Peltier device[115]. This time they used 4°C circulating water as the heat sink and observed a drop in temperature to 9°C directly at the cooling tip 4mm into their agar gel model and a drop to 20°C within a 1.6mm radius in the rat brain at a similar depth. These temperatures were able to reduce seizures to 68% of their previous amplitude, but highlighted that the 60s required to reach target temperature

would not be enough to prevent seizures from happening based on forecasting EEG signals which could only give between 5-80s warning. They also highlight the need for a thicker or multiple probes in human applications as the hippocampal region for seizures is larger and at a greater depth[115]. The engineering challenge involved in human implications is to design a probe that can sufficiently cool the brain at depths of up to 10cm, as this is the approximate location of the subthalamic nucleus where DBS is normally carried out[28,116].

2.7.2 Cooling Probe Coating Design

A cooling probe requires a highly thermally insulating coating to ensure the length of the probe is properly insulated. This allows cooling to only be delivered at the tip rather than along the whole length of the probe and therefore also maximises the temperature drop in this region. As thermal conduction and insulation are dependent on thickness, in order to reach the temperatures required and cool only the desired brain region, these probes and their coatings will be thicker in nature than their electrically stimulating counterparts. As such, in order to design a functional probe that can be inserted into the brain without causing excessive damage due to its size, a range of materials should be carefully selected and designed.

Polymers are the most frequently selected coatings for electrically stimulating or recording probes, however, their thermal conductivity values vary considerably and not all are suitable for preventing conduction of heat along the length of a probe into the brain. For example, hydrogels mainly consist of water so their thermal conductivities are similar to that of water and are therefore unsuitable for use as thin thermal insulators. Other polymers such as polypyrole and PEDOT variations have thermal conductivity of 0.3W/mK and 0.2-0.4W/mK respectively[117,118]. One paper assessing cooling for epileptic

seizure treatments in rats utilised a silicone coating and highlighted that it is a useful material as it can be manipulated so that it is electrically conducting or insulating depending on the desired properties[115]. Its thermal conductivity ranges between 0.2-3W/mK depending on the exact form used. Alternatively, ceramics could also be utilised as thermal insulators. Hydroxyapatite's conductivity ranges between 0.08-0.18W/mK between 0 and 500°C[119] and the lower range of this end could provide adequate insulation without increasing the thickness of the probe to an unfeasible thickness for insertion into the brain. The induction of porosity into ceramic coatings, as well providing potential drug delivery applications as discussed earlier, could also decrease thermal conductivity further[120].

As well as considering the coating and its properties, it is important to consider how the coating can be best attached to the probe to ensure good stability and the desired surface topography. Electrodeposition is one of the most common methods of depositing a conducting polymer on a metal surface by using electrolysis of a solution to galvanostically grow the coating onto the surface of a conducting substrate. It means the thickness of the coatings can be carefully controlled by duration and current used for the process, but some delamination of coatings over time has been observed. One study addressed this problem by pre-roughening the metal substrate in order to get better attachment and found that PEDOT with various dopants adhered to electrodes better over time[52].

PDMS is the most widely used silicon-based polymer in biomedical applications due to its rheological properties – when initially mixed with its curing agent it is a liquid that can be poured or spin coated but if left for hours or subject to heat it will cure into a

hard flexible polymer. For these reasons it is often utilised in soft lithography and microfluidics[121]. PDMS is hydrophobic but after exposure to oxygen plasma, the surface develops hydrophilic silanol groups (Si-OH), allowing the creation of strong Si-O-Si bonds when brought into contact with another charged surface, leaving a covalently bonded system that is irreversibly sealed[122]. These methods are used both to bond PDMS to other PDMS surfaces or glass and could be utilised in a coating application to ensure adherence.

Many of the coating techniques applied in previous probes for polymers are not suitable for a ceramic based coating, but studies of other applications of ceramic coatings can be utilised. Two of the most common ways to apply a hydroxyapatite coating were investigated by Wang *et al* (2006)[123]: plasma spraying and electrochemical deposition (ECD). Plasma spraying involves melting a material at a very high temperature in a plasma jet before propelling it towards the surface to be coated, where it solidifies and forms a deposit. Electrochemical deposition involves electrolysis of an aqueous solution containing ions of the desired coating material which is then thinly deposited onto the surface of another material that makes up the cathode[123].

Plasma spraying is the most popular technology used commercially for coating implants with HA as it can provide thick coatings of up to several millimetres at a high deposition rate. However, the high temperatures used can damage the materials coated[123]. Electrochemical deposition on the other hand uses much lower temperatures and allows greater control of the coating's composition and structure by manipulating the electrolyte properties or current density[123]. This study also demonstrated a technique for calculating porosity and solubility of each surface using submergence in distilled

water and then measurement of calcium ion release from the coatings with a direct current plasma atomic emission spectrometer[123]. Plasma sprayed HA coatings were significantly rougher (R_a 1300nm v R_a 480nm) and had a higher bonding strength between coating and surface than electrochemically deposited HA. Plasma spraying also resulted in a large globule like surface rather than showing individual HA crystallites like electrochemically deposited HA. However, plasmas sprayed coatings dissolved much more readily as calcium ions reached saturation in distilled water after 2 days, whereas electrochemically deposited HA had low levels of calcium dissolved after 10 days [123]. The effects of these calcium ions on neural cells may determine which coating process is best for this particular application.

Electrophoretic deposition (EPD) is a process similar to electrochemical deposition, as it uses a flow of electric current to create a coating on an electrode. However, in EPD, the media between the two electrodes has a low conductivity creating an applied potential difference across the space between the electrode which drives the electric field and the migration of the ions. The main advantages of are EPD that it uses simple equipment, has short processing times and can be adapted for use with a large range of materials. A study by Moskalewicz *et al* (2013) used this method to coat a PEEK/Bioglass coating on a metal alloy followed by a sintering step (355°C) to improve adhesion to the substrate and to make the coating more dense[124]. It was found that the combination of these two methods resulted in a lack of shrinkage of the coating and therefore a reduction in brittleness, as well as providing suitable adhesion between the surfaces[124]. The best coating ratio (between PEEK/Bioglass) resulted in a uniform coating of approximately 40µm with open porosity with micropores of 2-30µm (average 18µm)

and an overall porosity of 28%[124]. A study by Eliaz *et al* (2005) compared the EPC and ECD process and the coatings they produced and concluded that they produced very similar microporous dense coatings with similar stabilities, though it did not discuss the thickness produced by either method[125].

Another method that could be used to coat a metal probe with a ceramic is pulsed laser deposition (PLD). PLD involves focusing a laser beam on a material in a vacuum. This material vaporises in a plume which can then coat a nearby surface. Carrado *et al* (2011) successfully employed this method in order to coat titanium substrates with an excellent adhesion between the surfaces[126]. It was observed that a there was a range of particulate sizes from 100nm to 1µm, which could result in a high roughness of the surface. A thickness of approximately 2µm was achieved[126]. These results were similar to another study that coated a titanium alloy with HA using different laser parameters and examined the effects these had on the coating produced [127]. This study also found that the resulting surface was rough (R_a up to 680nm) and the thicknesses ranged between 0.1 and 2.1µm due to this roughness. This range would have to be reduced in order to provide sufficient insulation or several layers added in order to thicken up the thin areas. Changing the laser parameters did not affect the morphology of the coatings significantly as all coatings consisted of a dense layer of HA formed by grains of different sizes[127]. However, lower deposition rates were found to give smoother surfaces and a low rate of 0.0043A/shot gave a coating that was 100% HA with no other calcium phosphate phases such as α-TCP present. This was attributed to the fact that low rates allow a greater incorporation of OH^- ions, which are present in HA but not in many other CaP phases[127]. Finally, a study carried out by Tucker *et al* (1996) compared PLD with

plasma spraying. It highlighted the advantages of PLD in controlling crystallinity and phase composition of the layers and being able to produce much thinner layers of HA[128]. It also carried tests to ascertain which coating method resulted in a lower ion release and found that during both pre-conditioning steps and once coated, the samples coated using PLD exhibited a much lower release of ions and a slower dissolution rate[128].

All of the above techniques can prove to be both complicated and expensive. A simpler method that can be utilised, particularly in early stage research, is dip coating, as it is quick, inexpensive and can easily coat complex structures[129]. Dip coating involves dipping the substrate in a solution of the coating material, air drying it to remove the solvents and create an initial thin layer of coating and normally a sintering step after this to fully form the layer[130]. It is this final sintering step that often causes problems, as high temperatures can cause shrinkage of the coating material and cracking of the coating[129]. However, some studies use a surface induced mineralisation technique, whereby the surface is modified to introduce surface functionalisation before dipping, allowing the whole process to be carried out at 25°C[131]. A study by Wheeler *et al* (1997) also showed the adhesion of these coatings to be comparable to those that were plasma sprayed *in vivo*[131]. Alternatively, the sintering temperatures can be kept relatively low and a study by Mavis *et al* (2000) showed that when sintering at 840°C, 25µm thick crack free adherent coatings could be achieved, with thicker coating obtainable by reducing dip rate or repeated dips[132].

2.7.3 Modelling of Thermal Conduction of Probe

In order to ensure sufficient cooling of the target brain tissue, it is important to first model the heat transfer of a potential probe *in silico*, the results of which can be

validated by an *in vitro* test. One study investigated the modelling of the cooling potential of a Peltier chip based device for both surface and deep brain region cooling using first principal heat transfer equations and analysing the effect of key variables on the device output using Matlab[133]. The forebrain of the zebra finch was cooled by 7°C via a Peltier thermoelectric device with an airbased cooling system on the hot side of the device, negating the need for liquid coolants or restrictive connective tubing[133]. Derived heat transfer equations describing the system were utilised to analyse and optimise the effects of variable parameters before validation experimentally. They highlighted the necessity for thermal probes to be thicker than electrical ones due to the conduction of heat being dependent by area and showed that increasing the diameter of the probe would increase the axial heat conduction but would reduce the thickness of the insulation as the total probe diameter is limited by the potential for tissue damage upon insertion, resulting in an optimum ratio of the two materials. They utilised a total geometry of 800µm consisting of a silver probe with a polyimide tube as coating with a layer of air in between due to its low thermal conductivity and found a probe that is roughly 2/3 the inner diameter of the tubing produced optimal cooling. For a distance 2mm into the brain, these devices were able to cool the tip of the probe by 11°C as a result of the 15°C temperature drop at the cold plate, however, the tissue was only cooled by 4°C 500µm away from the probe and showed very similar results to the mathematical model[133].

Although not studying the effects of a cooling probe in the brain, a study investigating potential heat effects of a standard DBS electrode also offers some alternative ideas on how to model the potential heat transfer of a system *in vivo.* By utilising Comsol® to

design a 2D axisymmetric model of a DBS probe, the joule heating observed when an electric current was applied to the system was analysed. High levels of stimulation, defined as 10V for 21ms, were found to cause an increase in temperature of up to 0.8°C[134]. This model also incorporated the heat effects of blood flow to the brain and metabolic activity via a bio-heat transfer model equation, which increases similarity of the model to the actual brain environment. However, the model was never validated experimentally.

2.8 *In vitro* and *in vivo* Evaluation Strategies

In order to test the viability of any coating materials or design features of a neural probe, a number of tests have to be carried out and the results from these analysed and brought to a conclusion to guide the next stages of investigation. In this section a variety of common techniques and their usefulness will be evaluated in order to aid the planning of a good methodology.

2.8.1 Cell Types

When looking at the biocompatibility and immune response of cells there are a number of stages in the investigation process to be followed. *In vitro* tests are carried out first as they are quicker and easier and are good for screening large number of potential solutions. However, they can also prove to be limited and *in vivo* trials are the next stage in reaching clinical trials. Within both these categories there are different models and strategies for investigating cell response with a variety of success.

2.8.1.1 Cell Lines

PC12 cells are a cell line derived from rats' adrenal glands that have been found to behave like neural cells once NGF is added to allow neurite outgrowth. The advantage of using a cell line is their ability to proliferate so that as many cells as necessary can be produced. These can then also be stored as frozen cells and thawed when required rather than needing to be freshly harvested for every trial. PC12 cells terminally differentiate once nerve growth factor has been added. They are used regularly when looking at neural applications but with a range of levels of success. A study by Yao *et al* (2008) successfully used PC12 cells to show the inclusion of a peptide motif from laminin on a scaffold in a high concentration encouraged neurite growth towards it but did not affect the neurite length as predicted[135]. A second study by the same group was able to

use PC12 cells and their NGF aided neurite outgrowth to determine the effect of nanopatterning of PLGA surfaces[136]. They determined that patterning aided early guidance and that there was improved growth on the laminin peptide coated grooves than the collagen coated ones and smaller grooves showed significantly more parallel growth of neurites[136]. However, a number of papers have reported difficulty and inconsistency in neurite outgrowth from PC12 cells which is not helped by the huge variability in types and concentrations of NGF used between experiments. There is also a lack of studies that have followed up their initial PC12 tests with corresponding results using primary neuronal cells or in vivo studies. A study by Kajiwara *et al* (2008) investigating the attachment of neural cells to peptides, showed that although PC12 and hippocampal neural cells showed increased attachment with one sequence, another sequence significantly affected PC12 cells but not hippocampal neural cells[137], indicating that using PC12 cells may increase the risk of false positives from experiments.

Another useful cell line may be THP-1 cells: a human monocytic cell line derived from a leukemic patient which can differentiate into macrophages. As microglia are difficult to harvest and purify, these macrophage cells can be utilised as a model as they perform similar duties outside of the brain[138]. Both macrophages and microglia have the ability to differentiate into M1 pro-inflammatory or M2 anti-inflammatory phenotypes depending on how they are stimulated which makes monocytes a useful model for investigating the effects of a drug delivery profile on the brain[18,139,140].

2.8.1.2 Primary Neural Cells

Primary neuronal cells can also be harvested from animals and used in *in vitro* studies. This is primarily performed using rats but the methods of extraction vary and the age

and type of rats also varies considerably. Polikov *et al* (2006) utilised neurons which had been mechanically dissociated from the midbrains of day 14 Fischer 344 rats and obtained results which correlated well to results found *in vivo* and outlined the idea that this could be a standard procedure for *in vitro* trials in order to obtain more comparable results between different labs[2]. However, studies by Thompson *et al* (2011) using 4-6 day old pregnant Albino Wistar rats and Hogberg *et al* (2011) using embryonic 16-18 day rats indicate that these attempts at standardisation have not been implemented[15].

As discussed previously, astrocyte and microglia activation are key stages in the inflammatory process and when studying chronic inflammation of the tissue a concern is how to keep primary cells alive for extended periods of time. Incorporating astrocytes into 3D hydrogel models allows them to form networks and function as they would *in vivo* and could allow the cells to survive for longer and act in a more representative way of how they would in the body. One such study incorporated astrocytes into a hydrogel consisting of collagen, hyaluronic acid and matrigel and found that astrocytes exhibited similar amounts of glial fibrillary acidic protein (GFAP) to those in their resting state in the brain but did not determine how they behaved after more than 24hr[141].

An interesting experiment by Ereifej *et al* (2013)[59] conducted an in vitro test using brain slices cut from post-natal 5 day old Sprague-Dawley rat pups which were kept alive using media, an experimental design that could provide a more accurate picture of what would actually happen *in vivo*.

2.8.2 In vivo methods

Once prototype electrodes are created, these are normally tested *in vivo* in a variety of animals. The most common of these is rats, due to the similarity of the rat's brain to a

human brain, although the small size can lead to issues of scale[67,91,142–145]. Other rodents such as guinea pigs have also been utilised[48] or small mammals like cats or pigs[35,38,108] with a final stage before clinical trials using monkeys[14,70,108].

2.9 Conclusion – Emerging Research Questions

The academic literature examined in this chapter has provided a number of important insights. It is clear from the studies examined, that the formation of a glial scar around neural probes is widely accepted as the main cause of long-term failure of these probes, either due to the acute injury resulting from the insertion of the probe or in the longer term, chronic inflammation of the tissue, damage caused by micromotion, repeated electrical stimulation of the tissue or a combination of these. Academic research undertaken so far has focused on reducing the inflammation of neural tissue by reducing the size of electrodes, increasing their biocompatibility and incorporating anti-inflammatory factors into their coatings, measures which have achieved some success in reducing inflammation in the short-term (acute) phase, but with few long-term (chronic) benefits apparent. This lack of longer term benefits underpins the rationale for designing a probe coating capable of delivering anti-inflammatory factors to the brain for weeks rather than days in order to mitigate this chronic response of the brain tissue. A microfluidic design is proposed as the best method to ensure long-term administration of factors and will be the subject of rigorous investigation as part of this study.

In addition to this, the review of academic literature highlights that while only a limited amount of research has been undertaken on an alternative therapeutic strategy using focal cooling rather than electrical stimulation, it has the potential to interrupt brain signals in a reversible way without long-lasting damage and to reduce inflammation *in situ* at the functioning tip. This provides the rationale for investigating the possibility of developing a focal cooling probe as a clinical solution to reduce inflammation of brain tissue around the functioning tip, as this would allow improved patient outcomes long-

term. In particular, it is important to note that although several studies have achieved promising results *in vivo,* these have been carried out in small animals where the target zone is only a few mm below the surface of the brain. Achieving a therapeutic temperature drop in human patients approximately 10cm deep in the brain, whilst trying to keep the probe a viable diameter for clinical applications, is a significant challenge. For this reason, highly thermally insulating materials such as HA and PDMS will be investigated as potential coating materials for a cooling probe. These also have the added benefit of controllable surface topography to further reduce inflammatory response of brain tissue. HA is not traditionally used in neural applications so the interaction between it and the various neural cell types will need thoroughly assessed.

Two key issues therefore emerge from the literature review: firstly, the absence of longer term benefits from interventions based on smaller electrodes, electrodes with increased biocompatibility or with anti-inflammatory factors incorporated and secondly, the challenges of bringing about a significant temperature drop deep in patients' brains. In response to these two issues, the **hypothesis** for this study is two pronged:

1. *The development of a drug delivery system capable of releasing anti-inflammatory factors chronically from a probe will reduce the inflammatory response of the brain against an inserted therapeutic probe and therefore reduce the formation of scar tissue and extend the efficacy of the probe.*
2. *By utilising highly thermally insulating coatings with a controllable topography, a probe using cooling as its therapeutic action up to depths of 10cm can be*

designed as a viable clinical alternative to electrical stimulation, again reducing the inflammatory response of the brain to the probe.

In addition, it is hypothesised that integrating these two strategies will bring about a long-term reduction of inflammation of the brain following the insertion of such a therapeutic probe.

This chapter has examined the current literature on neural probes utilised for chronic implantation. It has indicated that there are a number of significant knowledge gaps in this field, gaps which in turn provide opportunities for further productive research. These are summarised below in the form of specific research questions that will be explored during the course of this thesis.

1. What are the effects of HA on neural cells and can the control of its topography reduce inflammation?
2. Which cell models are most appropriate for predicting cell immune response to probe coatings for chronic studies?
3. How can a coating best deliver anti-inflammatory factors to neural tissue chronically?
4. Can the long term delivery of these anti-inflammatory factors reduce the immune response of neural cells in an *in vitro* model?
5. How can a Peltier cooled device be optimised to maximise focal cooling in the brain?
6. What probe dimensions are required to deliver therapeutic cooling with a HA/PDMS coating and what are the clinical implications?

This literature review has assessed the current state of the art neural electrodes and their limitations and highlighted the evidence for the failure of these electrodes long-term being due to the formation of a glial scar around the implant. It has summarised

research undertaken to prevent the formation of this glial scar by reducing the brain's inflammatory response to the probes and documented the successes and failures of these attempts. This has formed the basis for the suggested research areas, the two pronged hypothesis guiding this research and the associated key research questions that need to be answered in order to achieve the thesis's overall aim of developing a functional neural probe with the potential to reduce inflammation of brain tissue post-implantation. Chapter 3 will address research questions 1 and 2 in order to assess the suitability of HA as a coating material for neural probes, investigate the effects of adaptable surface topography on neural cells and analyse the strengths and weaknesses of different cell models to predict this behaviour.

3 PC12 Cell, Primary Cortical Neuron and Astrocyte Response to Surface Topography of Coating Materials for Neural Probes

3.1 Introduction

Although the potential of cooling therapy using neural probes was first highlighted in the 1980s[107], electrical stimulation became the forerunner in the field and more in depth investigations into the cooling possibilities stopped. Since then, a number of studies have re-evaluated the idea but these have mainly focused on surface cooling devices rather than deep brain stimulation (DBS) type applications. For example, a study by Lomber *et al* (1999) used a cryoloop with cooling methanol to deactivate brain function in cats and monkeys[108]. However, the deepest tissue reached using these cryoloops was 1.5mm, still within the cortex which would not suit the purposes of DBS. Cerebral cortex cooling has also been tested in human trials and found to be safe and effective. Bakken *et al* (1999) found that cooling, using a cold saline input, could disrupt speech activity but that speech quickly returned once the cooling mechanism was removed[109]. In line with other studies they discussed the difficulty in cooling a region more than 4mm away from the probe and attributed the steep temperature gradient to the efficiency of the brain's blood vessel system[109].

With cooling efficiency being of the utmost importance, particularly at the depths of around 10cm to reach the subthalamic nucleus[116], the thermally insulating coating is a critical element of the design. Polymers are the most frequently utilised coatings for electrically stimulating probes, including polypyrole, poly(ethylenedioxythiophene) (PEDOT), polyvinyl alcohol (PVA), polyethylene glycol (PEG) and polydimethylsiloxane (PDMS) and their usability in neural applications has long been established[9,10,47,51,59,146].

However, their thermal conductivity properties are often higher than desired. For example, Tanaka *et al* (2008) conducted an experiment to assess the potential of a silicone coated cooling probe in rats and found temperatures of 20-25°C reduced all epileptic seizures[115]. Silicone's thermal conductivity ranges between 0.2-3W/mK depending on the exact form used but could be too high to ensure sufficient insulation for a probe long enough for insertion into the human brain as only depths of 2.5mm were required for the rats[115]. PDMS is often used in bioengineered constructs and its thermal conductivity ranges between 0.15-0.2W/mK which could be low enough to offer the required thermal insulation[147–149].

Hydroxyapatite's (HA) conductivity ranges between 0.08-0.18W/mK[119] which has potential to sufficiently insulate a cooling probe. It is regularly used in orthopaedic implants[125] due to its similarity in composition to natural bone but is not traditionally used in neural applications. Nevertheless, it was selected for further investigation because of its excellent thermal properties, biocompatibility (in orthopaedic applications), controllable porosity and controllable surface roughness. For this reason, before probe design and coating optimisation, the interaction of HA with neuronal cell cultures had to be assessed – firstly for cytotoxicity and then to optimise the survival of neurons and to reduce the activation of glial cells. Topography of surfaces is often used to manipulate neuronal cell survival[52,59,150] and HA's is easily adapted via coating methodologies and sintering regimes, also making it a good substrate to initially investigate the effects of this *in vitro*. Previous studies have indicated that the traditional methods of quantifying surface roughness do not capture these topographically caused differences in cell response well and proposed a wavelength method of describing

surface roughness[151]. For this reason 3 different surface roughnesses are described by their pressing and sintering conditions and resulting surface as an initial screening methodology. By testing the HA's reaction to a range of different cell lines and primary neuronal cells, the suitability of each cell methodology for predicting the brain's immune response to materials could also be assessed and a recommended cell testing regime established. The experimental plan to do this is outlined in the flow chart below.

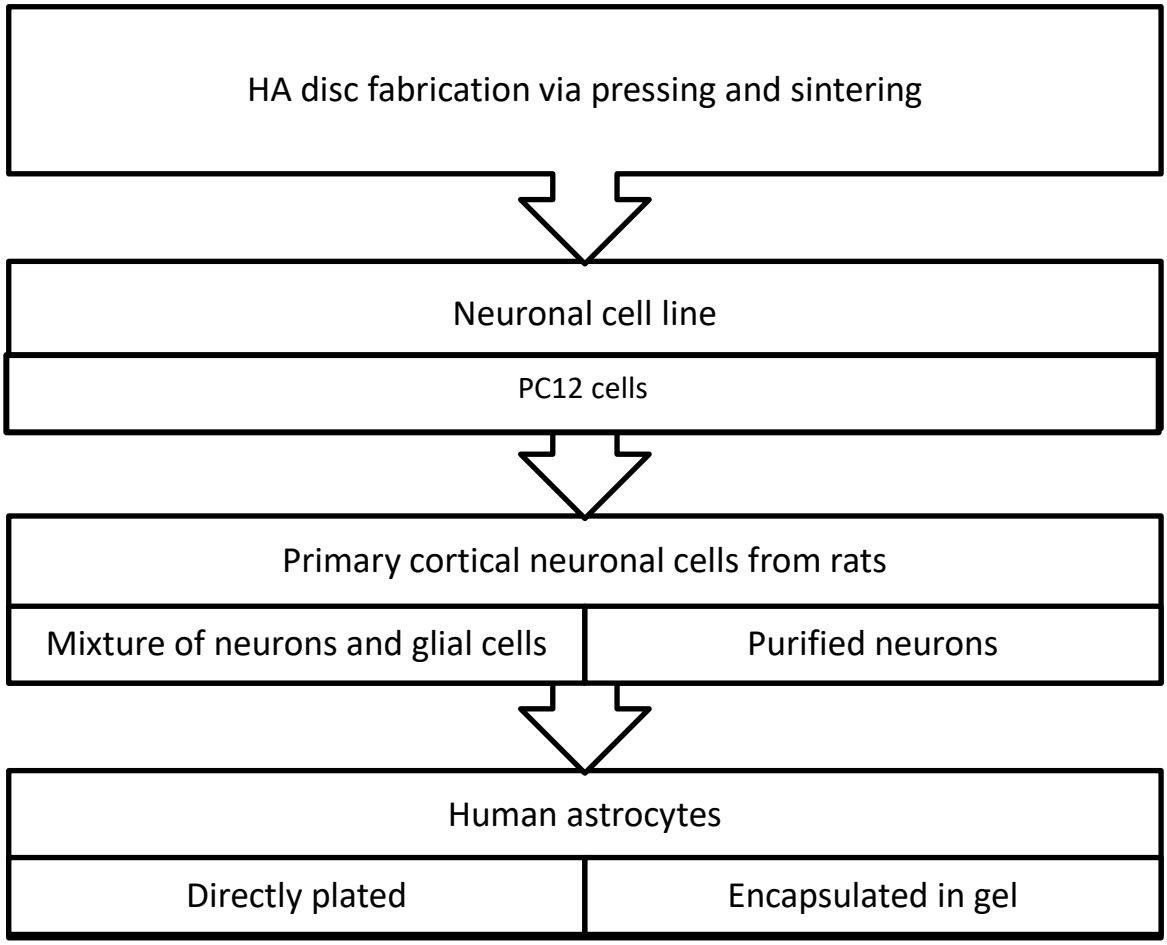

3.2 Methods

3.2.1 HA Disc Manufacture

HA discs were manufactured by compressing 200mg of HA powder (reagent grade, Sigma Aldrich) in a 13mm diameter die (International Crystal Laboratories, Garfield, NJ) under a 2kg weight for 2min (0.46 MPa/67psi). These discs were sintered for 3hr at either 1200°C or 1350°C to produce 2 different surface roughnesses (1200R and 1350R). Smooth HA discs (1350S) were formed by compressing the die under a pressure of 1.4MPa (200psi) for 2min before sintering at 1350°C. All design temperatures were attained using a heating cycle with a ramp of 3°C/min and an initial 1hr dwell phase at 250°C was used to burn off any organics.

3.2.2 Cell Culture

3.2.2.1 PC12 Cells

Cells were cultured for 7 days from frozen in DMEM media (+glutamax)(Sigma Aldrich) supplemented with 10% heat inactivated Horse Serum (Sigma Aldrich), 5% Fetal Bovine Serum (FBS) (Sigma Aldrich) and 2% penicillin-streptomycin (Sigma) at 37°C in a humidified 5% CO_2 environment.

3.2.2.2 Primary Neuronal Cells

Primary cortical neurons and glial cells were prepared from 1-day-old Wistar rats and maintained in neurobasal medium (Sigma Aldrich). Rats were decapitated, the cerebral cortices dissected and the meninges removed. The cortices were incubated in phosphate-buffered saline (PBS, Sigma Aldrich) with trypsin (0.25 μg ml^{-1}, Sigma) for 3min at 37°C. The cortical tissue was then triturated (× 3) in 6ml of Dulbecco's Modified Eagle Medium (DMEM, Sigma Aldrich). The suspension was centrifuged at 2000RPM for 3min at 20°C and the pellet resuspended in 5ml of DMEM and triturated (x3). The

suspension was passed through a cell strainer before centrifuging again at 200RPM for 3min at 20°C. The pellet was resuspended in 5ml of DMEM and triturated (x3) so that cells were ready for plating.

3.2.2.3 Human Astrocytes

Primary human astrocytes (ScienceCell) were cultured in suspension for at least 7 days before use in media (DMEM:F12 with L-glutamine + HEPES, Thermoscientific) supplemented with 10% FBS, 10% Astrocyte Growth Supplement (ScienceCell) and 1% Penicillin-Streptomycin (Sigma Aldrich) at 0.5-2 million cells/ml media. Cell media was changed at least every three days, retaining 50% of the old media.

3.2.3 Cell Plating

All discs were placed in 24 well plates and 100,000 cells were added in 50µl of relevant media (see above) with 10ng/ml of nerve growth factor (NGF, Sigma Aldrich) included for PC12 cells. A further 250µl media was added after 3hr to flood the wells. For primary neuron only culture, 20µl/ml cytosine beta-D-arbinofuranoside (Ara-C, Sigma) was added to media for first 3 days of culture. Circular 10 mm diameter coverslips were coated with poly-L-lysine (50 μg ml^{-1} Sigma). These glass coverslips, coated with Poly-L-lysine, were used as a positive control with uncoated ones used as the negative control. The coating procedure added sterilised coverslips to poly-L-lysine and di-ionised (DI) H_20 solution and incubated them in a humidified atmosphere containing 5% CO_2 : 95% air at 37°C for 2hr. Once they were removed from solution they were left to dry on filter paper for another 2hr.

3.2.4 Metabolic Assays

A 0.01% resazurin solution was made up by mixing 50mg of resazurin powder (Sigma) with 50ml of DI H_20. This was sterile filtered and stored at 4°C. All media was removed

from samples and 270µl of warm media and 30µl of resazurin solution were added. Well plates were returned to the incubator (5% CO_2:95% air at 37°C) for 2hr. Colour change was measured using a Gen5 Microplate Reader (Biotek). The plate reader measured the fluorescence of each sample using an excitation filter of 530/25 and an emission filter of 590/35. The percentage reduction of each sample was calculated versus a sample that was completely reduced in the autoclave.

3.2.5 GelMA Fabrication

Gelatin from porcine skin (Sigma Aldrich) was melted in 100ml PBS (10%w/v) at 50°C and continuously heated at this temperature and stirred with a magnetic stirring bar at 240RPM for 1hr. The slow addition of 8ml methacrylic anhydride (Sigma Aldrich) followed and the emulsion was stirred and heated under the same conditions for a further 2hr. After this time, 100ml of preheated DPBS was added and further mixed at 50°C in order to stop the reaction. Dialysis membranes (Spectro/Por membrane tubing MW 12-14000, Fisher Scientific) were cut into 20cm lengths and tied at one end before the addition of the mixture and sealing of the open end. These tubes were transferred to a 5L beaker of distilled water and heated to 40°C to allow dialysis to occur. Water was changed twice daily for 7 days and the tubes were inverted several times to homogenize content. On day 7, the contents of the tubing was added to 200ml of ultrapure water and heated for 15min at 40°C, before filtering the solution using a vacuum filtration cup with 0.22µm pores (Millipore). This solution was transferred into 50ml falcon tubes in 30ml batches and cooled to -80°C before freeze drying for 5days.

3.2.6 Astrocyte Encapsulation

Astrocytes were capsulated in 5% GelMA with 0.1-0.5% photoinitiator (2hydroxy4(2hydroxyethoxy)2methylpriopiophenone 98%, PI, Sigma Aldrich) in PBS at a

density of 1 million cells/ml. These solutions were crosslinked using UV light at an intensity of 6.9 mW/cm^2.

3.2.7 ELISA Assays

TNF-α and IL-6 sandwich ELISAs (R&D systems) were carried out according to instructions. Briefly, 50µl of assay diluent and 200µl of sample were added to each well and left for 2hr. Following 4 washes with the wash buffer, 200µl of either TNF-α or IL-6-conjugate was added to each well and left for a further 2hr period. After another wash cycle, 200µl of the substrate solution was added and left for 20min before the stop solution was added and the assay was measured at 450nm and 540nm using the plate reader.

3.2.8 Statistical Analysis

All data is expressed as mean±standard deviation. T-tests or 2 way anova tests were performed where appropriate with $p<0.05$ being viewed as significant. These tests were carried out both on the individual timepoints for each test but also on the regression lines in order to analyse the trends over 7 days to allow more robust conclusions to be drawn from the study.

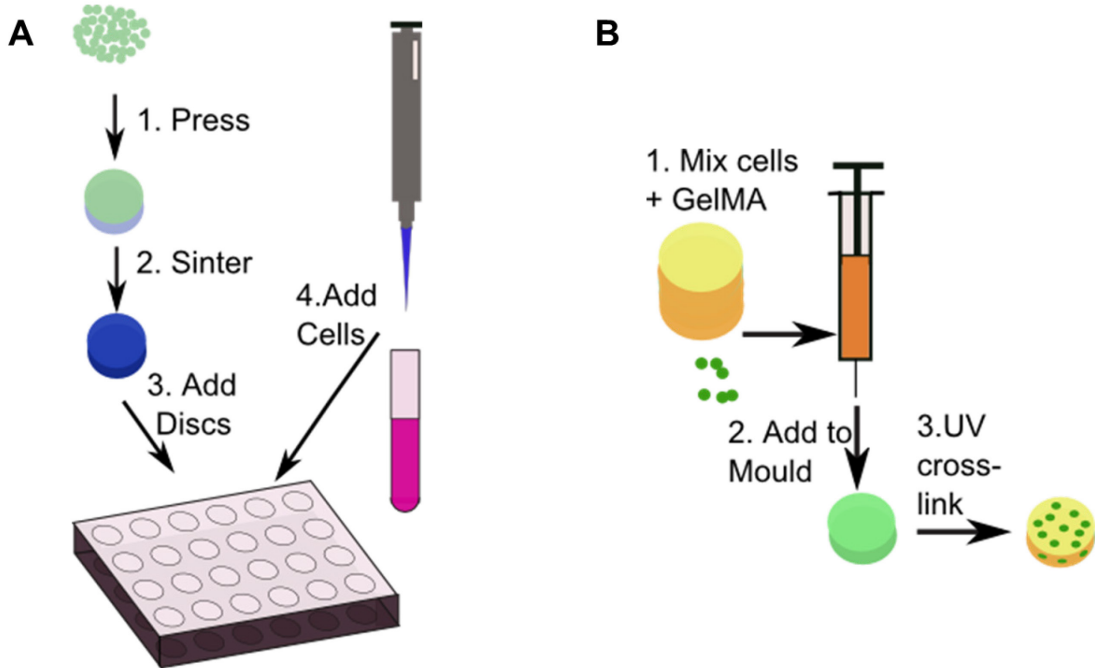

Figure 3.1. Schematics showing the A) fabrication of HA scaffolds via pressing and sintered before addition to the 24 well plate; B) encapsulation of cells in hydrogel.

3.3 Results

3.3.1 Disc Fabrication and Manipulation of Surface Roughness

SEM images were taken to analyse the different roughnesses created by pressing the HA powder at different pressures and sintering at different temperatures (Fig. 3.2).The hard-pressed and sintered at 1350°C discs (1350S) were clearly the smoothest surface with only minor cracks of less than 1µm interrupting the flat surface (Fig. 3.2A and D). Light pressing and sintering at 1350°C (1350R) produced a moderately rough surface with a much higher number of cracks and large surface features of up to 20µm (Fig. 3.2B and E). As expected, light pressing and sintering at 1200°C (1200R) produced the roughest surface with no smooth areas and a large number of small surface features of 1-2µm (Fig. 3.2C and F). A previous study analysed the traditional surface roughness values for these samples and attempted to correlate them with mesenchymal stem cell attachment and survival[151]. Ra values are calculated as an average surface roughness and did not capture the differences between surface profiles accurately, resulting in a lack of correlation between the values and cell attachment and survival – despite trends that were visible to the eye. However, the surface wavelengths of each disc were measured and showed a clear progression from rougher surfaces sintered at lower temperatures to smoother surfaces at higher temperatures. These measurements, did then in fact correlate with cell survival and attachment, implying that these are a more accurate representation of a surface roughness. These wavelengths were measured as 2.85µm, 2.68µm and 2.30µm for 1350S, 1350R and 1200R respectively[151].

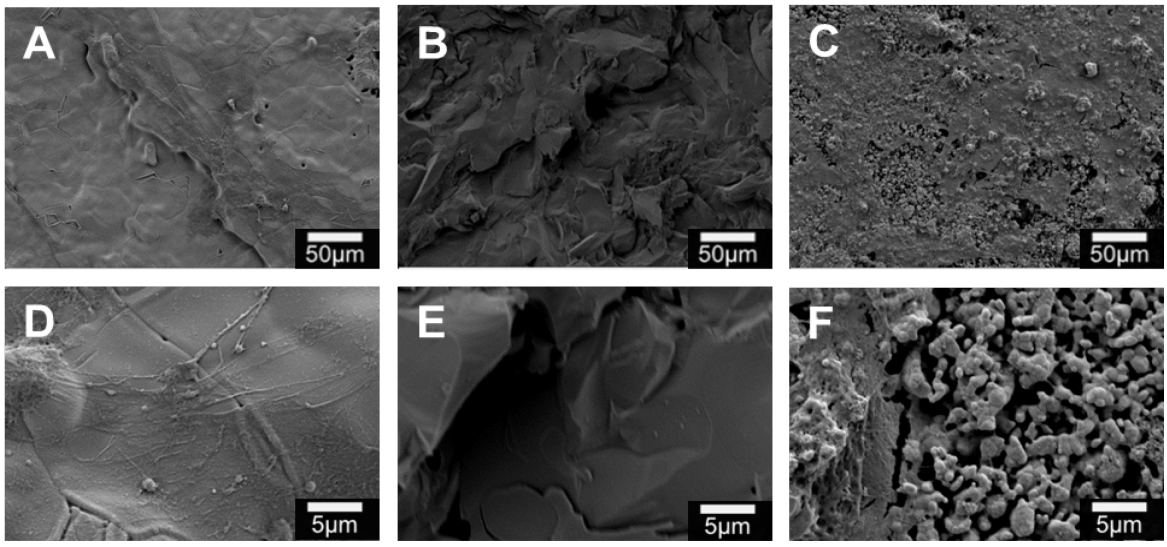

Figure 3.2. SEM images of HA discs created at different pressures and temperatures to produce different roughnesses. A) Hard pressed and sintered at 1350°C at 1000x; B) light pressed and sintered at 1350°C at 1000x; C) Light pressed and sintered at 1200°C at 1000x; D) Hard pressed and sintered at 1350°C at 6000x; E) Light pressed and sintered at 1350°C at 6000x; F) Light pressed and sintered at 1200°C at 6000x.

3.3.2 PC12 Cell Study

PC12 cells attached to each of the three surfaces were counted (via metabolic activity) at day 1, 4 and 7 in order to analyse cell interaction with the different surfaces over time.

Of the three materials, the moderately rough surface 1350R showed the highest cell count and was not significantly different from the positive control at day 4 (Fig. 3.3). 1350S has the next highest count, with significantly higher cell numbers than that of the negative control or 1200R at days 4 and 7. On day 4, 1350R was statistically the same as the positive control, 1350S was lower than the positive control but higher than negative control and 1200R was lower than the negative control. On day 7, 1350R was worse than the positive control but better than 1350S with 28% of metabolic activity vs 41% and 24% respectively. 1350S was statistically better than the negative control (5%) which was the same as 1200R (7%).

The comparison of the regression lines over the week corroborated the timepoint findings. As expected, the positive control had the best increase in number of attached cells over time as it had the highest gradient and therefore increase in cell count but the difference between it and the next best material 1350R was not statistically significant(p=0.25) (Table 3.1). 1350S had significantly less cell survival and attachment than both 1350R (p=0.04) and the positive control (p=0.03) but more than 1200R and the negative control which were statistically the same over the whole time period (p=0.51).

3.3.3 Cortical Neuronal Cell Study

On day 4 and day 7 the positive control had the highest number of cells attached and the 1200R had the lowest (Fig. 3.4). On day 4, 1350S, 1350R and the negative control were not significantly different but by day 7, 1350R was significantly better than both the 1350S and the negative control with 33% metabolic activity versus 30% and 29% respectively. The trendline analysis confirmed these results – the positive control had the most attached cells and the 1200R the fewest and 1350R, 1350S and the negative had the most attached cells and the 1200R the fewest and 1350R, 1350S and the negative control were all statistically the same (Table 3.1). Despite not being significantly different, 1350R still exhibited the best results of the three HA samples, results consistent with those shown using the PC12 cells.

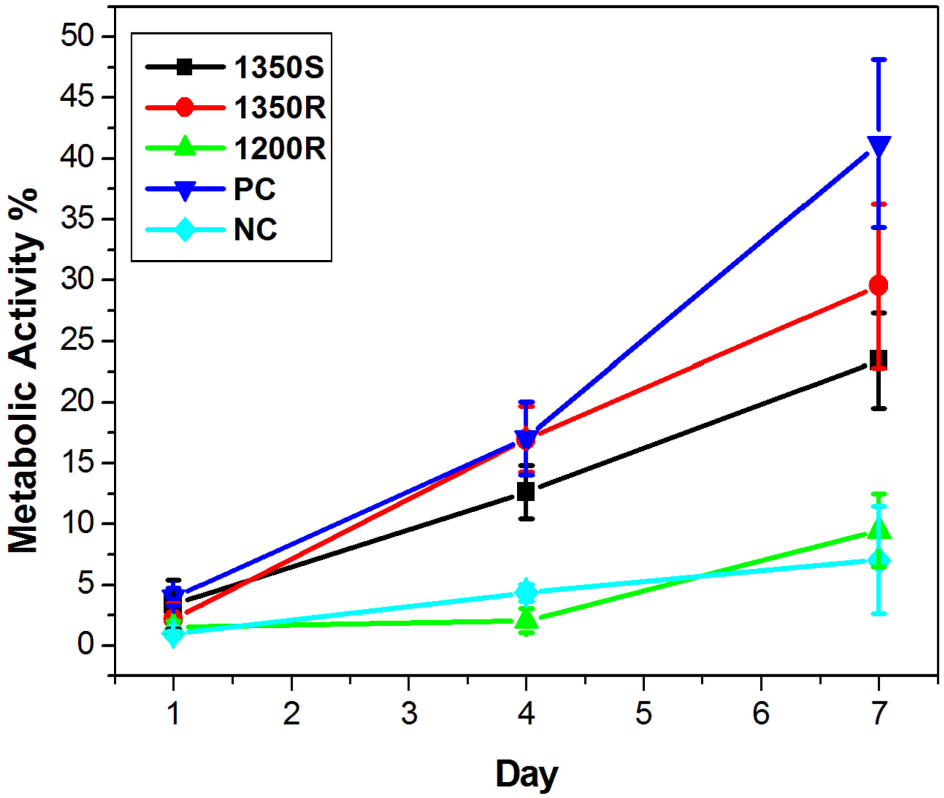

Figure 3.3. Measured metabolic activity of attached PC12 cells on 1350R, 1350S, 1200R surfaces at Day 1, 4 and 7 showing 1350R with significantly the highest metabolic activity % of the 3 HA discs (n=4).

Table 3.1. Table showing the gradient and standard deviations of the trend lines for each roughness and cell type.

Material	Neuron and microglia gradient	PC12 gradient	Neuron only gradient
1350S	4.34±0.21	3.42±0.23	-0.09±0.02
1350R	4.44±0.20	4.19±0.36	0.10±0.05
1200R	0.69±0.11	1.25±0.20	0.39±0.08
PC	6.49±0.29	5.56±0.67	0.05±0.06
NC	4.38±0.20	1.02+0.29	-0.16±0.07

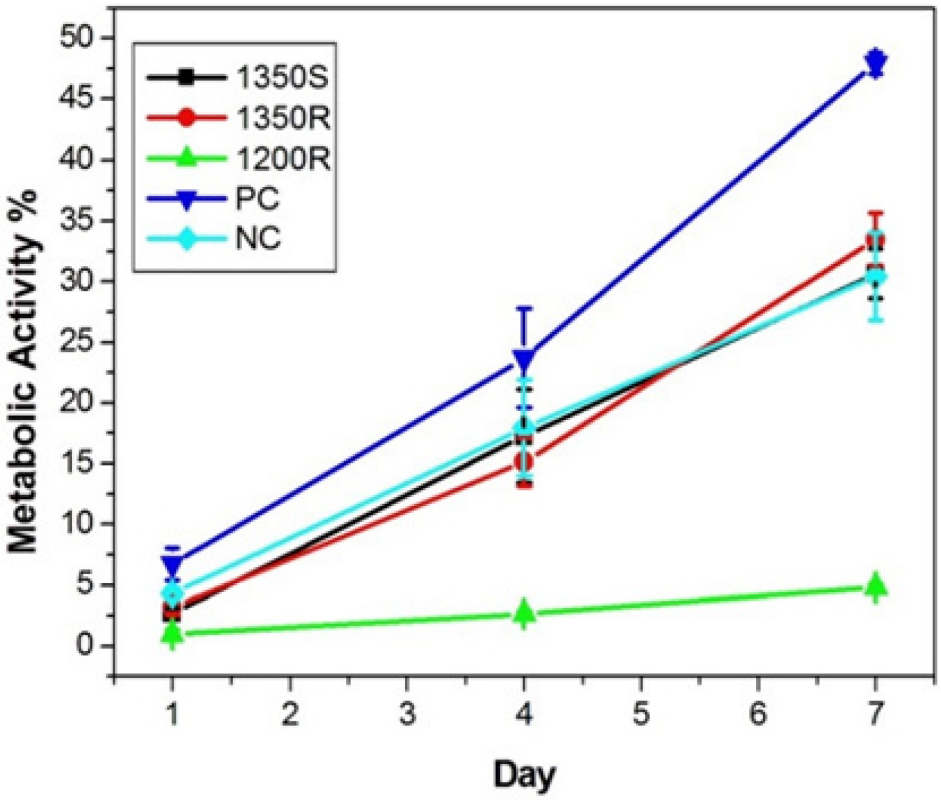

Figure 3.4. Measured metabolic activity of attached glial cells on 1350R, 1350S, 1200R surfaces at Day 1, 4 and 7 showing 1350R with the highest metabolic activity at Day 7 (n=4).

A culture of purified neurons was created by adding Ara-C to destroy glial cells by blocking their ability to proliferate[152]. This was done after plating as primary neurons do not survive if left in suspension. This meant that the effective day 0 (once Ara-C media had been removed and replaced by normal media) commenced with each disc having a different initial number of cells. For this reason, all subsequent measurements have been normalised to the day 1 results (Fig. 3.5A). On both day 4 and 7, 1200R showed the best cell attachment, with 1350R and the positive control performing next best at day 7 while being statistically the same. Also on day 7, the negative control showed the lowest number of attached cells and 1350S the second lowest as both of these decreased vs their day 4 results. When looking at the trendlines, the best performer was significantly

1200R; 1350R showed the second best attachment and was not different from the positive control, whereas 1350S showed a reduction in attachment and was not different from either the positive or the negative control which also had a negative gradient and performed the worst. These results contradicted PC12 and neuronal mixture findings as it implied that the rougher the surface the more likely the primary neurons are to attach to the surface. However, the non-normalised data also provided some useful information (Fig. 3.5B). The apparent strong increase in neuronal cell attachment is actually a result of very few cells being attached at effective day 0 – so a small increase in cell attachment appears larger proportionally. In fact it is clear that 1350R once again performs similarly to the positive control with a greater initial amount of surviving neurons attached on effective day 1 and a small increase towards day 7. As shown in the normalised graph, 1350S has a decrease in cells between day 1 and 4 but still has cell levels just below those of 1350R and the negative control.

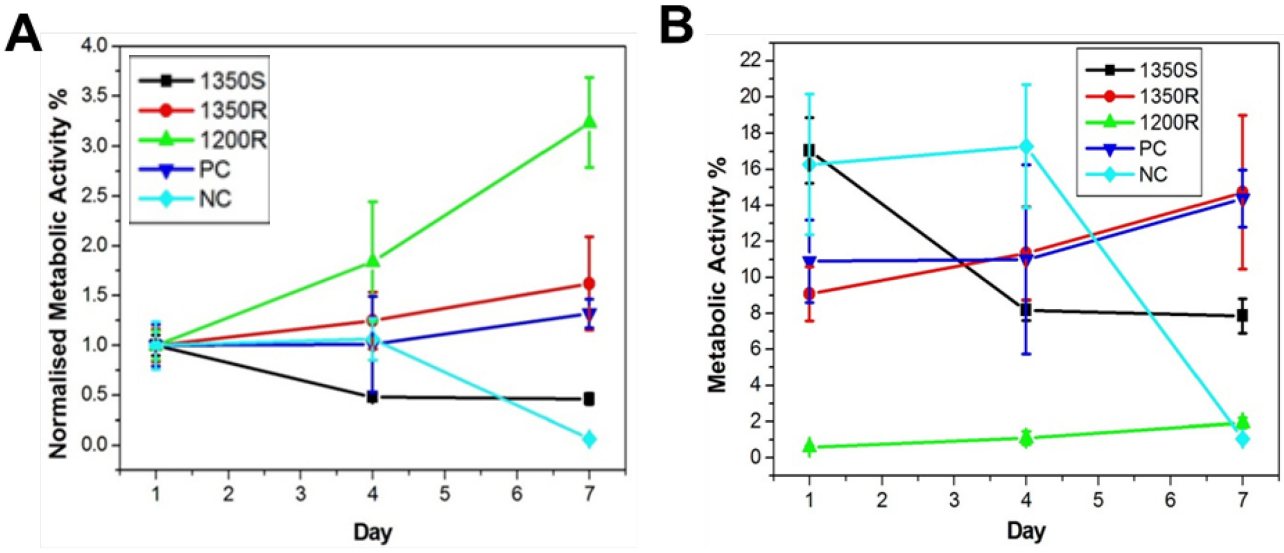

Figure 3.5. Measured metabolic activity of attached cells on 1350R, 1350S, 1200R surfaces at Day 1, 4 and 7 A) Isolated primary cortical neurons (normalised to day 1) (n=4); B) Isolated primary cortical neurons unnormalised (n=4).

3.3.4 Direct Astrocyte Culture

Confocal microscope images were taken at day 7 in order to examine the health of the astrocytic cells. As the HA is opaque and has a rough surface, the images were less clear than normal (Fig. 3.6). However, it is still possible to see that on 1200R surface (Fig. 3.6), cells are fewer and less healthy than those on 1350R (Fig. 3.6B) and 1350S (Fig.3.6C) surfaces, where cells are more plentiful with better networks, particularly on the 1350R surface.

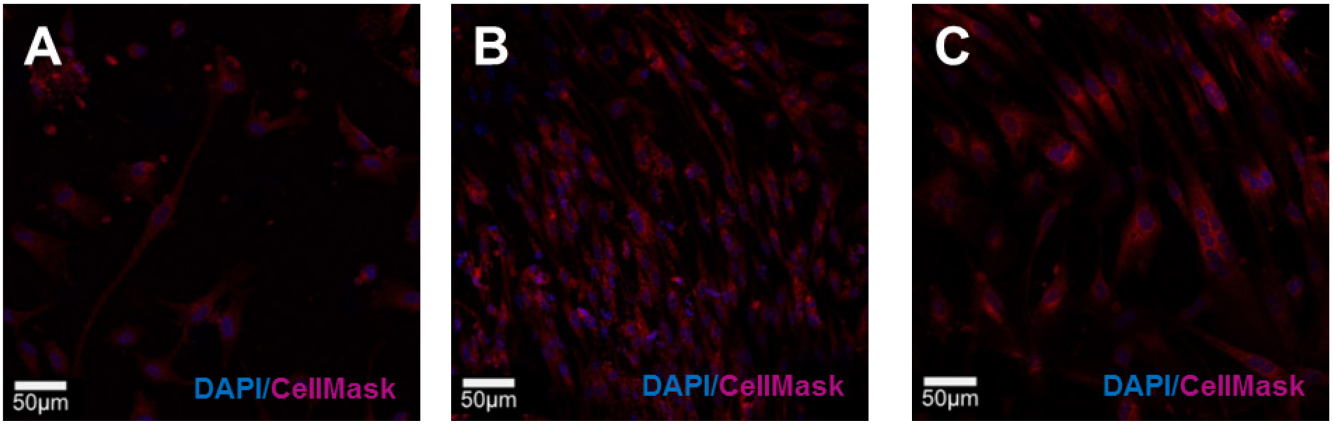

Figure 3.6. Astrocytes cultured directly onto HA discs: Confocal images after 1 week stained with DAPI (blue) and cell mask (red): A) 1200R; B)1350R; C)1350S.

In order to further analyse the astrocytes response, the expression of TNF-α and IL-6, two common inflammatory markers[64], was measured. This measurement was carried out at both day 1 and 7 to reduce the chances of results being skewed by cell death as astrocyte survival levels without an extracellular matrix is reduced after a few days[153]. TNF-α levels decreased with decreasing roughness at both day 1 and day 7 with 1200R eliciting the greatest expression of the three surfaces and 1350S eliciting the least which was not significantly different from the results experienced by the negative control ($p=0.067$) (Fig. 3.7A). This trend was also seen with IL-6 expression, however, variation

in the data meant that only the roughest surface 1200R's expression of IL-6 was statistically different to the negative control (p=0.0231) (Fig. 3.7B).

Cell metabolic activity indicated that both the positive control and 1350R increased the number of cells, whereas 1200R decreased the number of cells slightly over time. 1350S showed cell numbers in the same range as both the control and 1350R but seemed to decrease over time although there was a large variance in this data, particularly by day 7 (Fig. 3.8).

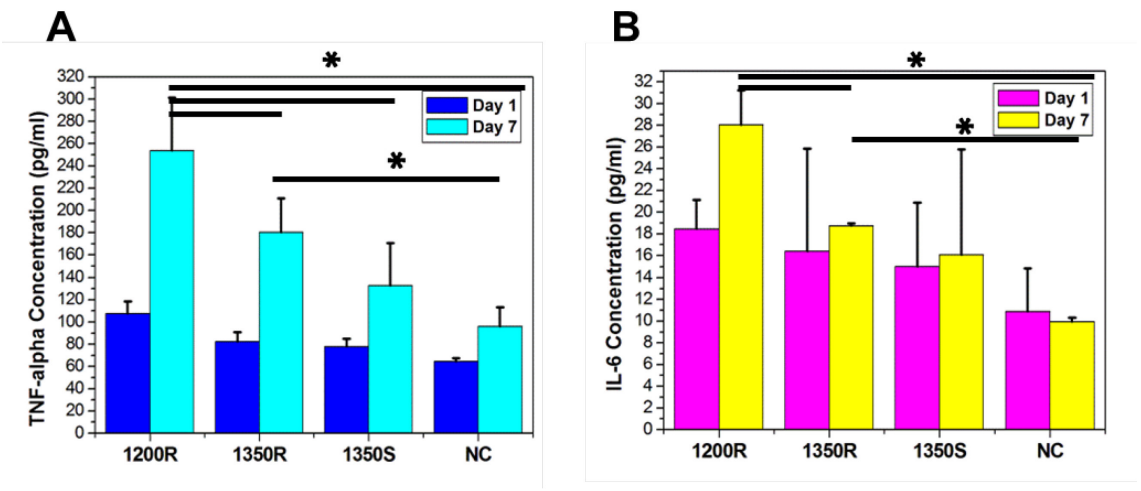

Figure 3.7. Pro-inflammatory markers released by astrocytes encapsulated in hydrogel placed on top of HA discs after 1 week A) TNF-α release (n=4); B) IL-6 release (n=4).

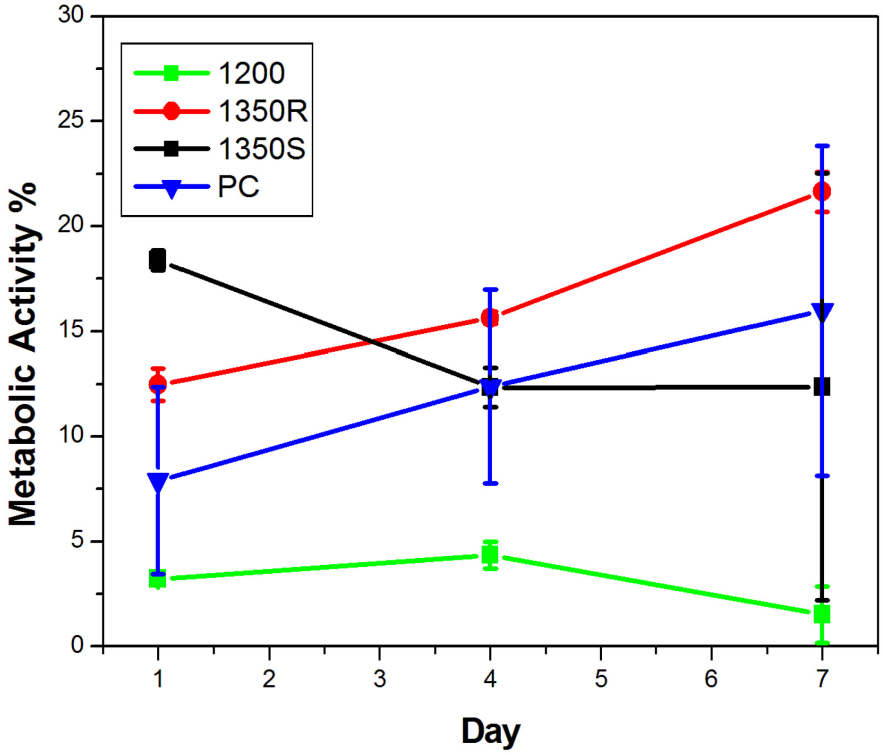

Figure 3.8. Astrocytes cultured directly onto HA discs. Astrocyte metabolic activity over one week using metabolic resazurin assay (n=4).

3.3.5 Astrocytes Encapsulated in Gels

Three dimensional (3D) astrocyte models are advantageous as, without a matrix to support their growth and network formation, cells will die within a few days which means chronic studies cannot be carried out[141]. 3D systems are also more physiologically accurate models of what is happening in the brain. In order to form networks, astrocytes need a precise extracellular environment, otherwise the cells will stay small and circular and die without behaving as astrocyte cells would *in vivo*[153]. For this reason, a variety of different percentages of PI and seconds of UV light exposure were tested in order to find the optimum for healthy network formation. Table 3.2 highlights these conditions, with

some being discarded immediately for being too weak to encapsulate cells properly and survive long term in an *in vitro* environment.

Table 3.2. Astrocyte model testing conditions varying % photoinitiator and duration of UV radiation.

UV (s)	**PI (%)**		
	0.1	0.3	0.5
10	Too weak	Too weak	Too weak
20	Too weak	Too weak	Assess Cell Growth
30	Too weak	Assess Cell Growth	Assess Cell Growth
40	Too weak	Assess Cell Growth	Assess Cell Growth

These cells were encapsulated and left to survive *in vitro* for a week in order to give the cells time to extend and make connections. These hydrogels were then imaged up to 200µm deep into the structure so that a 3D representation of the cells could be built up. Both 20s UV/0.5% PI and 40s UV/0.5%PI were not suitable with very few cells having outgrowth and a lot of cell death apparent (Fig. 3.9A and D). Both 30s UV/0.5%PI and 40s UV/0.3% PI showed some cell network formation but also a lot of round dead cells (Fig. 3.9B and C).

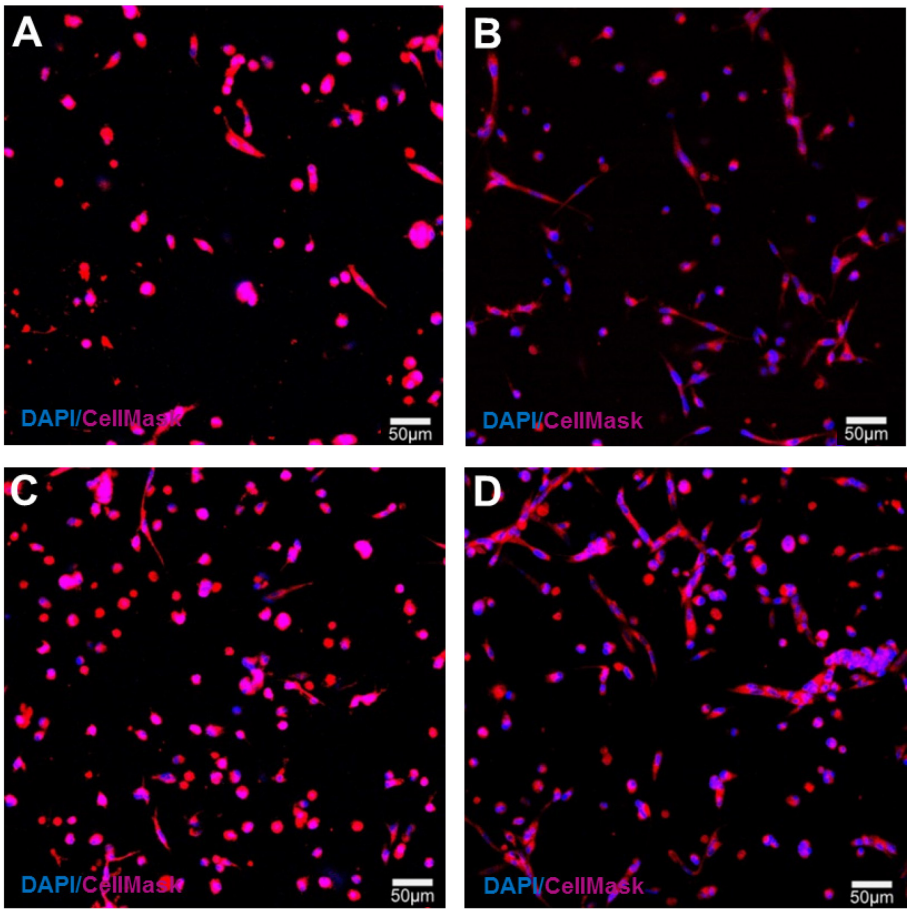

Figure 3.9. Confocal stacks of unsuccessful astrocyte models after 1 week of culture in a 5% GelMA hydrogel structure with varying % PI and UV radiation exposure**.** DAPI staining (blue) for nuclei and Cell Mask 649 (red) for cell structure A) 20s UV 0.5% PI; B) 30s UV 0.5% PI; C) 40s UV 0.3% PI; D) 40s UV 0.5% PI.

The optimum conditions for cell network formation were found to be those in the hydrogel with 0.3% PI and 30s UV exposure, as the majority of the cells had outgrowth with multiple connections and strong networks (Fig. 3.10A). The cross section of the 3D image shows how this network spreads throughout the entirety of the hydrogel (Fig. 3.10B) and for this reason these conditions were chosen for the astrocyte model to test the surface roughnesses.

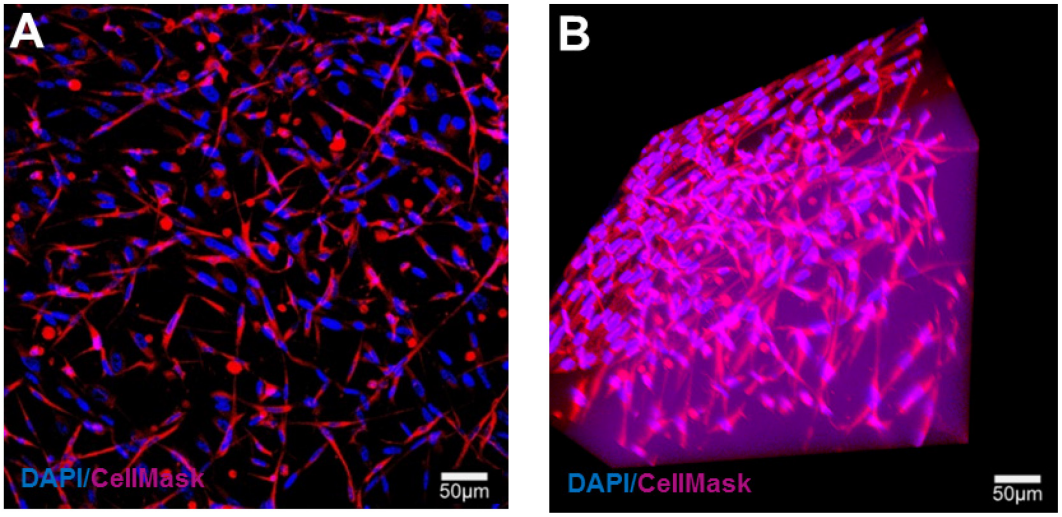

Figure 3.10. Confocal stacks (200µm thick) of astrocyte model after 1 week of culture in 5% GelMA hydrogel structure with 0.3% PI and 30s UV radiation exposure. DAPI staining (blue) for nuclei and Cell Mask 649 (red) for cell structure A) topview; B) sideview.

Confocal images were taken at day 7 in order to examine the health of the astrocytic cells with a stack depth of 200µm being combined into a single picture to give a better view of the network of cells formed in the gel. Once again the hydrogel encapsulated astrocytes on the rough 1200R surface (Fig. 3.11A) were fewer and more rounded up dead cells were visible than those on 1350R (Fig. 3.11B) and 1350S (Fig. 3.11C) surfaces,

where cells are more plentiful with better networks, with very high numbers of astrocytes on the 1350R surface.

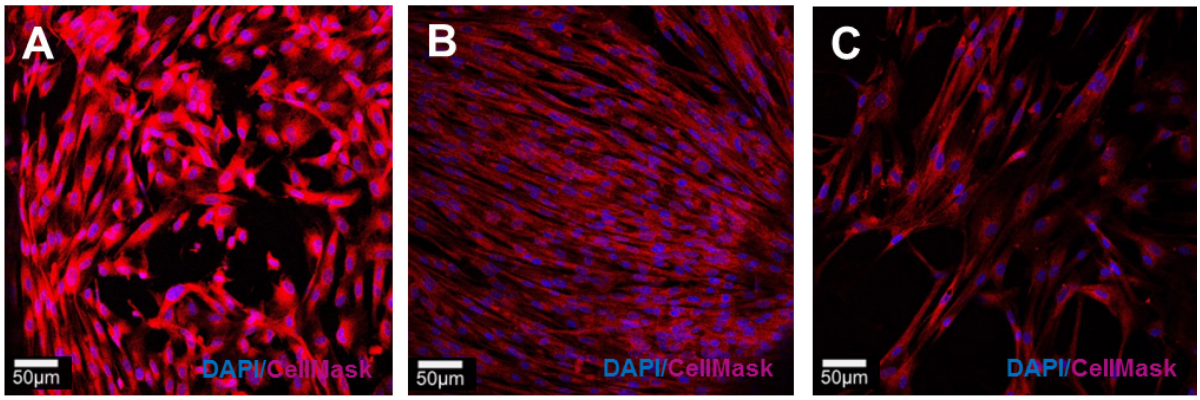

Figure 3.11. Astrocytes encapsulated in hydrogel on top of HA discs: Confocal microscopy images after 1 week stained with DAPI (blue) and cell mask (red): A) 1200R; B)1350R; C)1350S.

As cells have been shown to survive weeks in these hydrogel matrices, inflammatory marker expression was only measured at day 7 this time[153]. The TNF-α levels decreased with decreasing roughness once again, however, 1350R and 1350S were not significantly different from each other (p=0.39) and still elicited a higher expression of TNF-α than the negative control (p=0.0062 and 0.0029 respectively) (Fig. 3.12A). This trend was also seen with IL-6 expression, with 1350R and 1350S not significantly different (p=0.801) but both released significantly less IL-6 than 1200R (p=0.0011 and 0.0013) but more than the negative control (p=0.0129 and p=0.0238) (Fig. 3.12B).

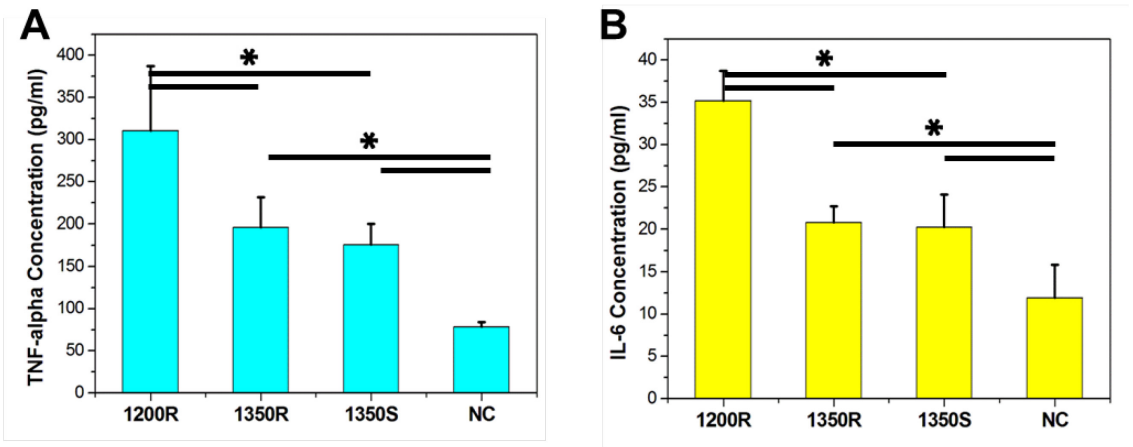

Figure 3.12. Pro-inflammatory markers released by astrocytes cultured in hydrogel on top of HA discs after 1 week. A) TNF-α release with the highest inflammation that of the roughest surface 1200R (n=4); B) IL-6 release with the highest inflammation that of the roughest surface 1200R (n=4).

3.4 Discussion

Pressing and sintering HA discs at different pressures and temperatures successfully created a wide range of surface roughnesses. These surfaces were identified as 1350S, 1350R and 1200R by these conditions and their surface roughness values were defined by previously measured surface wavelengths of 2.85µm 2.68µm and 2.30µm respectively as these are thought to describe the surface in the most comprehensive manner[151].

The behaviour of cells added to samples was assessed using metabolic activity as a measure of cell functionality as an indicator of cell survival and attachment. This is regularly used as a measure in studies as the number of cells correlates strongly with the output of mitochondrial activity calculated. The 1350R surface showed the best PC12 cell attachment out of the 3 different HA samples, on day 4, 7 and over the whole week period, during which it exhibited the same potential for attachment as the positive control. 1350S showed the next best attachment and survival and cells with 1200R and the negative control having the poorest attachment. Firstly, this supports the idea that surface morphology can be manipulated to affect neural cell survival and attachment[46,52]. Secondly, the moderately rough surface showing better attachment than both the smooth and very rough surfaces corroborates the hypothesis that there is an optimum level of roughness to enhance cell survival.

Although PC12 cells are a useful cell line due to their similarities in behaviour to neural cells, they do have a number of limitations dependent on culture conditions so a further set of experiments was carried out using primary neuronal cells[154].

A mixture of primary neurons and glial cells was added to the discs in the same way as the PC12 cells were and the same tests carried out. A mixture of cells was used as this would be more typical of what the probe would encounter during implantation into the brain. The data showed similar trends to the PC12 cells in that 1350R showed the best cell attachment out of the HA samples, although it was not significantly different from 1350S, and 1200R had the least cell attachment over the week long period. However, the dramatic increase in the number of cells attaching to the negative control versus the PC12 results implied that one of the glial cell types was multiplying rapidly and attaching in a response to the material, which highlights a limitation of the assay for counting cells in co-cultures – it is impossible to separate which cell type's metabolic activity is reducing the resazurin. Attempts were made to differentiate the cell type using cell staining and confocal microscopy, however the combination of the rough surfaces and weak stains made this an unreliable method of quantification (Appendix 1).

For this reason, further testing using a culture of primary neurons only was carried out by adding Ara-C to destroy glial cells and measuring from an effective day 0 with each disc having a different initial number of cells. When cell metabolic activity data was normalised to the day 1 results, the results initially looked dramatically different to those shown with the PC12 cells as 1200R had the strongest increasing gradient over the week, followed by 1350R and 1350S. This implied the rougher the surface the more likely the primary neurons are to attach to the surface. However, looking at the non-normalised data is also important for correct interpretation. The apparent strong increase in neuronal cell attachment is actually a result of very few cells being attached at effective day 0 – so a small increased in cell attachment appears much larger than it is when

normalised. In fact, neurons will not replicate under these conditions so any increase is due to variability in the samples[155]. It is clear from the unnormalised results that the 1350R HA exhibited the most favourable conditions for neuronal attachment, with similar survival rates to those of the positive control.

As well as assessing the effect of the HA on neural cells in isolation, looking at the glial cells in isolation was also important to the study. Although there is a relationship between neuronal cell death and activation and proliferation of glial cells, the interaction of these glial cells with the material itself is perhaps more important as these cells will drive the brain's reaction to an implant and physically form the glial scar which is encapsulating the probes. As described in the literature review, astrocytes play a major role in the inflammatory process and although microglia are the initial response to a trauma, astrocytes react in similar ways and form the majority of the scar tissue[17], while it is also possible to produce almost pure cultures of human astrocytes, unlike microglia. For this reason, these cells were chosen as a method of determining the inflammatory effect HA might have *in vivo*.

Initially, these cells were directly plated onto the HA discs and cell staining and counts were carried out. Both the confocal images and the cell count indicated that the 1200R surface had fewer astrocytes growing on the surface, which implies the astrocytes were finding the very rough surface more difficult to attach to than the smoother 1350R and 1350S. This could be viewed as a positive but the lack of networks forming on the 1200R indicated that the astrocytes were less healthy. In fact, when the release of pro-inflammatory cytokines was assessed, it was clear that both TNF-α and IL-6 were upregulated by the very rough 1200R surface when compared to the smoother surfaces

and the positive control. It is also important to note that for all surfaces, TNF-α expression increased between day 1 and 7 indicating that continued presence of a foreign material will upregulate expression of pro-inflammatory cytokines, even at lower levels. This implies that although manipulating surface roughness may be able to reduce the formation of a glial scar, it does not eliminate neuronal cells response. The 1350R and 1350S results were indistinguishable from each other for both inflammatory markers and not significantly different from the positive control for IL-6. IL-6 data had larger variation but 1200R was significantly causing both an increase of IL-6 expression through the week and elevated values compared to the smoother surfaces, indicating that the very rough surface may be having an undesired inflammatory effect on the glial cells alone without even the involvement of dying neural cells.

As discussed, *in vivo* the astrocyte cells are supported by an extracellular matrix and this 3D network has important effects on cell behaviour before and after the insertion of a foreign body into the brain[153]. Therefore the final stage of investigation involved recreating this environment using GelMA, a photocrosslinkable hydrogel, which could encapsulate the cells and provide a support network in order to compare the 2D and 3D structures' effects on results and get a more accurate representation of the astrocyte reaction *in vitro*. This model had to be carefully devised in order to assure than in the initial state the astrocytes were extending and interacting as they would in the brain. This is primarily controlled by the mechanical properties of the surrounding material, with something as close to the ECM as possible required. Although gelatin is found in the body it is not a component of ECM, so therefore it is just the spatial effect that is being captured. The weaker and stronger gels that were tested resulted in many

rounded dead cells, with 30s UV and 0.3% PI having the best network of healthy cells spreading throughout the entirety of the hydrogel. For this reason these conditions were chosen for the astrocyte model to retest our drug delivery profiles.

Cell counts with the resazurin assay were attempted for this study as well but failed to work as the colour was absorbed by the gels rather than being left in the media so could not be accurately sampled or measured. The hydrogel encapsulated astrocytes on the rough 1200R surface were again fewer than those on 1350R and 1350S surfaces, where cells are more plentiful with better networks, with very high numbers of astrocytes on the 1350R surface.

The TNF-α levels decreased with decreasing roughness once again, however, 1350R and 1350S were not significantly different from each other and still elicited a higher expression of both TNF-α and IL-6 than the negative control. It is also interesting to note that TNF-α and IL-6 expression levels are similar whether astrocytes were plated directly onto scaffolds or were encapsulated in the 3D hydrogel matrix. This implies that even though the 3D matrix is a more accurate representation of the cell environment *in vitro* a 2D representation will return very similar and therefore useful results in terms of inflammatory response testing. The 3D model would however be more useful for chronic studies of over one week.

3.5 Conclusions

This chapter focused on answering research questions 1 and 2 in order to achieve the first of the two overall objectives of this thesis – to design a thermally insulating coating capable of reducing the inflammation of glial cells and promoting the survival of neuronal cells. As HA is not a material usually inserted into the brain, its potential cytotoxity was assessed, while simultaneously analysing how topography could affect neuronal cell survival and glial cell activation.

The survival of all cell types on various HA discs for periods of up to one week indicates that HA is non-cytotoxic. A range of surface roughnesses of HA was created ranging from very rough surfaces of lightly pressed powder sintered at 1200°C (1200R) to almost smooth surfaces of hard pressed powder sintered at 1350°C (1350S). The moderately rough surface 1350R caused the greatest increase in PC12 cell attachment and the best cell survival of primary neurons, both by themselves and in a mixture with microglia, closely followed by 1350S, with the roughest surface 1200R performing poorly in all tests. This implies that there may be an optimum level of surface roughness of a neural probe coating material to reduce inflammation at the surface of a probe.

In order to assess the performance of materials in the longer term, a 3D cell model capable of surviving weeks was also developed. This involved encapsulating astrocytes in a GelMA hydrogel. These cell survived in an *in vivo* mimicking environment for a week without viability being tested for further timepoints. Results with astrocytes also showed the roughest 1200R surface caused the most cell death and resulted in the highest expression of inflammatory markers TNF-α and IL-6. These tests also indicated

that 2D models of astrocytes for inflammatory marker expression are a reliable substitute for 3D models for studies lasting a week. For all samples, including the negative control, TNF-α expression increased over a week, implying that although surface topography can reduce the glial response, in order to progress towards complete eradication, a more sophisticated anti-inflammatory strategy is required.

In conclusion therefore, and in response to research question 1, this study indicates that HA may be a suitable coating material for a cooling probe as it is non cytotoxic and that while adjusting topography can reduce inflammation, it also highlights the limitations of utilising surface topography to reduce inflammatory response and strengthens the case for the design of a coating capable of delivering anti-inflammatory factors to the brain chronically. In relation to question 2, this study indicates that the combination of PC12 and astrocytic cell responses gives the best indication of how neuronal and glial cells will respond to a surface. Having answered these two initial questions, chapter 4 now reports on the design and assessment of a coating that will permit the long-term release of anti-inflammatory factors.

4 A Dual-layered Microfluidic Coating for Long-term Controlled *In Situ* Delivery of Multiple Anti-inflammatory Factors for Chronic Neural Applications

4.1 Introduction

As much of the reduction in a probe's effectiveness is attributed to both the acute[62] and chronic[2,40] inflammation of the neural tissue post insertion, drug delivery strategies to attenuate this response are a key area of research within the field. This chapter presents the work carried out in developing a functionalised coating capable of delivering anti-inflammatory factors to neural tissue chronically.

Drug delivery options are wide ranging, both in choice of delivery method and the molecules to be delivered. Delivery methods previously investigated include microspheres[74], liposomes[79], degradable coatings[75] and microfluidic systems[85,86,156]. Some of these studies have been shown to effectively reduce the acute inflammatory response to electrode implantation. For example, an *in vivo* study in guinea pigs whereby dexamethasone was encapsulated in PLGA nanoparticles and released from alginate gels for up to two weeks, showed that the electrical impedance of a conducting electrode due to the formation of the glial scar was unchanged in the 3 week period, whereas the impedance of the non-eluting control had tripled by 2 weeks and then began to stabilise[82]. Another study showed that immobilising alpha-MSH to the electrode surface could significantly attenuate the glial response to implants in rats over a 4 week period[8].

However, several recent studies have shown that strategies which effectively reduce the acute anti-inflammatory response to implants often are indistinguishable from

untreated devices at the chronic stage of implantation. For example, a study by Potter *et al*[76] where neural implants released curcumin from polyvinyl alcohol film coatings over time, with most of the release occurring in the first 10 hours, showed a reduction in scar tissue and an increase in functioning neurons surrounding the implant at 4 weeks. However, once 12 weeks was reached, there was no statistical difference between the implants which were drug eluting and those that were not. Although not a drug eluting probe, the same phenomena was found when investigating the shape and size effects on glial scarring in a study by Szarowski *et al*[40]. Smaller rounded implants showed a reduction in the acute response of microglia (defined as less than 2 weeks in this study) but chronic results from 2 weeks up to 12 weeks showed no significant difference between all designs[40].

These studies indicate that in order to create viable probes for long term implantation, a strategy to reduce the inflammatory reaction of brain tissue in its chronic phase is required. In order to allow release of anti-inflammatory factors for months not weeks, a microfluidic system is required. Some investigations into these systems has been carried out, however difficulties with controlled release[85] and repeated administration of drugs were reported[86]. For this reason the aim was to design an easily refillable microfluidic system which would allow the slow and steady delivery of an optimised profile of anti-inflammatory factors long term. Inspiration was also drawn from advancements in microneedle technology whereby swellable tips allow better tissue adhesion with reduced dimensions and insertion forces required[58]. The introduction of a dual layer swelling element to the system, could not only reduce insertion trauma but also reduce micromotion and mechanical property mismatch of the probe once implanted and

manipulation of both layers of the system could allow improved control of release profiles.

Therefore, it was hypothesised that being able to sustain anti-inflammatory factor delivery, reduce insertion trauma and micromotion and change the factor being delivered would significantly reduce the inflammatory reaction of neural cells, leading to a reduction in scar tissue formation and a probe that functions better long term.

In order to assess these claims, the anti-inflammatory factors to be delivered had to be selected. In future, a patient specific anti-inflammatory profile could also be developed, whereby key molecules could be delivered in synchronisation with specific occurrences in the inflammatory process but initially only two such factors were investigated. Dexamethasone (DEX) is a non-steroidal anti-inflammatory drug that has been shown to reduce inflammation in multiple areas of the body, including the brain[91,157]. However, this is an aggressive corticosteroid which can potentially have detrimental effects with chronic administration[2]. IL-4 is an anti-inflammatory cytokine which has been shown to have the ability to polarise macrophages and microglia into their anti-inflammatory M2 phenotypes, as opposed to the pro-inflammatory M1 variety which are believed to increase the formation of scar tissue. It must be noted that this isn't always a clear boundary and some macrophages can exhibit properties of both M1 and M2 or neither but the overall trend gives an excellent indication of the reaction of the cells[81,94,96].

In order to bring all aspects of the investigation together, several stages of assessment were carried out. Firstly, the design of the microfluidic channel containing dual layered system was optimised utilising different hydrogel concentrations and sacrificial fibre

methodologies. A chip version of the system was then devised to provide assessment of the diffusion profile of different sized molecules and plan the infusion profiles for cellular work. Finally, hydrogel brain models containing monocytes and astrocytes were optimised to allow assessment of the effects of chronically released DEX and IL-4 release. The outline of this workplan is shown below.

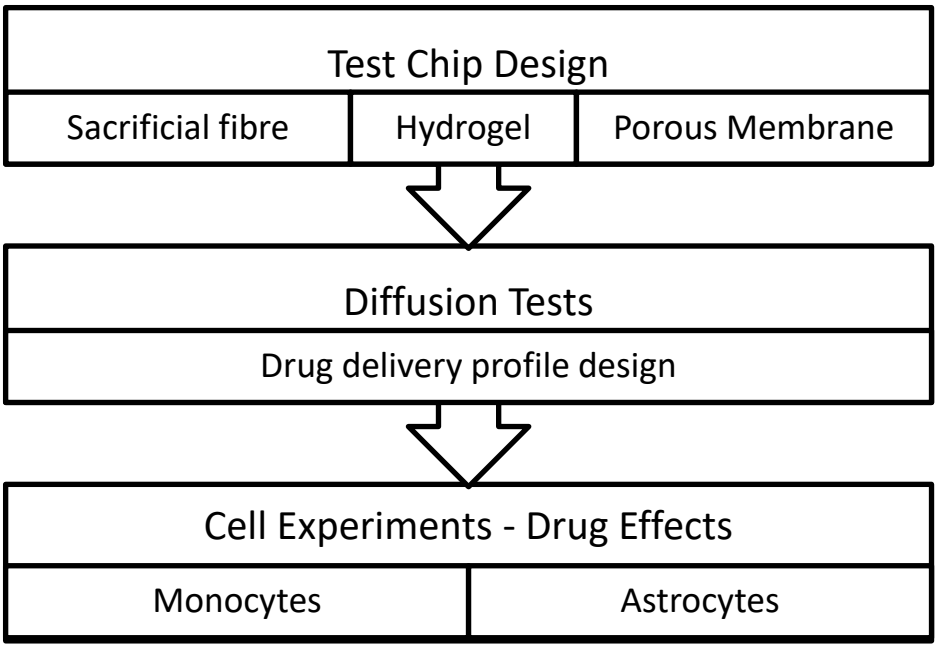

4.2 Materials and Methods

4.2.1 Synthesis of Gelatin Methacryloyl (GelMA)

The methods used here were identical to those described in Section 3.2.5.

4.2.2 Agarose Fibres

A 4% agarose solution (Sigma Aldrich) in PBS was heated to 60°C and stirred gently to ensure no bubbles were present. A 250µm inner diameter glass capillary (outer diameter 350µm, length 85mm, Organovo, CA) was placed in the solution as a complementary glass piston was pulled upwards from the other end, drawing the solution into the tube. This tube was placed on an ice block for 10s before pushing the piston back through the tubing to extrude the solid fibre.

4.2.3 GelMA Solutions

Pre-polymer solutions of 5% GelMA for cell encapsulation were prepared with 0.5% photoinitiator (PI) (2-hydroxy-1-(4-(hydroxyethoxy) phenyl)-2-methyl-1-propanone 98%, Sigma Aldrich) in PBS. For scaffold manufacture, 10% GelMA, 2% PEG (1000 MW, Polysciences), 0.5% PI solutions were used. These solutions were crosslinked using UV light at an intensity of 6.9 mW/cm^2.

4.2.4 Fabrication of PDMS Membranes

All PDMS was prepared at a ratio of 10:1 with its curing agent (Sylgard 184 Silicone Elastomer Kit, Dow Corning). PDMS membranes that were 100µm thick were fabricated using a silicon wafer with 100µm diameter posts spaced 400µm apart. The thin PDMS membrane was formed using a spin coater at 3500RPM for 2min before scraping over the posts with a glass slide. Partially cured PDMS frames of 0.5cm (width)× 0.5cm (length) (cured for 20min in 80°C oven) were added on top of the fresh PDMS on the

mould before curing at 80°C for 2.5hr to produce membranes with attached frames (Fig. 4.8).

4.2.5 Scaffold Fabrication

Moulds of 0.25cm^2 were manufactured from PDMS. Small metal connectors (100µm inner diameter) were punched through the middle of the mould and a sacrificial fibre of 80µm thickness was passed through the connectors. Initially, 40µl of 10% GelMA-2%PEG solution was poured into the mould before UV crosslinking for 20s at 6.9 mW/cm^2 and then a further 40µl of solution was crosslinked on top for 40s. These samples were air dried for 12hr. The PDMS membrane and frame was then plasma bonded on top and PBS was added to allow reswelling of the construct for 5hr. At this stage the sacrificial fibre was removed to create a microchannel of 80µm diameter through the centre of the construct (Fig. 4.1).

4.2.6 Diffusion Studies

Diffusion was first calculated optically using fluorescein isothiocyanate (FITC)-Dextran with 20kDa MW, 40kDa MW and 392Da MW FITC isomer (Sigma Aldrich). A solution of 20mg/ml of FITC-Dextran in PBS was injected into the microchannel until it was full and fluorescent images were taken from above every 5 minutes at 37°C. The fluorescent intensity at a fixed point was calculated over time using Image J software[158] in order to calculate a value for the diffusion coefficient. The equation used for this was:

$$D = \frac{n_0^2 x^2}{t\pi(n_0^2 + 4n^2 - 4nn_0)}$$

where n is the intensity of the fluorescent signal, x is the distance from the microchannel and t is time. A 100µl PBS reservoir was added to the top of the PDMS membrane and the whole construct was placed in a humidified chamber in an incubator at 37°C. Every

24hrs the reservoir was replaced in order to maintain sink conditions and the fluorescence of 2µl of the solution was measured using Nanodrop2000 (Thermo Fisher Scientific).

4.2.7 Microscope Imaging

All bright field and fluorescent images were taken on a Zeiss Axio Observer D1 Fluorescence Microscope (Carl Zeiss, Germany) and all scanning electron microscopy (SEM) images were taken on a Hitachi Model S4700, Japan. Confocal images were taken on Leica SP5X MP, Germany.

4.2.8 Nanodrop

Blank measurements were conducted using PBS and all measurements were completed using triplicates of 2µl samples. FITC-Dextran was measured at 494nm excitation levels and concentrations were calculated using a calibration curve.

4.2.9 Instron

Mechanical properties of the gels were calculated using Instron 5524 mechanical analyzer (*Instron*, Canton, MA) compressive tests with a 10N load cell. Compressive modulus was calculated between 10 and 20% loading of 600µm thick samples with a 5mm diameter with 6 replicates for each sample.

4.2.10 Monocyte Culture and Encapsulation

Human monocyte cells (THP-1) were cultured in suspension for at least 7 days before use in media consisting of Roswell Park Memorial Institute Medium (RPMI) media (Life Technologies) supplemented with 10% FBS (Gibco BRL) and 1% Penicillin-Streptomycin (Gibco BRL) at 0.5-2 million cells/ml media. Cell media was changed every three days, retaining 20% of the old media. Monocytes were encapsulated in 5% GelMA with 6

million cells/ml and50µl of this solution was added on top of the chip and UV crosslinked as before for 20s.

4.2.11 Astrocyte Culture and Encapsulation

Primary human astrocytes (ScienceCell) were cultured from in suspension for at least 7 days before use in media (DMEM:F12 with L-glutamine + HEPES, Thermoscientific) supplemented with 10% FBS (Sigma Aldrich), 10% Astrocyte Growth Supplement (ScienceCell) and 1% Penicillin-Streptomycin (Sigma Aldrich) at 0.5-2 million cells/ml media. Cell media was changed at least every three days, retaining 50% of the old media. Astrocytes were encapsulated in 5% GelMA with 0.3% PI at a density of 1 million cells/ml and 50µl of this solution was added top of the chip and subject to 30s UV light exposure.

4.2.12 Chronic Cell Studies

Each sample had an initial infusion of 0.1mg/ml DEX (Sigma Aldrich) or 10ng/ml IL-4 (R&D Systems) through the microchannel, excluding negative controls. Selected samples then had repeated infusions (every 3.5 days) of IL-4 or DEX (Table 4.1), with media added every 3.5 days immediately before injections. Immunostaining was carried out at day 7, 14 and 21.

4.2.13 Live/Dead Assay

Assays were carried out at day 1 and 7 using Live Dead kits for mammalian cells (Life Technologies). After washing all samples in warm PBS, a mixed solution of ethidium homodimer-1 and calcein was prepared in a ratio of 4:1 and 300µl of this solution and incubated for 15min. After this period, samples were washed in PBS three more times, before being left in PBS for microscope imaging.

4.2.14 Immunostaining

All cell encapsulated hydrogel samples were washed with PBS before fixation in 4% paraformaldehyde (PFA) (Sigma Aldrich) at room temperature for 30min. Samples were stored overnight at 4°C in PBS at this stage if required. Samples were then incubated in 0.1% triton x-100 (Sigma Aldrich) for 30min at room temperature. Blocking was carried out in 1% bovine serum albumin (BSA) (Sigma Aldrich) in PBS for 1hr at room temperature. For monocyte samples, the primary antibody for CD206 (R&D Systems) was diluted at 1:100 in PBS with 1% BSA and samples were incubated at 4°C in a humidified chamber overnight. The Alexa 488 or Alexa 594 conjugated secondary antibodies (Molecular Probes) were added at a dilution at 1:200 in PBS with 1% BSA and incubated for 1hr at room temperature in a dark humidified chamber. The primary and secondary antibody addition steps were repeated for 27E10 (R&D Systems) before adding 4, 6-diamidino-2-phenylindole (DAPI, Vector Laboratories Inc.) at 1:1000 dilution for 10min at room temperature whereby samples were ready for observation under the microscope. Between each stage 3x5min washes in PBS were carried out. For astrocyte samples, DAPI was added at 1:2500 dilution as well as Cellmask 647 membrane stain (Sigma Aldrich) at 1:1000 dilution in a PBS 10% goat serum (Gibco BRL) solution for 10 minutes at room temperature whereby samples were ready for observation under the microscope. Between each stage 3x5min washes in PBS were carried out.

4.2.15 ELISA Assays

The methods used here were identical to those described in Section 3.2.7.

4.2.16 Statistical Analysis

All data is expressed as mean ± standard deviation. T-tests or 2 way anova tests were performed where appropriate with $p<0.05$ being viewed as significant.

4.3 Results

4.3.1 Fabrication of Microchannels

GelMA is a biocompatible photocrosslinkable hydrogel that has been shown to support cell growth when cells are in contact with its surface or encapsulated within its structure[159]. It is also an interesting material for drug delivery applications as its porous structure can be fine-tuned to control the rate of drug release into the surrounding environment[160,161]. By optimising the photocrosslinking time, mechanical properties of the gel can also be exploited to easily fabricate and retain microchannels within the structure. The concept and process for fabricating this system is illustrated in Figure 4.1.

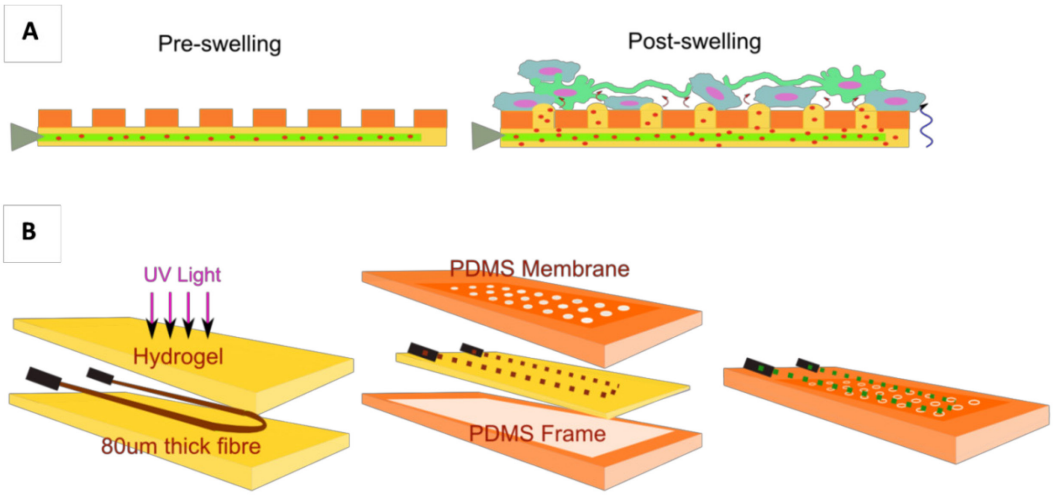

Figure 4.1. Construction of dual-layered microfluidic system and its concept**.** A) Schematic diagram illustrating the concept of the transformation from dry insertion state to drug delivering implantation state. B) Preparation procedure of microchannel in GelMA hydrogel construct surrounded by microporous PDMS membrane.

Before the hydrogel system design could begin, the sacrificial fibre fabrication method needed to be selected. Initially, 250µm and 500µm agarose fibres were printed using a glass capillary system. A 4% concentration of agarose in PBS was chosen as higher concentrations would not be drawn into the glass capillaries easily and lower concentrations resulted in more breakable fibres. This technique had some success when printing simple straight channels on non-dried systems (Fig. 4.2A). However, once loop systems were utilised and gels had been dried and reswollen, fibres were repeatedly breaking inside the gel instead of being removed as a result of the added force required. The addition of Triton-X to the solution in various concentrations had no effect on the removal success. The fibres were also shrinking and deforming during the drying stage resulting in a smaller microchannel (Fig. 4.2B).

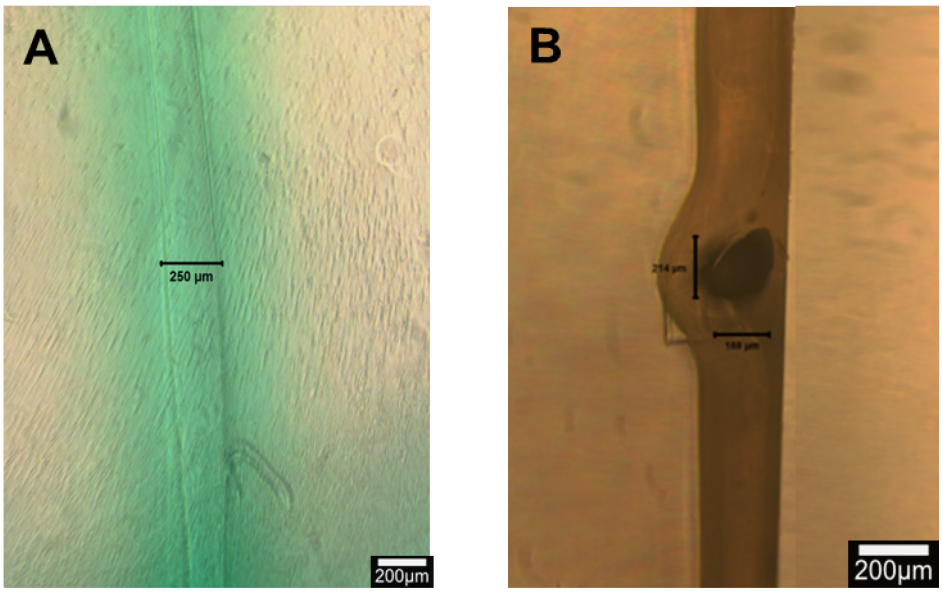

Figure 4.2. Agarose microchannel optimisation**.** A) 250µm microchannel formed by removal of 4% agarose fibre and successfully filled with dye; B) Cross-section of microchannel post drying and reswelling stage showing shape formation and shrinkage.

As the objective is to bioprint these fibres in exact configurations in future, an alginate bioprinting system was also explored. A biaxial needle system allowed Calcium Chloride to be printed alongside the alginate itself causing it to crosslink *in situ*. There were several problems with this. In order to allow the fibre to print where it was supposed to, the rate needed to be slowed to a point where the fibre was unevenly printing (Fig. 4.3A). As well as this, printing directly onto the hydrogel was not possible as there was not sufficient traction to anchor the fibre resulting in it sliding along the surface as the printing path was followed. Finally, hair was investigated as an option as it is strong and flexible and so can be easily manipulated into any shape. It retained a constant thickness of 80±16µm channel that was unaffected by the drying and reswelling stage (Fig. 4.3B). It tended to float to the top of the hydrogel so crosslinking of the hydrogel had to be completed in two halves to ensure the anchorage of the fibre in the middle of the gel. The addition of 100µm microconnectors to the mould ensured exact placement of fibre and allowed easy precise filling of the microchannels.

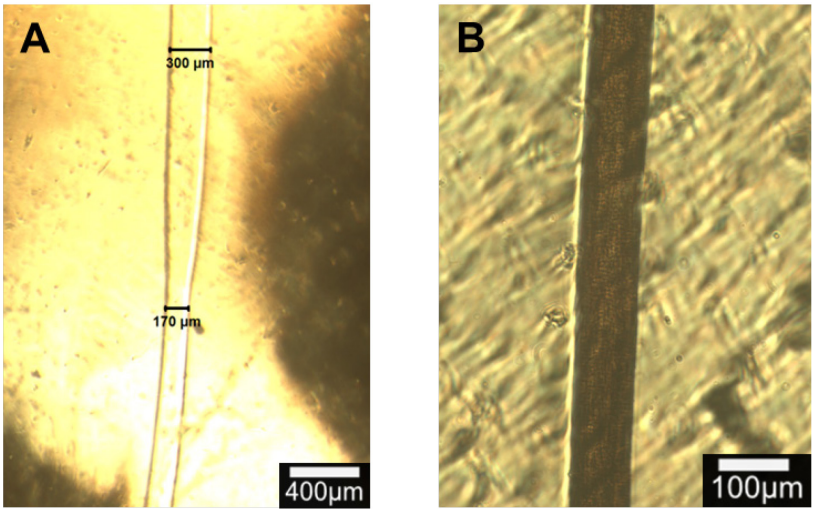

Figure 4.3. Alternate sacrificial fibre formation strategies. A) Bioprinted alginate fibre exhibiting uneven nature; B) Hair showing uniform diameter.

4.3.2 Hydrogel Optimisation

In addition to optimising the properties of the sacrificial fibre, the properties of the hydrogel also affected the microchannel structure integrity over an extended period of time. Concentrations of below 5% GelMA resulted in channels leaking and not being able to retain their shape after a number of days of infusion (Fig. 4.4A). It was also important to ensure that a loop system could be easily created and the channel filled successfully (Fig. 4.4B) as highly crosslinked gels (10% GelMA, 40s UV) broke when more complex shaped fibres were removed.

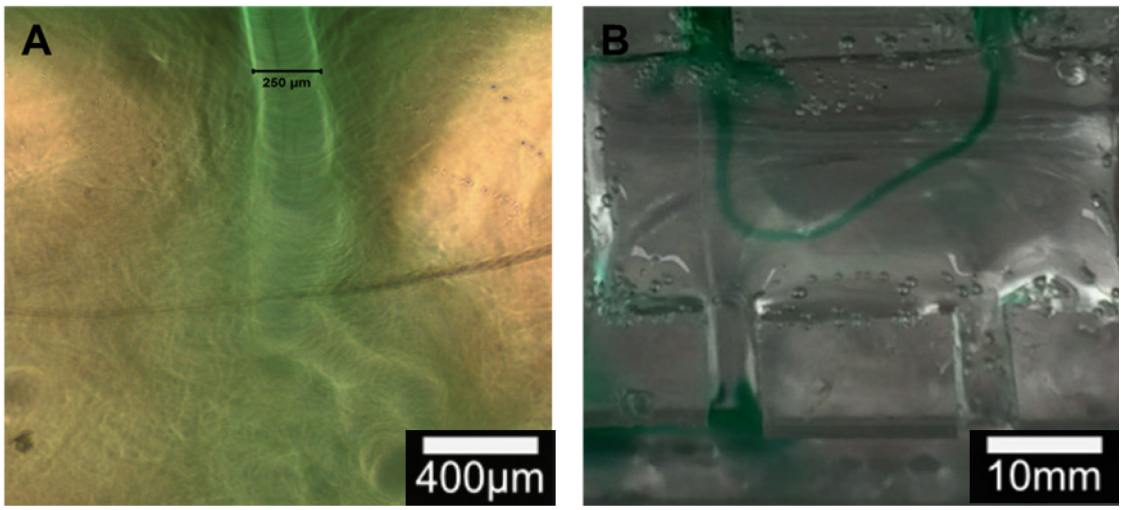

Figure 4.4. Microchannel integrity in GelMA. A) Demonstration of microchannel failure in weak GelMA gel; B) successfully filled looped microchannel.

During the developmental process it was also noticed that the drying and reswelling stages were having an adverse effect on the integrity of the hydrogel, particularly if they were left for more than 3 days in the dry state. After these preliminary studies had been carried out, three different hydrogel formulae were investigated: 5% GelMA, 10% GelMA and 10% GelMA/2%PEG. The addition of the PEG as a long chain crosslinking monomer between GelMA chains was to provide extra crosslinking and resistance to cracking upon drying. Firstly, their mechanical properties with varying degrees of

photocrosslinking post drying and reswelling were analysed. The compressive moduli of 5% GelMA, 10% GelMA and 10% GelMA/2% PEG were 2.83±0.40kPa, 3.26±0.45kPa and 6.41±0.67kPa, respectively (Fig. 4.5A). The reswelling profiles of the three formulations were also assessed in order to ascertain if they would exert undue pressure on the brain and if their reswell time had the potential to be problematic in surgery as sometimes implants have to be removed and reinserted several times during this time[162]. All three formulations had a similar reswelling profile with total reswell within 4hr in PBS (Fig. 4.5B).

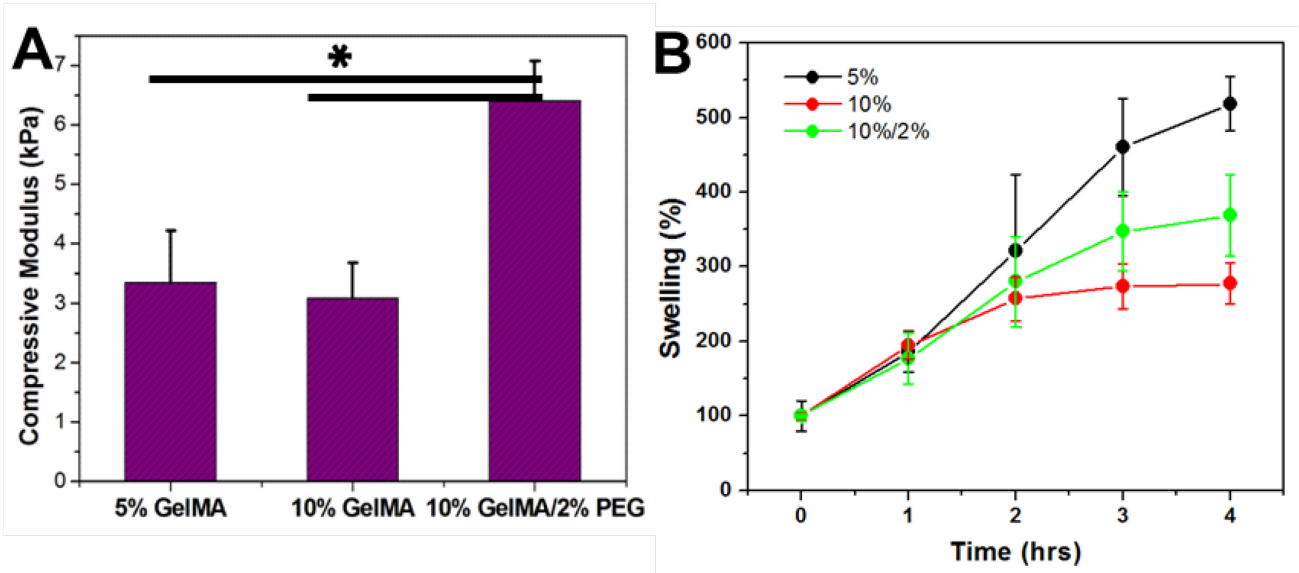

Figure 4.5. Hydrogel optimisation**.** A) Compressive modulus of three different concentrations of GelMA/PEG hydrogel composites (n=6). B) Reswelling profiles of three different concentrations of GelMA/PEG hydrogel composites (n=5).

The thicknesses of the gels in their dry state were 210±40µm, 430±20µm and 350±20µm respectively. After 72hr drying in air, 10% GelMA/2%PEG was the only formulation which remained entirely crack free in all samples. SEM images taken of this hydrogel (Fig. 4.6)

show the porous structure of the gel with pores of 90±37µm in diameter, as measured across 3 different cross-sectional images.

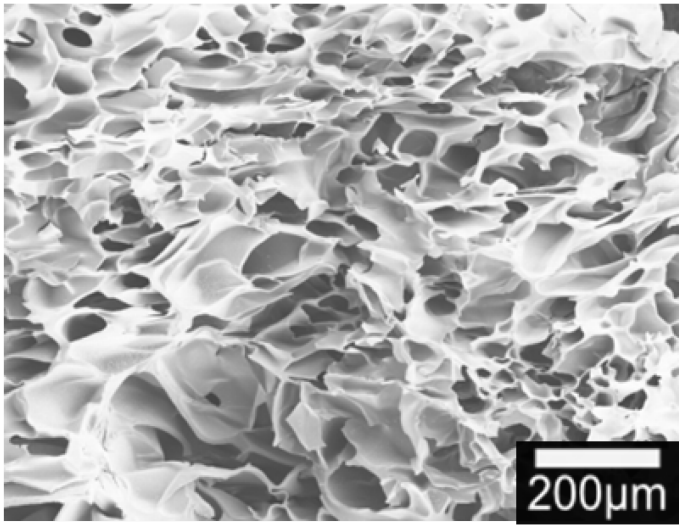

Figure 4.6. SEM image showing GelMA/PEG porous structure**.**

4.3.3 PDMS Membrane Construction

Particularly at lower concentrations, GelMA can degrade quickly over time and diffusion through the gel can be quick[163]. For these reasons, as well as preventing excessive reswelling post-insertion and allowing even greater control over the drug release, a porous PDMS membrane layer was added to the microchannel containing GelMA gel. PDMS is also non-toxic and non biodegradable[164,165] and the reduced surface area for diffusion through the hydrogel based microfluidic system further slowed the release of active molecules. The spin coating process over the silicon wafer with a pillar system created a porous membrane, the spacings and sizes of which could be manipulated. One recurring problem was ensuring that all pores were fully open as often excess PDMS resulted in pits being formed instead of pores (Fig. 4.7). An extra stage of removing any excess PDMS post spincoating using a glass slide was added to the protocol at this point.

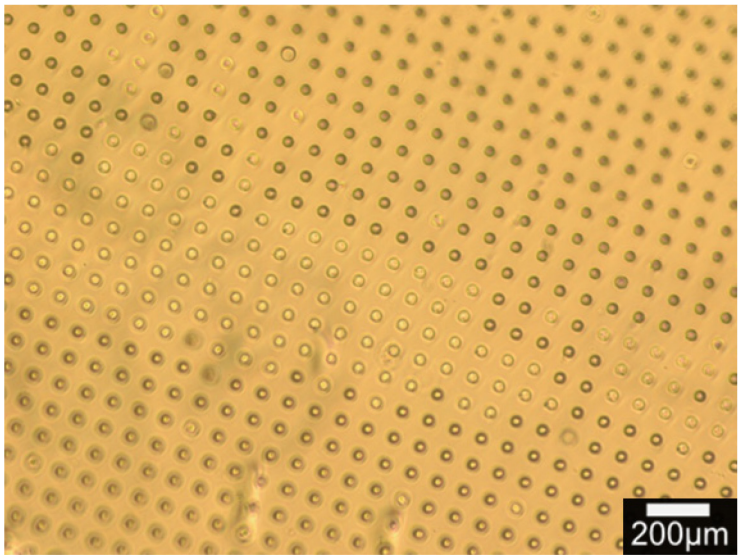

Figure 4.7. PDMS Membrane formation**.** Microscope image showing open pores (dark) and closed pits (light).

The technique to combine the hydrogel layer with the PDMS membrane also had to be carefully thought through. Plasma bonding was a suitable method by which to do this as it is relatively simple, results in a strong bond and negates the need for glue or extra chemicals[122]. GelMA cannot be activated by oxygen even in its dry state so a thin mould of PDMS was left surrounding the dry GelMA which could be activated and bonded with the membrane. However, the membrane itself was too thin and fragile to be utilised in the plasma bonder alone, so a method of anchoring the membrane in some way became necessary. A method of partially curing PDMS membrane frames which could then be pressed onto the PDMS loaded wafers and added to the oven to completely cure was devised. This ensured the membrane could not only be safely placed in and sufficiently activated in plasma bonder but also be easily removed from the silicon wafer mould without tweezers or the risk of ripping in the first place (Fig 4.8). This thicker frame could be removed at a later stage to minimise the thickness of the whole system.

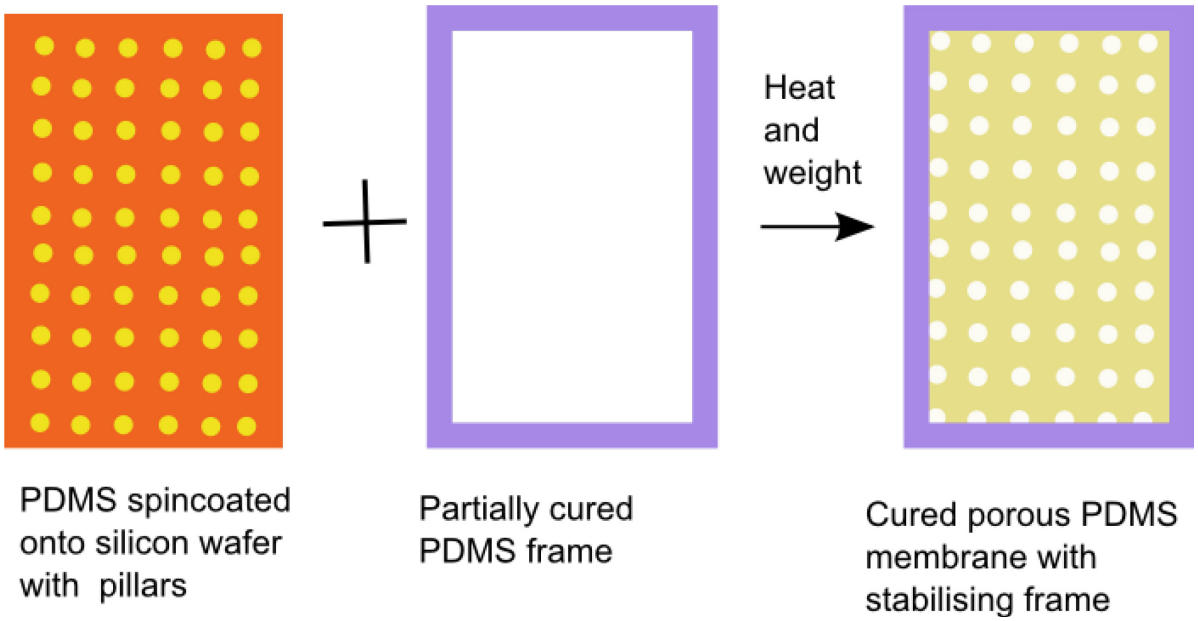

Figure 4.8. Construction of PDMS membrane and frame. Schematic demonstrating addition of partially cured PDMS frame to membrane pre-curing.

4.3.4 Chip Development

Once the individual properties of the dual layered microfluidic system had been designed it was time to devise something we could use for our cell experiments. The chip itself was designed as a square piece with one single cylindrical microchannel of 80±16µm through the hydrogel in order to simplify the calculations for diffusion (Fig. 4.9A). The appearance of the chip itself as well as the microchannel and porous membrane under the microscope are shown in Fig. 9B-E with the hydrogel stained green.

4.3.5 Diffusion through the Scaffold

In order to calculate the diffusion co-efficient of potential anti-inflammatory factors such as drugs and interleukens through our system, FITC-Dextran with various molecular weights (MW) was used. DEX is a commonly used anti-inflammatory drug, particularly at the acute stage of inflammation and has a MW of 392Da[82,91,157] . FITC isomer has a

MW of 389Da and was used as a model for DEX and other small drugs. Interleukens are a family of cytokines involved in the inflammatory process and some of these, such as IL-4, have been shown to have anti-inflammatory effects[94,96]. IL-4 has a MW in the range of 12-20kDa, so FITC-Dextran with 20kDa MW was chosen as a model for this cytokine, with tests also being conducted with 40kDa FITC-Dextran as a model for larger proteins that may be investigated at a later date. In order to calculate the diffusion co-efficient for these FITC based molecules, sample chips were placed under the fluorescent microscope and a single injection of the substance was added to the microchannel (Fig. 4.10A). The channel and its surrounding area were imaged every 2min until the dye had diffused throughout the chip (Fig. 4.10B).

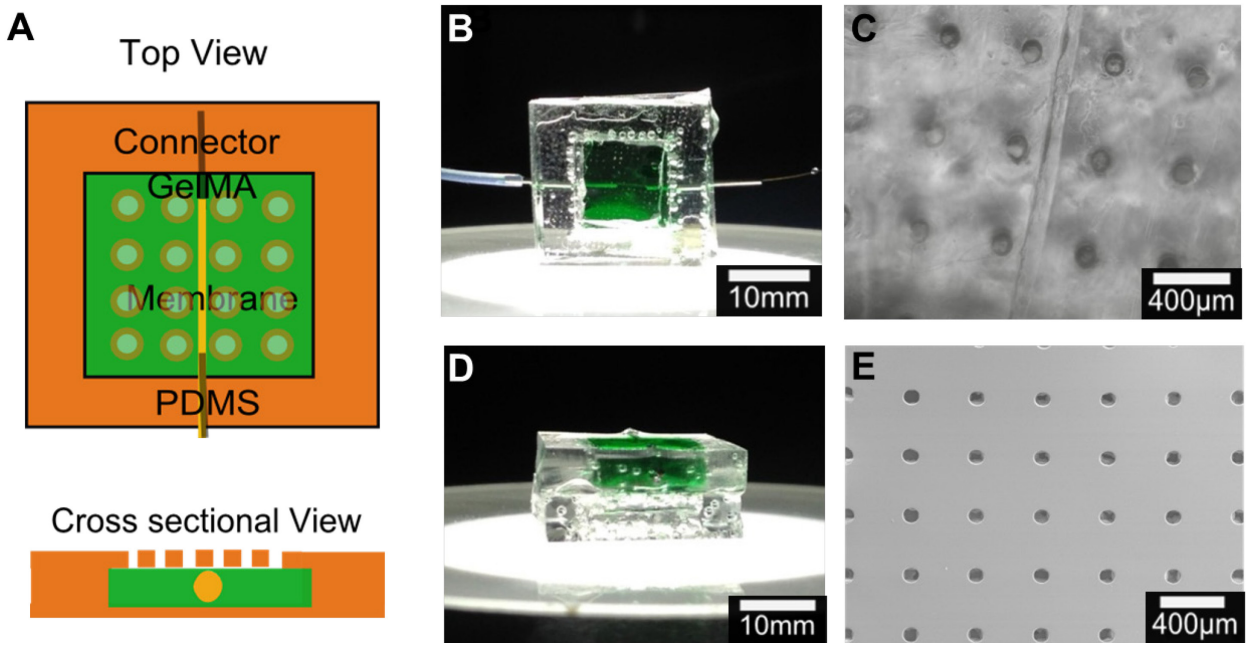

Figure 4.9. Chip design optimisation**.** A) Schematic of chip design B) Top view of sample chip with GelMA/PEG section stained green C) Top view of chip showing 100µm channel and 100µm pores D) Cross sectional view of sample chip E) SEM image of PDMS membrane with 100µm pores with 400µm spacing.

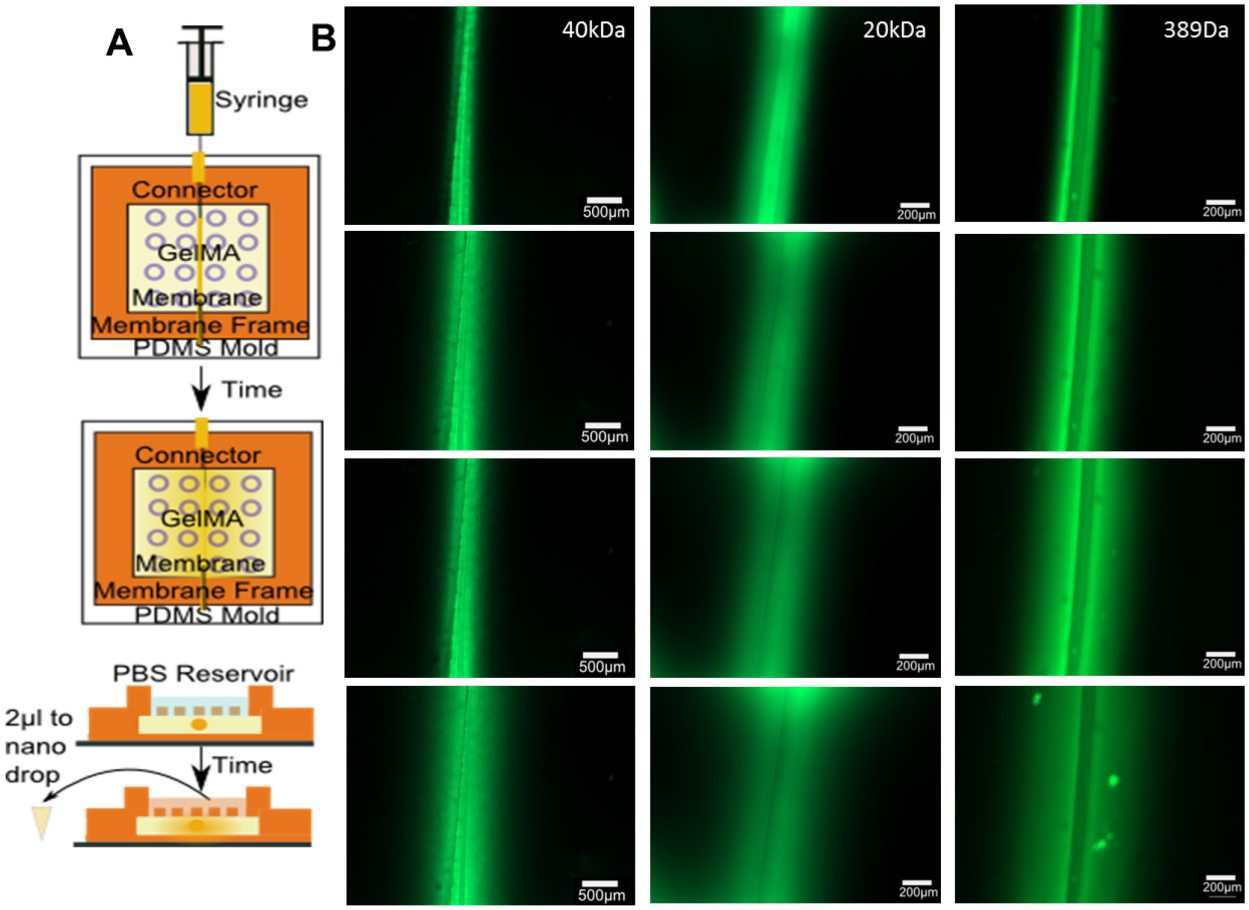

Figure 4.10. Diffusion profiles of FITC variants with different molecular weights through chip system. A) Schematic of tests to show diffusion: optical set-up using microscope images and quantification using nanodrop to measure diffusion into a PBS reservoir. B) Optical images over time of FITC-Dextran (40kDa MW and 20kDa MW respectively) and FITC isomer (389Da MW) showing effect of molecular weight on diffusion time.

Change in fluorescent signal at a fixed point outside the channel was quantified using Image J and a diffusion co-efficient was calculated *via* the diffusion equation listed in the methods section and verified using the gradient of the plot of all the points on the graph (Fig. 4.11).

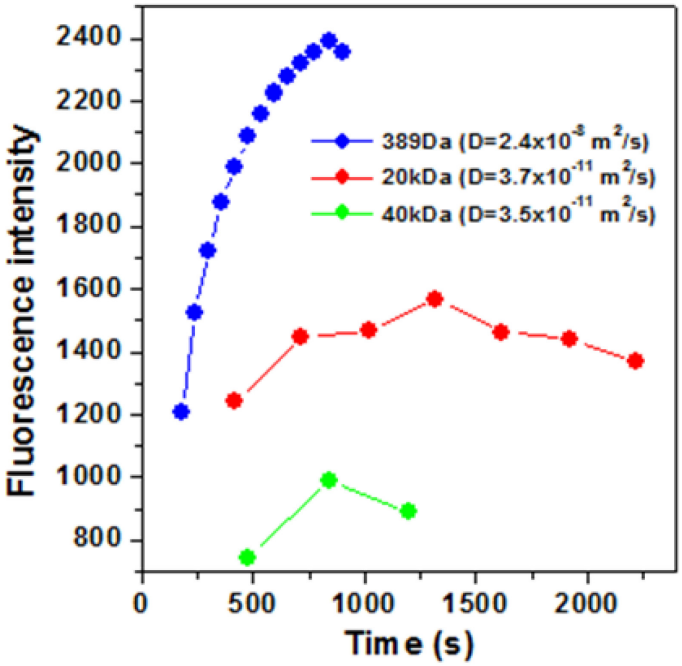

Figure 4.11. Diffusion profiles of FITC variants with different molecular weights through chip system. Progression of fluorescent signal is measured at a fixed point as FITC diffuses through hydrogel system to calculate diffusion co-efficient D.

The diffusion co-efficient is a useful measure of diffusion through a substance, however, the diffusion of the anti-inflammatory factors through the whole chip including the porous PDMS membrane and into the brain tissue on the other side is actually more relevant to our studies as this will allow us to specifically target different points in the inflammatory process with our molecules in future. This was calculated by adding a PBS reservoir on top of the chip (which was held in the PDMS frame surrounding the membrane) into which the FITC variants could diffuse over time. Samples of this PBS's fluorescence were measured using the nanodrop at regular intervals and the entire PBS reservoir was replaced to maintain sink conditions similar to those in the brain. Concentration of the FITC present was plotted against time at 24hr intervals to identify peak release from the system and allow understanding of the release profile (Fig. 4.12A).

The 40kDa FITC-Dextran had its peak release at 48hr with both 20kDa and 40kDa FITC-Dextran still being released from the system up to four days after the initial infusion through the microchannel. As the release of FITC isomer and 20kDa FITC-Dextran both peaked at 24hr or before, the experiment was repeated with 8hr time points (Fig. 12B). This showed the initial release of the 20kDa FITC-Dextran was steady over the first 24hr and there was minimal burst release of the FITC isomer.

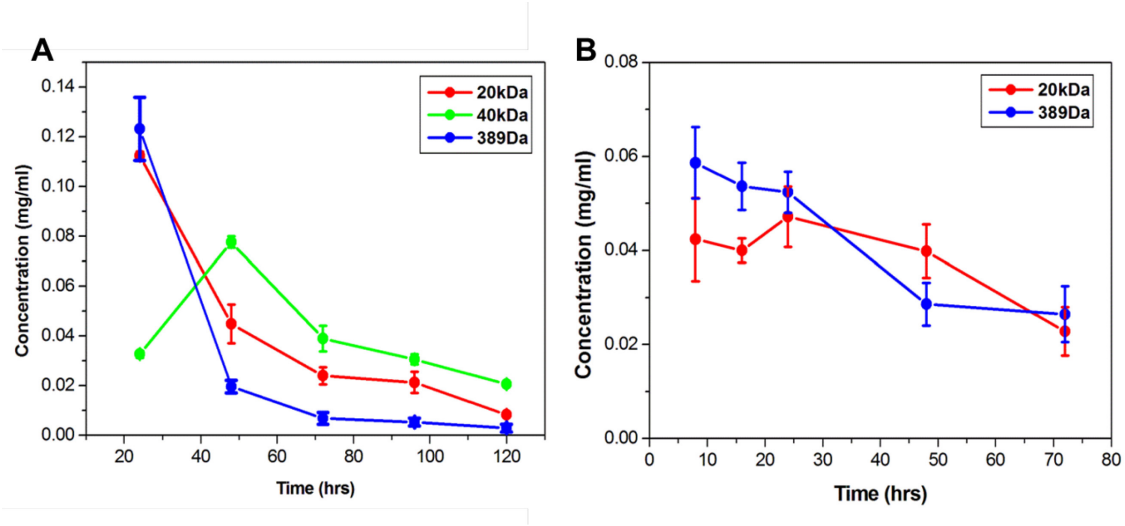

Figure 4.12. Diffusion profiles of FITC variants with different molecular weights through chip system (n=6). A) Quantity of FITC diffused through system at 24 hr time points showing 40kDa FITC-Dextran has peak release after 48hrs B) Quantity of FITC of different molecular weights diffused through system at 8hr time points as demonstrating steady release over 24 hours and minimal burst release.

4.3.6 Brain Model Development

Once the drug delivery chip had been designed and optimised, a cellular model for neural tissue was required. As microglia are the first response to any injury in the brain, moderating their response can affect the whole chain of inflammation events[19]. Microglia are sometimes referred to as the macrophages of the brain as they carry out

many of the same duties that macrophages carry out in the rest of the body[138]. Microglia are very difficult to harvest and purify without having other remaining cell types whereas macrophages can be formed from monocytes using a well-established cell line THP-1. As both microglia have the ability to differentiate into M1 or M2 phenotypes, which correspond to pro-inflammatory and anti-inflammatory macrophages respectively, monocytes are a suitable model for investigating the effects of a drug delivery profile on the brain[18,139,140]. In order to create a more brain-like environment and allow longer survival of the cells, GelMA was used as a 3D scaffold to imitate the brain like extracellular matrix. The photocrosslinkable nature of this hydrogel allowed the fine-tuning of the mechanical properties to mimic brain tissue as 20s UV light exposure resulted in a compressive modulus of 1.27±0.17kPa which is similar to brain tissue[166](Fig. 4. 13).

Live/dead analysis of the encapsulated monocytes at these conditions was carried out at day 1 and day 7 of encapsulation without drug delivery treatment (Fig. 4.14). The green stain show the live cells and the red the dead cells with over 90% cells remaining viable at day 1 and over 80% at day 7.

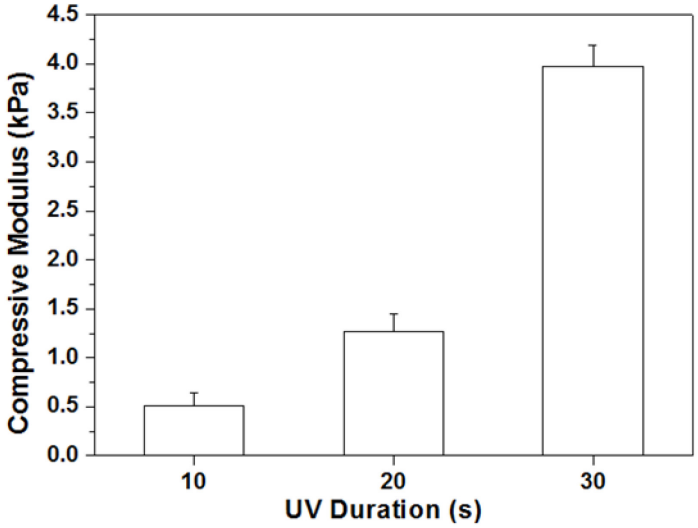

Figure 4.13. Mechanical properties of in vitro brain model. Compressive modulus of monocytes encapsulated in 5% GelMA photocrosslinked with varying UV light durations indicates 20s as optimum time for similar mechanical properties to brain (n=5).

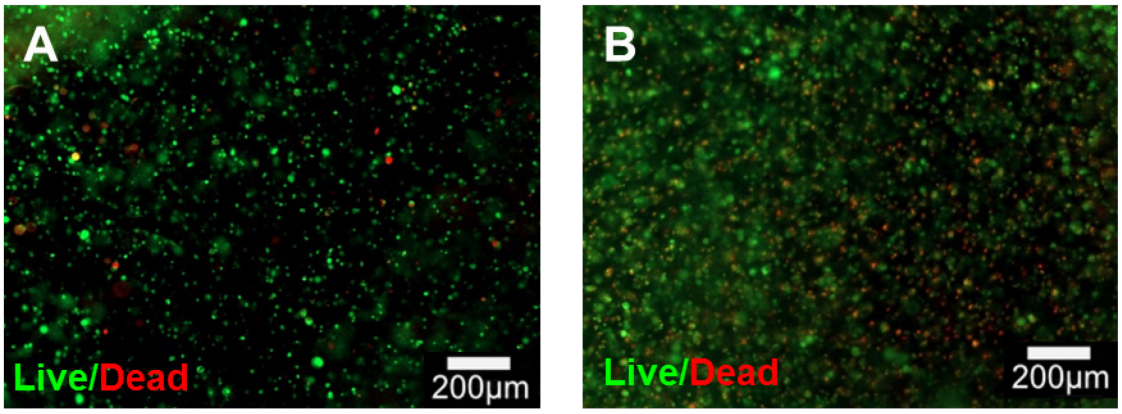

Figure 4.14. Survival of monocyte cells encapsulated in 5% GelMA system as an *in vitro* model for brain immune response. A) Monocytes stained using calcein (green) for live cells and ethidium homodimer-1 (red) for dead cells showing minimal cell death during procedure at day 0. B) Monocytes stained using calcein (green) for live cells and ethidium homodimer-1 (red) for dead cells showing minimal cell death during procedure at day 7.

4.3.7 Chronic Studies: Monocyte Model

Once the monocyte model had been created, different test conditions for the drug delivery profile had to be designed. The profiles chosen are shown in Table 1 with all except the negative control receiving an initial infusion of DEX or IL-4 and three of those then receiving twice weekly infusions of either DEX or IL-4.

Table 4.1. Drug delivery profile of each test condition for chronic 3 week study.

Delivery Profile	A	B	C	D	E
Initial Infusion	None (NC)	DEX	IL4	DEX	IL4
Repeated Infusion	None	DEX+	None	IL4+	IL4+

Firstly, samples were analysed for cell survival, which was quantified using Image J (Fig. 4.16A). As is apparent in the microscope images themselves, the samples from week 1 (Fig. 4.15A-E) have significantly better cell survival than those at week 2 (Fig. 4.15F-J).

When quantifying the ratio of cells with M2 (green) pro-healing versus M1 (red) pro-inflammatory phenotype, the negative control showed an increase from week 1 to week 2 without any infusion of anti-inflammatory factors (Fig. 16B). At week 2, the negative control statistically had the same ratio of M2:M1 cells as the samples with only one infusion of IL-4 and was performing better than those with repeated injections of DEX. By week 2 both conditions which involved repeated injections of IL-4 resulted in significantly increased ratios of M2:M1 macrophages, with the IL-4 initial and IL-4 follow up injections samples increasing the ratio 6 fold versus the negative control at this time point. In order to strengthen these findings, the next stage was to repeat the tests with

primary astrocytes (the main cell type in a glial scar) and carry out immunoassays for released inflammatory cytokines.

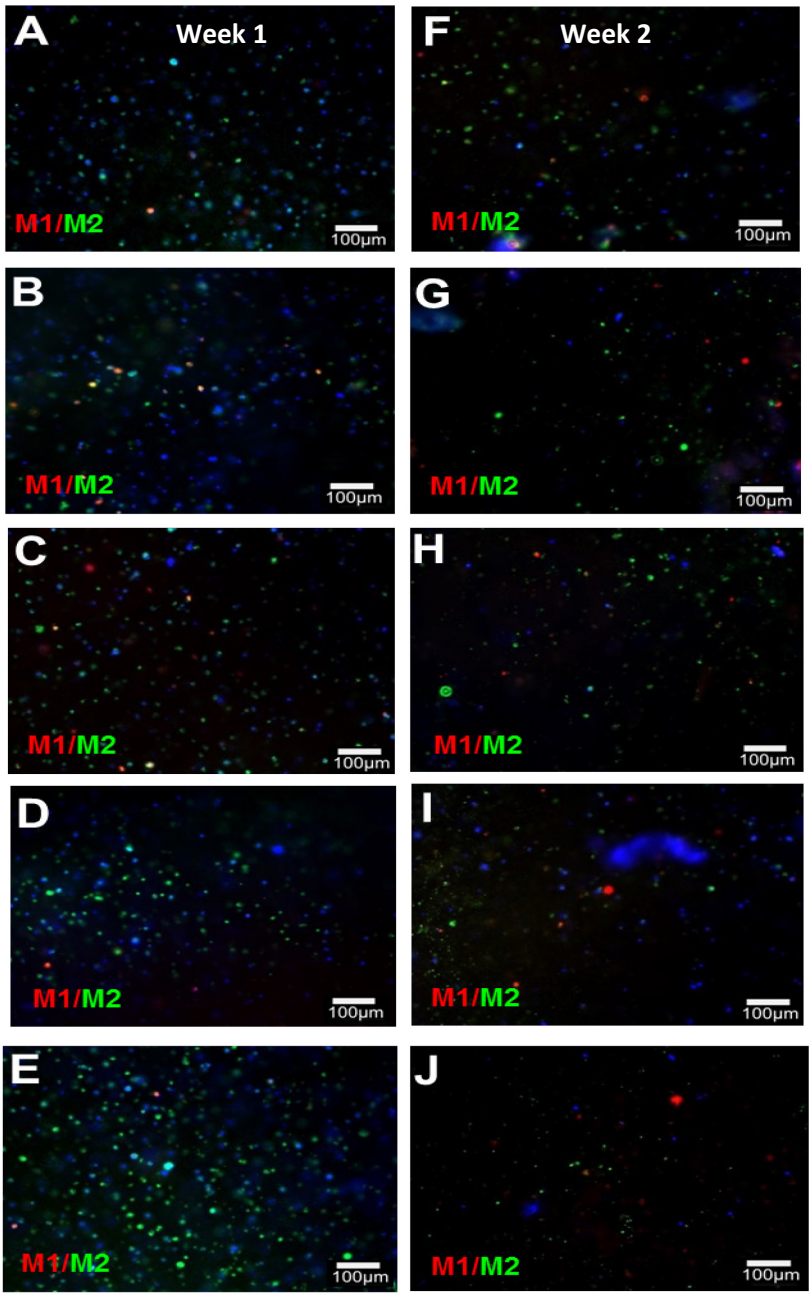

Figure 4.15. Phenotype of monocytes after different drug delivery profiles through hydrogel system. Immunostaining of CD206 (green) as an M2 macrophage, nuclei (blue), and 27E10 (red) as an M1 macrophage at week 1 for profiles listed in Table 1 A) delivery profile A; B) delivery profile B; C) delivery profile C; D) delivery profile D; E) delivery profile E and for week 2 for F) delivery profile A; G) delivery profile B; H) delivery profile C; I) delivery profile D; J) delivery profile E.

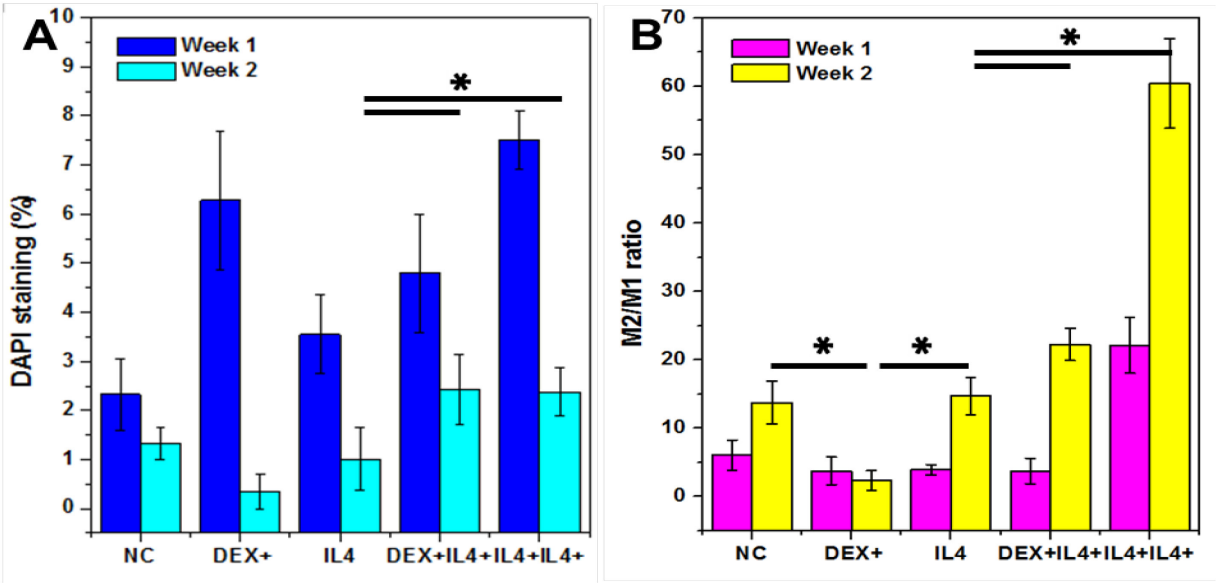

Figure 4.16. Quantification of macrophage survival and phenotype A) Surviving cell count at weeks 1 and 2 determined by percentage DAPI staining evident B) Ratio of M2/M1 differentiated macrophages for all delivery profiles at 1 and 2 weeks indicating that repeated infusion of IL4 significantly increases the presence of pro-healing M2 macrophages (n=4, average of 5 images per sample quantified).

4.3.8 Chronic Studies: Astrocyte Model

In contrast to the monocyte cell results, there was no evidence of significant cell death between weeks, which resulted in tests being run for three weeks rather than two. By the end of three weeks, both the negative control and the samples with DEX injections only had some astrocytes with long extended features but no evidence of a strong network of cells (Fig. 4.19A and B). The samples with a single injection of IL-4 showed an increased number of living cells with a more substantial network (Fig. 4.19C), however, the samples with repeated IL-4 injections clearly had the healthiest networks of astrocyte cells (Fig. 4.19D and E). Attempts were made to quantify the inflammation of cells using GFAP marker but the staining was minimal and inconsistent (Appendix 2).

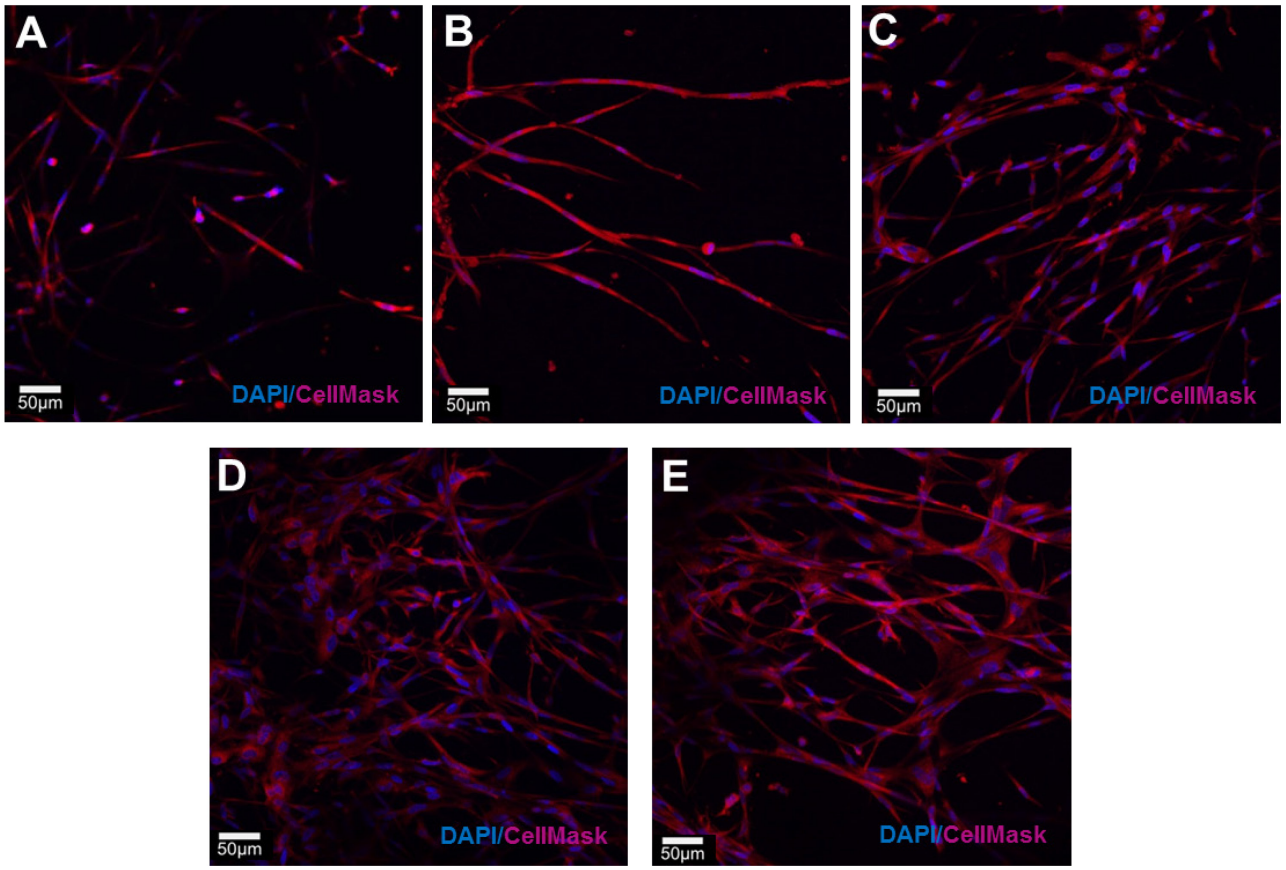

Figure 4.17. Confocal stacks of astrocytes after 3 weeks of different drug delivery profiles through hydrogel system**.** DAPI staining (blue) for nuclei and Cell Mask 649 (red) for cell structure A) delivery profile A, B) delivery profile B, C) delivery profile C, D) delivery profile D, E) delivery profile.

ELISA immunoassays were also used to calculate the expression of inflammatory markers from the cell encapsulated hydrogels at week 1 and week 3. TNF-α is often viewed as the most consistent and unambiguous marker for cell inflammation and its release from samples was measured at week 1 and week 3 (Fig. 4.20A). There was no significant difference between samples at one week and three weeks indicating that inflammation is stable throughout this period. The negative control (profile A) had significantly increased inflammation versus those with an IL-4 injection, DEX and a

repeated IL-4 injection and IL-4 repeated injections only with p values of 0.03, 0.0004 and 0.0002 respectively. Repeated DEX injections did not cause significant changes in inflammation versus the negative control or the IL-4 single injection, however, both DEX (p=0.02 and p=0.03) and IL-4 single injections (p= 0.01 and p=0.02) had significantly higher amounts of TNF-α released than either of the repeated IL-4 injected samples. There was no significant difference in the repeated IL-4 injections between those injected with DEX or IL-4 initially. IL-6 is another marker of inflammation and its expression was also measured at 1 and 3 weeks (Fig.4. 20B). There were no significant changes in inflammation between the negative control, the repeated DEX injections or the IL-4 single injection. All samples with repeated IL-4 injections had significantly reduced release of IL-6 versus the negative control (*p*=0.01 and 0.003) or the repeated DEX injected samples (p=0.04 and *p*=0.002).

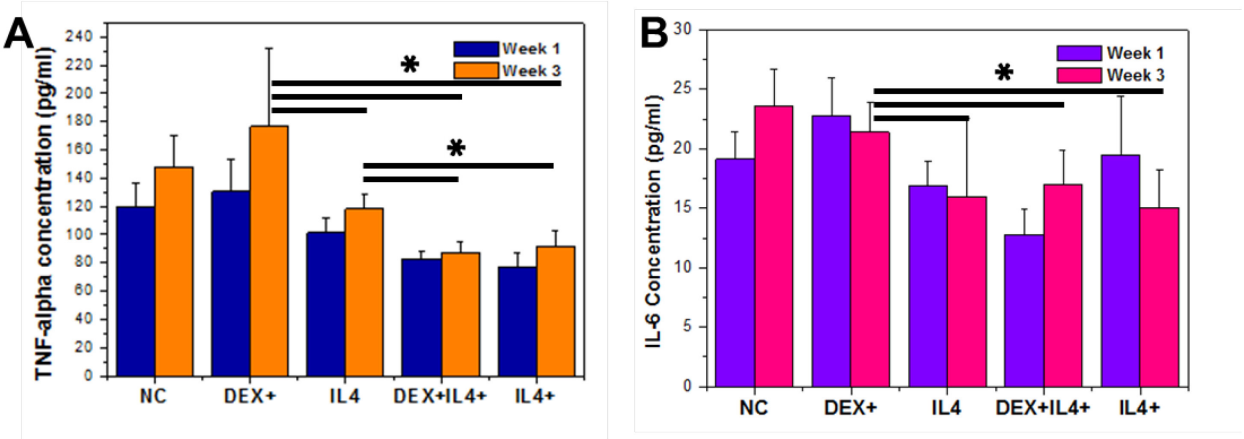

Figure 4.18. Pro-inflammatory marker release from astrocytes after 3 weeks of different drug delivery profiles through hydrogel system A) TNF-α at Week 1 and 3; B) IL-6 at Week 1 and 3 (n=4).

4.4 Discussion

The concept of the dual layer system is to minimise the brain's inflammatory reaction through a variety of key features as well as providing steady release of anti-inflammatory factors. It involves a drying stage to minimise the size and increase the stiffness of the implant for easy insertion. It also allows reswelling of the coating on insertion which could reduce the damage to the surrounding tissue caused by micro-motion of the electrode as well as making the electrode surface more mechanically compliant and similar to brain tissue. The multi-faceted nature of such a design meant that every stage of material choice and fabrication design needed careful analysis.

The contraction of agarose derived microchannels during the drying stage of fabrication could be an advantage when looking to miniaturise the system, however, it does affect the reproducibility of the microchannels. Overall, they had limited potential for success in this system due to high breakability, particularly in their post drying and reswelling state or in complex architectures. Alginate suffered similar reproducibility problems with fibres being uneven and although bioprinted, could not adhere to where they were printed in the hydrogel and often had to be repositioned manually. For this reason, the utilisation of hair as a strong and consistently small diametered fibre was ideal for this application. In future this could be replaced by a similar polymer fibre with precisely defined properties.

The hydrogel selection process highlighted the necessity for a strong enough formulation to retain the microchannels through all processing steps without excessive crosslinking resulting in sacrificial fibres being too difficult to remove when required. As the compressive modulus of brain tissue is around 1kPa[166] all 3 of the formulations

investigated were strong enough to resist deformation by the brain tissue itself whilst not being so stiff that they caused a mechanical mismatch between the implant surface and the brain which has been shown to increase the brain's immune reaction to implants[57]. The reswelling profiles of all formulations were similar and should result in better anchorage of the implant post insertion, reducing damage due to micromotion[48]. As 10%GelMA/2% PEG was the only formulation to remain crack free throughout all drying and reswelling processes it is presumed that the long chain crosslinking monomer is situated between GelMA chains and provides extra crosslinking and therefore resistance to cracks. For this reason, as well as its thickness of only 350±20µm in the dry state, this formulation was chosen for the chip.

The PDMS membrane was added to the system to prevent degradation of the system and to slow down diffusion over time. A membrane with 100µm pores with a 400µm spacing was utilised for this purpose but smaller pores or different configurations could be used in future.

All elements of the dual layered drug delivery system were brought together in the form of a simple square chip in order to test the drug delivery profiles of different potential anti-inflammatory factors. Fluorescently labelled molecules allowed the simple quantification of diffusion over time with different molecular weights of FITC-Dextran and the FITC isomer being used to represent cytokines and small drugs. As the molecules have no charge and their MW is directly related to the hydrodynamic radius which affects their diffusion, this is often used as a quantification method[167].

Both 40kDa and 20kDa FITC-Dextran could be released for up to four days, which allowed infusion profiles for cell testing to be twice weekly to ensure cells would have a constant supply of our anti-inflammatory factors delivered to them. The 40kDa FITC-Dextran's delayed peak release at 48hr is something that could be utilised when trying to release factors at precise stages of inflammation reaction for an optimised drug delivery profile in future. The repeated trials with 8hr timepoints for the smaller molecules confirmed the steady release of 20kDa FITC dextran over this period and also showed minimal burst release of even the small drug molecule model FITC isomer. As burst release profiles are a common problem in drug delivery systems, this indicates that this system could release factors in a much more controlled method than previous studies[76,83,85]. These results showed an interesting contrast to the simple diffusion co-efficient calculated optically through the hydrogel, where the co-efficient for 20 and 40kDa FITC-Dextran were not significantly different. This may be due to the addition of the porous PDMS membrane to the system or the diffusion co-efficient only looking at 2D diffusion but emphasises the importance of setting up experiments that really mimic the conditions you will see *in vivo*. It is also important to note that drug dosages were selected based on previous work whereby drugs were administered directly to cell culture system. Further optimisation could be carried out in order to determine a graded concentration-response curve and to determine the initial infusion dose required to give the desired response once the drug has traversed the system.

In order to allow monocytes to survive for weeks in *in vitro* experiments and to exist in a more brain-like environment, they were encapsulated into a 5% GelMA hydrogel that could be contained by the chip's membrane frame to ensure direct contact during tests.

The photocrosslinking properties of GelMA allowed the fine-tuning of the mechanical properties to mimic brain tissue as 20s UV light exposure resulted in a compressive modulus of 1.27±0.17kPa which is similar to brain tissue[166]. Live/dead tests also showed that the cells showed good survival over 1 week as more than 80% of cells were still viable at this stage.

However, during chronic tests with our different drug delivery profiles, it was clear that samples from week 1 had significantly better cell survival than those at week 2. This may be due to the sample brain model thickness of 600µm being too thick to allow nutrients to pass through the gel, particularly at such a high density of 6 million cells/ml. The negative control which had no infusion of anti-inflammatory molecules had a high number of M2 anti-inflammatory macrophages present, implying that the chips themselves do not have an adverse effect on the cells.

Despite the reduction in cell survival and the loss in integrity of samples between weeks 1 and 2, there were still clear trends in polarisation of the monocytes. Even a one time injection of IL-4 improved the ratio of M2:M1 polarisation with repeated injections showing significant effects including a six-fold increase for the IL-4 initial and repeated infusion profile versus the negative control. The relative lack of success of DEX injections was a surprising result as DEX is a well-established anti-inflammatory drug but it may have its effect without altering the phenotype of the macrophages. Alternatively, the mechanisms of action may be similar to that of IL-4, resulting in complementary action when the two strategies are combined – resulting in no measurable reduction in inflammation by the addition of DEX. DEX's mechanisms of action are not clearly defined so this would require further testing to confirm.

In order to investigate further, the drug delivery trials were repeated with an astrocyte brain model (see Chapter 3). In this case the hydrogel system allowed the cells to survive easily for a 3 week period so cell networks were only imaged as this was the latest timepoint measured and can be considered a chronic stage of inflammation[40]. The improved cell survival may be due to the robust nature of astrocyte cells, an increase in GelMA strength of surrounding material or most likely is a reflection of the reduced cell seeding density of 1 million cells/ml which ensured all cells would receive more nutrients. Again, the microscope images show the positive effects IL-4 had on creating a healthy network of astrocytes. The ELISAs for TNF-α showed no significant difference in the repeated IL-4 injections between those injected with DEX or IL-4 initially, which implies that it is the repeated nature of IL-4 injections causing the reduction in inflammation over the three week period as they have the lowest values.

Interestingly, there was no significant difference in IL-6 release between any of the repeated IL-4 injections or a single IL-4 injection which implies that the first few days of inflammation may be the most significant for this cytokine. Overall both TNF-α and IL-6 release data shows that repeated injections of IL-4 could be used to reduce the inflammatory response of brain tissue to an electrode over time, although it must be noted that TNF-α expression did still slightly increase between week 1 and 3.

4.5 Conclusions

The previous chapter has indicated that the reduction of the brain's inflammatory response to an implant could not be controlled by surface topography alone and that a more aggressive strategy to realise the second objective of this thesis was required. This chapter has reported on the findings of the experiments undertaken as part of this study. These experiments took the form of designing a drug eluting coating capable of delivering anti-inflammatory factors to brain tissue for weeks rather than days and required several stages of optimisation and assessment and in doing so, the chapter provides answers to research questions 3 and 4.

Firstly, a dual layered microfluidic system was developed. It can be inserted in a thin dry state and then be held firmly in place by its own reswelling, protecting the brain against damage caused by micromotion of the probe. This system consists of an 80±16µm channel created by a sacrificial fibre in a thin GelMA-PEG composite hydrogel surrounded by a PDMS membrane with a microporous structure, which can be dried to 350±20µm thickness propagating increased stiffness for easy insertion. Next, it was established that the system can easily be infused with a range of anti-inflammatory factors at body temperature for a period of at least three weeks without degradation. Furthermore, the system allows the slow steady release of cytokine like molecules for at least four days and shows minimal burst release of small drug like molecules. This allowed a test profile of varying combinations of IL-4 and dexamethasone to be designed.

Once the system had been shown to successfully deliver multiple factors long term, a brain-like cell model needed to be developed in order to assess the potential of these anti-inflammatory factors to reduce inflammation of the brain chronically. Hydrogels encapsulated with monocytes were developed and were able to last in an in vivo mimicking environment for a minimum of 2 weeks. The previous astrocyte hydrogel model also allowed survival of cells for up to 3 weeks. Finally, upon delivery of the anti-inflammatory profiles, the repeated infusion of IL-4 caused both an upregulation in M2-induced macrophages over 2 weeks and a down regulation of both TNF-α and IL-6 in astrocytes over a 3 week period. DEX infusion had no effect on either of these measured outputs, however, further work must be done to assess the mechanisms of DEX's anti-inflammatory effects as these are well recognised elsewhere in the body.

In summary, this chapter answered research question 3 by showing that a dual-layered microfluidic system was capable of delivering anti-inflammatory factors with steady release for up to 96hrs and that these infusions could be repeated easily over 3 weeks. The chapter also answered research question 4 by showing that these infusions resulted in improvements in anti-inflammatory effects in vitro – which in turn strongly implies that repeated infusions of anti-inflammatory factors like IL-4 for weeks via this microfluidic system could be utilised in the future to reduce the formation of a glial scar around neural implants. The final experimental chapter will involve determining the dimensions of a probe that are required to successfully deliver therapeutic temperatures to the depths required in the human brain and optimising such a system in order to address the final two research questions and achieve the thesis's first objective.

5 An experimentally validated Thermal Model for Cooling Neural Probes

5.1 Introduction

Cooling has long been a method employed in healthcare to reduce damage to tissue. Reducing the body temperature of patients after cardiac arrest when blood flow to the brain has temporarily stopped is now common practice. This is known as Targeted Temperature Management or Protective Hypothermia and functions by mitigating neuronal damage and The potential of neural probes to offer therapeutic cooling was first highlighted in the 1980s.[107] However, no studies have attempted to ensure sufficient cooling below brain temperature can reach the depths of the human hippocampus and sub thalamic nucleus, where the majority of interventions are needed for debilitating neural conditions[12,26,168]. The exact temperature of brain tissue required to deliver therapeutic advantages is reported as being anywhere between 20-30°C, with discrepancies in the difference between the cortical surface temperature and the resulting target area temperature of approximately 5°C.[109,110,112,113,115,169] For this reason, a 10°C drop in temperature between the probe tip temperature (27°C) and the brain tissue (37°C) was selected as an initial target.

Despite the shift in research towards electrically stimulating probes for DBS, some studies have been carried out to demonstrate the potential of alternative focal cooling techniques in animal models. One such study designed a probe system for cooling the forebrain of the zebra finch via a Peltier thermoelectric module[133]. Derived heat transfer equations describing the system were utilised to analyse and optimise the effects of

variable parameters before validation experimentally. A probe with a total diameter of 800μm consisting of a silver probe with a polyimide tube as coating with an entrapped layer of air was used due to its low thermal conductivity. A core with two thirds the inner diameter of the polyimide tubing, the remaining third being the air gap, produced optimal cooling. For a distance of 2mm into the brain, these devices were able to cool the tip of the probe by 11°C as a result of the 15°C temperature drop at the Peltier device.

Another interesting thermal model of a DBS electrode was devised by Elwassif *et al* (2006) in Comsol® in order to assess the effects of joule heating on the surrounding brain tissue during periods of electrical stimulation[134]. They found that temperature of the brain tissue could be increased by 0.8°C during periods of high stimulation and prolonged durations of stimulation exacerbated these outcomes. Although not increasing to a dangerous level, it was noted that temperature increases of 1-2°C could affect neuronal function and advised the design of DBS electrodes to take this potential effect into account when specifying maximum operating ranges. Although no experimental validation was carried out, their work demonstrated the design of a simple finite element method (FEM) model of a neural probe and the characterisation of important effects.

This chapter presents the numerical and experimental work carried out to assess the viability and performance of a cooling probe capable of reaching the hippocampus and subthalamic nucleus in humans. An FEM model was used to assess the optimal ratio of a thermally conductive core to insulating coating within a 2mm probe to deliver the maximum cooling to brain tissue 10cm deep. Once this was established, the model was

used to determine the minimum temperatures that can be achieved 10cm into the brain using a 2mm diameter probe with prospective insulating coatings. These results were used in equations to choose a Peltier cooling device and heat sink set up to achieve this, before validating the model experimentally. Once the model was validated, it was used to predict the required thicknesses of conducting core and insulating coating material to reach specific target temperatures.

5.2 Methods

5.2.1 Probe Design

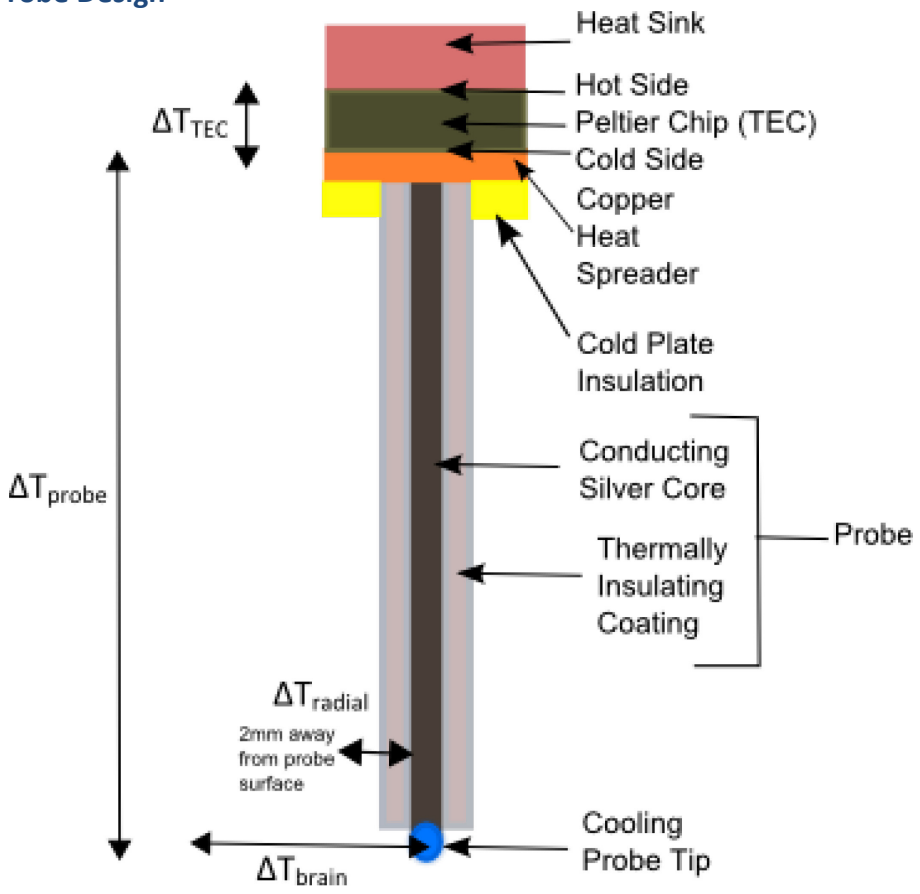

Figure 5.1. Design and components of a Peltier cooled neural probe, defining all temperature differences to be used throughout this chapter. The probe consists of two parts which will be referred to as core or insulation, probe refers to the combination of the two.

The probe consists of a conduction core and thermally insulating layer connected to a Peltier chip. An electric current passes through the Peltier and generates a cold temperature at one plate and a hot temperature at the other. The probe is connected to the cold plate via a heat spreader and the hot plate is cooled via a heat sink. Probe diameter dimensions are referred to in terms of the ratios of core:insulation as outlined in Table 5.1. The probe length is a constant 10cm for all trials.

Table 5.1 Ratios of probe to insulation according to their total probe diameter.

Probe Total Diameter (mm)	3:1 core:insulation dimensions (mm)	1:1 core:insulation dimensions (mm)	2:3 core:insulation dimensions (mm)
2	1.5:0.5	1:1	0.8:1.2
3	2.25:0.75	1.5:1.5	1.2:1.8
4	3:1	2:2	1.6:2.4
5	3.75:1.25	2.5:2.5	2:3
6	4.5:1.5	3:3	2.4:3.6

5.2.2 Probe Comsol® Model

A steady state heat transfer model was developed using Comsol® 4.3. As the probe is cylindrical and therefore exhibits symmetry through the centre of the probe, it was modelled using 2D axisymmetric methods. The core was made of silver due to its high thermal conductivity and inert nature, with models using HA and PDMS of various thicknesses as the insulating coating as well as an uninsulated control. Brain tissue was modelled as a solid with a thermal properties from the literature[133]. The design utilised for the model is outlined in Figure 5.1 and include a copper heat spreader, with an insulating poly(methyl methacrylate) (PMMA) layer as cold plate insulation between the copper and the brain. Temperature boundary conditions were set as 37°C for the brain temperature at 5cm distance from the probe in any direction to represent the brain temperature as an infinite solid with the ability to constantly maintain a temperature of 37°C due to vascularisation of tissue. The cold plate temperature was a variable input above the heat spreader in order to identify different temperature profiles. The Comsol® configuration is shown in Figure 5.2.

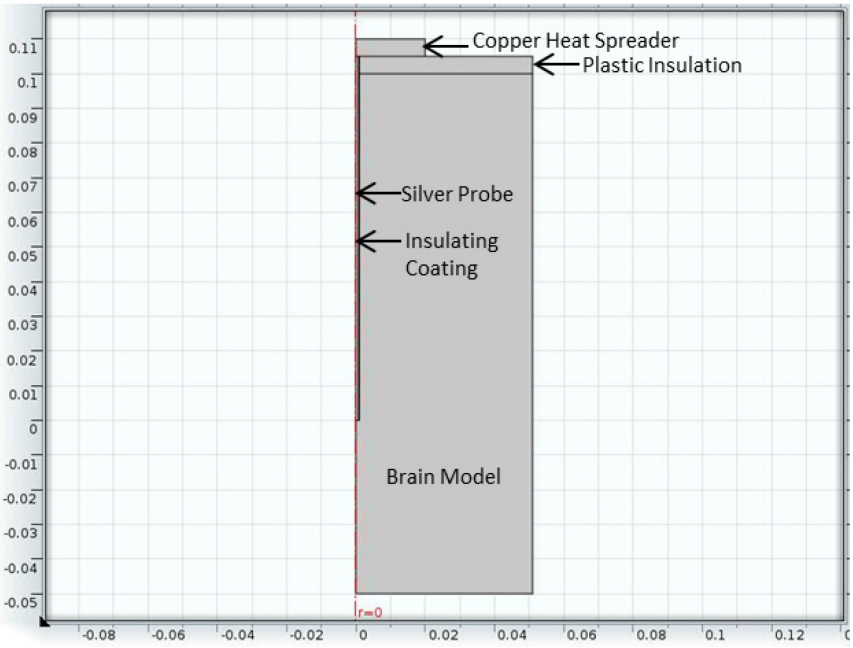

Figure 5.2. Initial model dimensions in Comsol®.

5.2.3 Thermoelectric Module and Heat Sink Design

Thermoelectric modules and the required heat sink parameters are modelled using the Peltier manufacturer's specifications and the heat flux magnitude calculated from Comsol® and the following heat transfer equations readily available in the literature[170]:

$$Z = \frac{2\Delta T_{max}}{(T_{h-}2\Delta T_{max})^2} \tag{5.1}$$

$$S_m = \frac{V_{max}}{T_h} \tag{5.2}$$

$$K_{m=}\frac{(T_h - T_{max})V_{max}I_{max}}{2T_h\Delta T_{max}} \tag{5.3}$$

$$R_{m=}\frac{(T_h - T_{max})V_{max}}{T_h I_{max}} \tag{5.4}$$

$$Q_c = S_m T_c I - 0.5I^2 R_m - K_m \Delta T \tag{5.5}$$

$$V = S_m \Delta T + I R_m \tag{5.6}$$

$$R_{HS} = \frac{T_h - T_a}{Q_c + Q_p} \tag{5.7}$$

Where: T_C is cold side temperature, T_h is hot side temperature, T_a is the ambient temperature, Q_C is the heat pumped at the cold side of the Peltier, Q_p is the power input for the Peltier, ΔT_{max} is the maximum temperature difference between the plates, I is current, V is voltage, Z is the figure of merit for the Peltier, S_m is the device's Seebeck resistance, R_m is the device electrical resistance, K_m is the device thermal conductance and R_{HS} is the thermal resistance of the heat sink.

5.2.4 HA Dipcoating

A slurry consisting of 30% HA (Sigma Aldrich), 20% de-ionised (DI) water, 50% ethanol (Sigma Aldrich), 3% polyethylene glycol (Sigma Aldrich) and 7% Glycerol (Sigma Aldrich) was homogeneously mixed in an ultrasonic bath for 1hr. A 100mm long silver wire (99.99% annealed, Advent Materials) was dipped in the slurry and removed at a rate of 200mm/min before drying in a furnace (Lenton, Hope, UK) at 150°C for 30min. Once the sample had cooled, this practice was repeated 4 times before a final sintering stage at 750°C for 3hr. Average thicknesses of the coatings were measured using Vernier Calipers at 4 points along each probe. HA's conductivity can be analytically calculated using values of porosity and density, however, these values are not always accurate and porosity and density values themselves are difficult to assess. It can also be determined experimentally using precise dimensions and conduction of a known temperature gradient across resistors. However, the dipcoated coatings were unable to be separated

in one piece from the probes or a plate they were coated onto so an average value was taken from the literature[119,120,171].

5.2.5 PDMS Coating

PDMS (Sylgard 184, Dow Corning) was mixed at 10:1 ratio with its curing agent and allowed to rest for 1hr to ensure there were no remaining air bubbles entrained in the liquid. The PDMS was then poured into a petri dish to the required depth and partially cured in oven at 60°C for 20min. A partially cured strip with 20mm diameter was removed from the dish and wrapped vertically or diagonally around the silver wire leaving 5mm exposed at the tip before returning to the oven for a further 40min to complete the curing process. The conductivity of PDMS was taken from the literature[147–149].

5.2.6 Brain Analogue

A porous plant foam (Amazon) was utilised as a thermal model for brain tissue as it could be saturated with 37°C water resulting in similar thermal properties to those of brain tissue. It still retained excellent mechanical properties when saturated allowing probe insertion and support of the device.

5.2.7 Scanning Electron Microscopy (SEM)

All images were captured using a Zeiss Ultra Scanning Electron Microscope (Carl Zeiss Microscopy, Jena, Germany) following surface coating with gold-palladium using a sputter coater (Cressington Scientific Instruments, Watford, UK).

5.2.8 Experimental Validation

A schematic of the experimental set up is shown in Figure 5.3. The probe was soldered to a copper heat spreader (40mm*40mm) and then coated as required. The copper heat spreader was anchored to a Peltier chip with a fan cooled heat sink on the other side

using thermal paste. This probe model was inserted into the brain model encased in a 3D-printed 100mm*100mm support cage and placed in a water bath at 37°C. The current applied to the Peltier device was varied and the temperature of the hot plate, cold plate and the tip of the probe recorded using thermocouples and temperature probes.

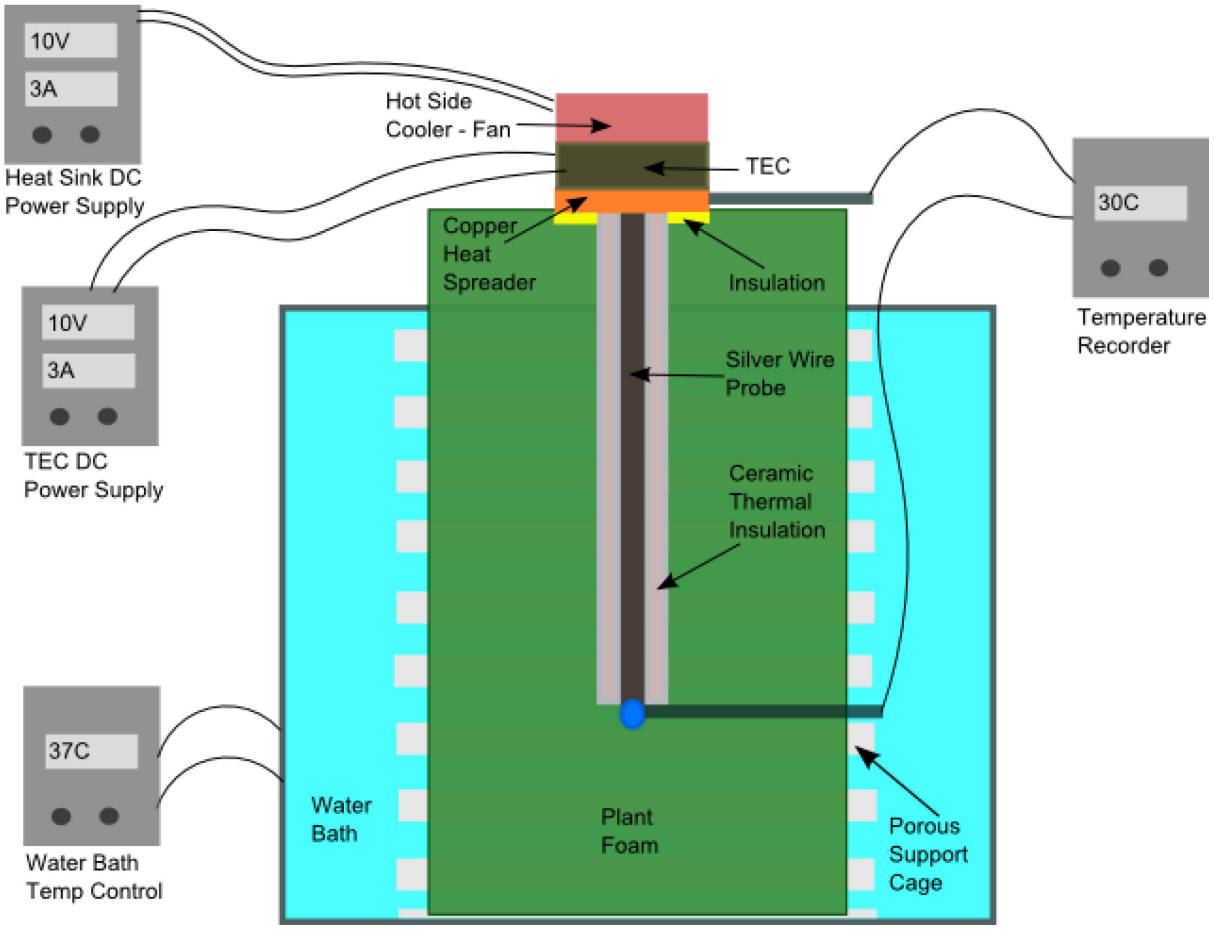

Figure 5.3. Schematic of experimental setup for validation.

5.3 Results

5.3.1 Probe Coating

During preliminary work with HA slurry creation, 10/20/30% HA solutions were tested. The 10% slurry did not provide enough HA to allow build-up of layers to a thick coating and 30% HA causing clumping of HA and an uneven coat. Further optimisation studied a range of 16% to 24% HA whereby 20% was found to be the optimum level for building layers of even thickness. In order to achieve thicknesses of 230±22µm, 4 dip coats with intermediate sintering stages (to 150°C) were required before final sintering at 750°C. Although coatings with a 20% slip solution ensured an even layer per dip, the repeated nature of the dips required increased the number of cracks in the coating (Fig. 5.4). With two coats of HA only, cracks were not visible to the naked eye, and were less than 20µm in width (Fig. 5.4A-C), whereas with 4 coating stages, the cracks were clearly visible, more frequent and increased in size to approximately 50µm width (Fig. 5.4D-F). Some evidence of aeration was present with bubble outlines of up to 500µm diameter present on the surface of the sintered coatings.

PDMS coating was tackled with 3 main strategies with varying degrees of success. A simple dip coat resulted in solidified drips attached to the coating (Fig. 5.5A). A diagonal wrap of partially cured PDMS left a tightly would coating with all junctions fused by the final curing step, whereas a simple horizontal wrap resulted in a less tight and uniform structure (Fig. 5.5B and C).

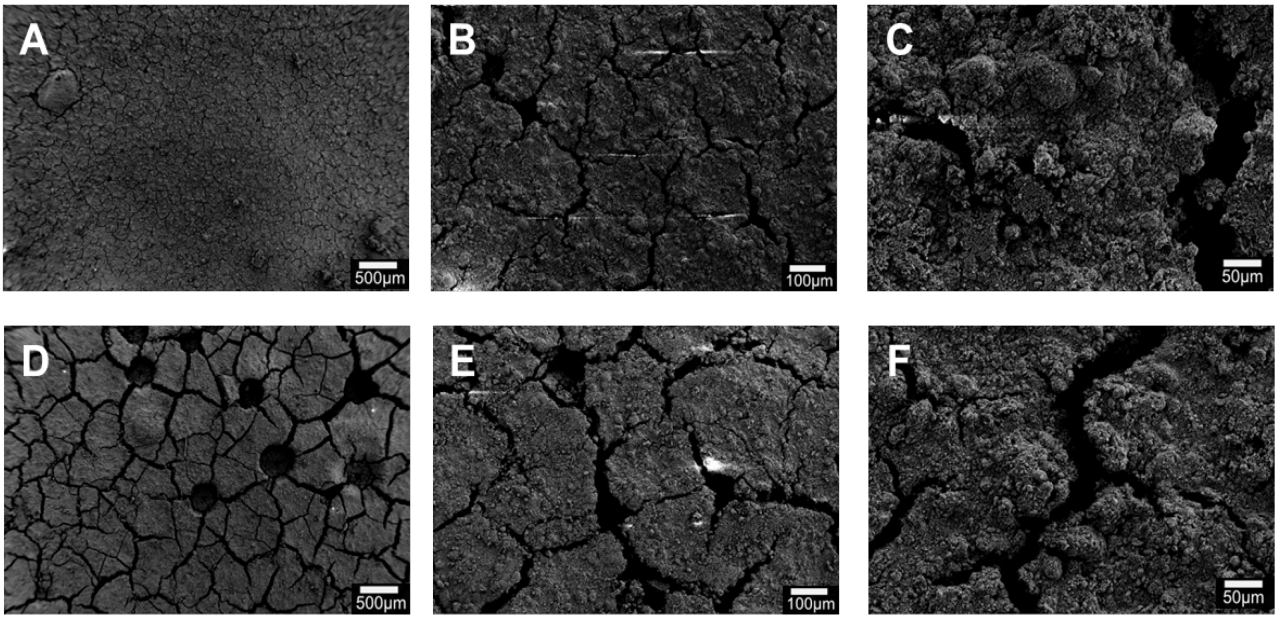

Figure 5.4. SEM Images of HA dipcoated coatings A) 2 coats of HA at 25x magnification; B) 2 coats of HA at 100x magnification; C) 2 coats of HA at 600x magnification; D) 4 coats of HA at 25x magnification; E) 4 coats of HA at 100x magnification; F) 4 coats of HA at 600x magnification.

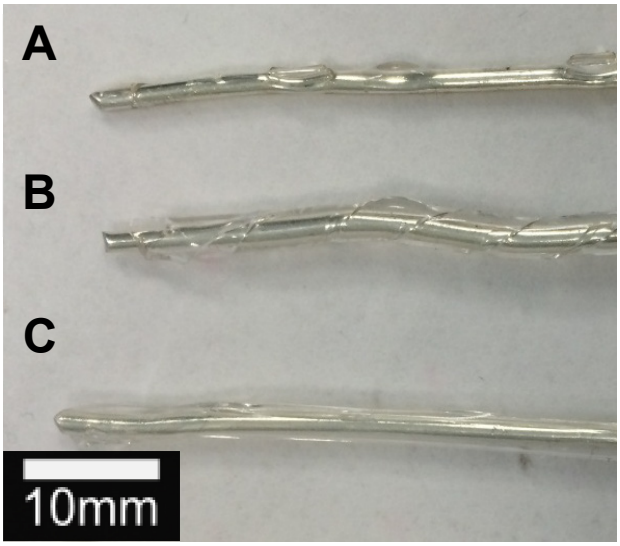

Figure 5.5. Image of PDMS coated probes A) dipcoated; B) Diagonally wrapped partially cured PDMS; C) Horizontally wrapped partially cured PDMS.

5.3.2 Probe Comsol® Model: Thickness Ratio

In order to determine the optimum ratio of thermal conducting core to insulating coating, identical 2mm diameter probes were numerically modelled using standard dimensions of silver wire as the conducting core, with the remaining thickness consisting of HA. A T_C of 0°C was initially utilised to compare the cooling capacity of each probe. By plotting the temperature profile along the length of the probe, it is clear to see that 1.5mm and 1.75mm silver probes offer enhanced cooling at the tip, with 33.9°C and 33.3°C tip temperatures respectively, whereas 0.5mm and 1mm silver probes resulted in tip temperatures of only 35.6°C and 36.8°C respectively (Fig. 5.6).

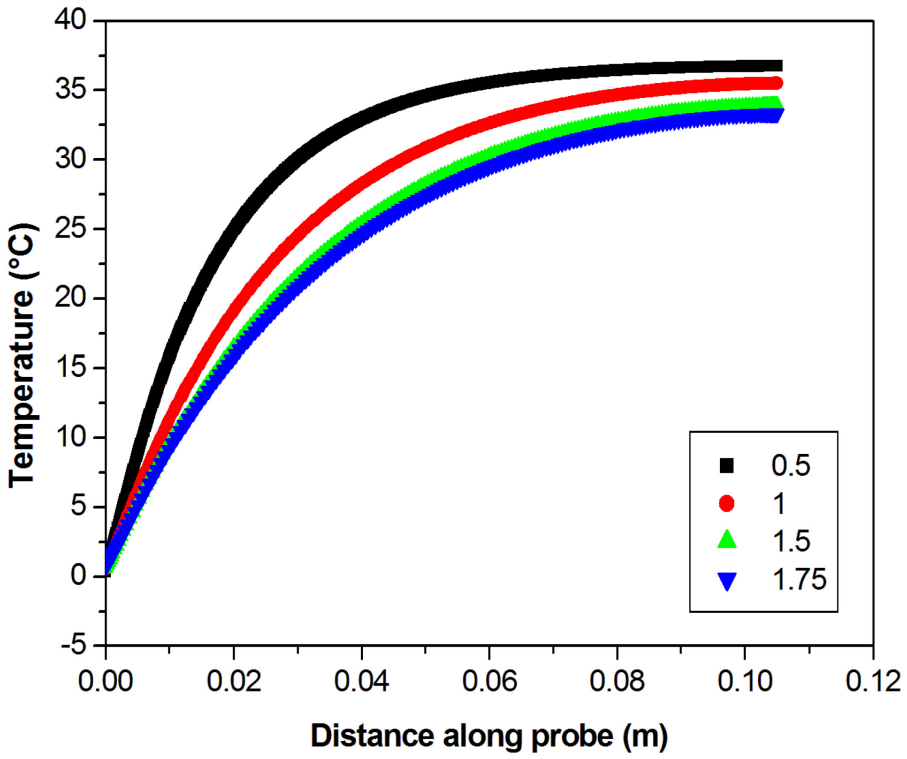

Figure 5.6. Influence of increasing thicknesses of silver cores between 0.5mm and 1.75mm on temperature profile along probe length. The lowest temperature at the tip is achieved with the thickest silver core (1.75mm).

However, the radial temperature profiles along the probe must also be considered in order to assess the insulating function of the coating. In order to do this, the radial temperature was modelled at the probe mid-point and the probe tip. At the midpoint of the probe there is a temperature difference of 1.6°C between the 1.5mm and 1.75mm probe at the coating-brain interface – the 1.5mm probe with the added 0.125mm HA insulation results in a brain temperature of only 31.4°C compared to 29.8°C (Fig. 5.7).

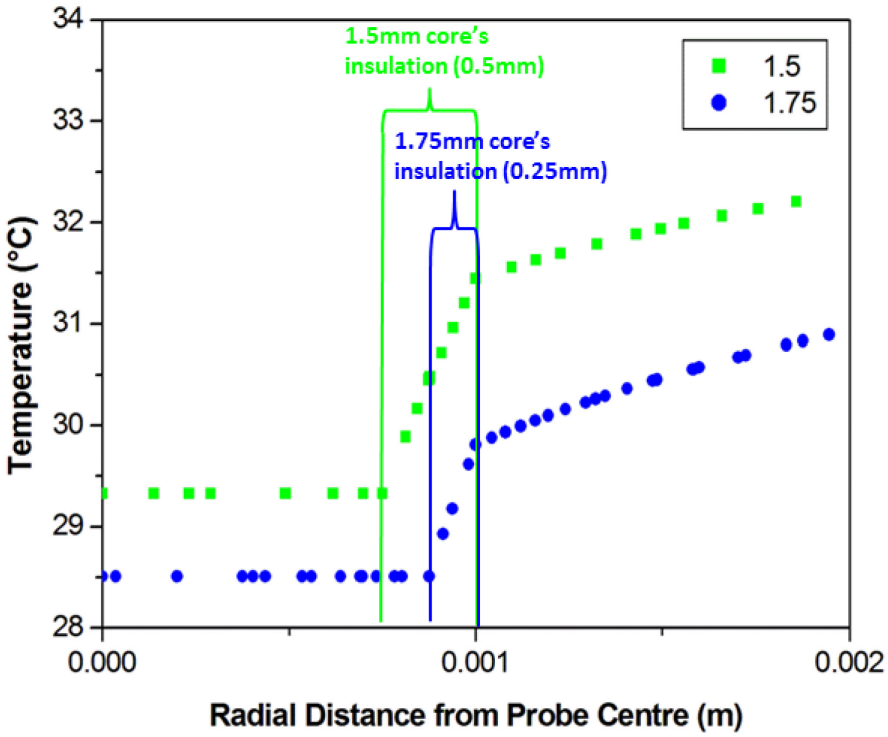

Figure 5.7. Influence of increasing insulation thicknesses on temperature radially for core diameters of 0.5mm to 1.75mm. The added insulation for the 1.5mm silver core results in better insulation along the probe length with a temperature difference between the two models of 1.6°C at the midpoint vs only 0.6°C at probe tip.

5.3.3 Peltier Chip Design

Before building and validating the model, the feasibility of using a Peltier chip to reach the temperatures required had to be assessed using the heat transfer equations listed

in the methods section - calculations which also help design the heat sink system. Figure 5.8 shows the T_C required to achieve a range of ΔT_{brain} for different core thicknesses for a total probe diameter of 2mm. In order to achieve even 4°C cooling at the probe tip, a T_C of -10°C is required at the cold side of the Peltier with a 1.5mm or 1.75mm core.

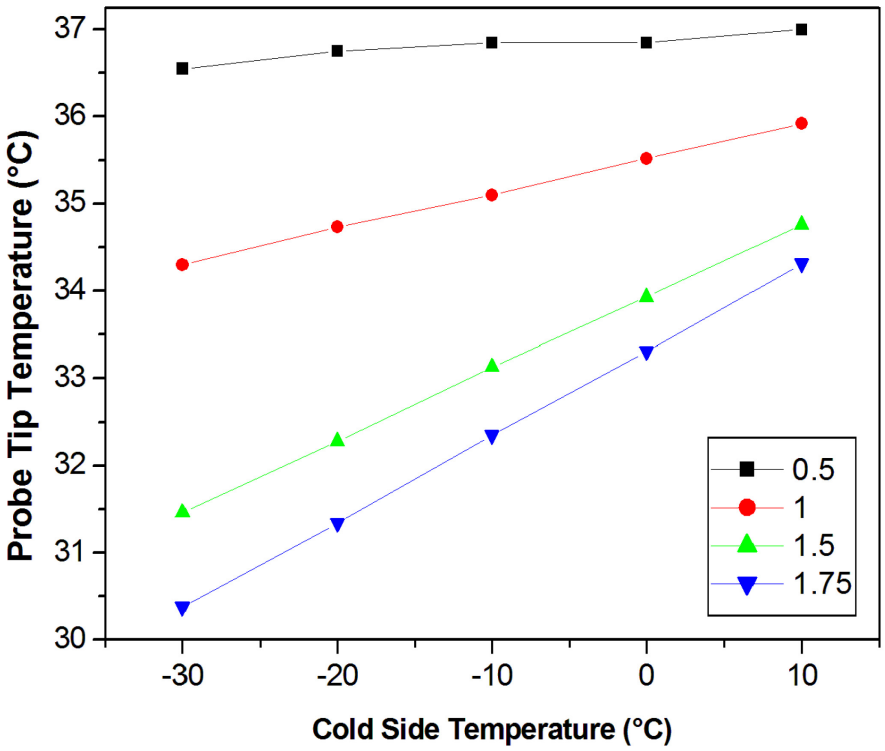

Figure 5.8. Assessment of cold side temperature required to achieve various temperature drops at the probe tip for core diameters of 0.5mm to 1.75mm. A temperature drop of 4°C requires a T_C of -10°C for a 1.5 or 1.75mm core.

The Comsol® model also offers total heat flux as an output via surface integration calculations. Therefore, to cool to the brain by even 4°C with a temperature of -10°C at the cold plate, it is necessary to absorb 16.97W of heat at the Peltier surface. The equations detailed in the methods section (5.1, 5.2, 5.3 and 5.4) allow the calculation of the Peltier properties Z, S_m, R_m and K_m using the basic manufacturer defined specifications. Utilising these values and fixing the Q_C value and T_C values from the

model, it is then possible to vary the theoretical current applied to the Peltier and determine the theoretical temperature drop across the Peltier using equations 5.5 and 5.6. As current increases, so does the power of the Peltier chip and therefore the temperature drop across the device increases with a linear relationship (Fig. 5.9). With a T_C of -10°C required, a ΔT_{TEC} of approximately 40°C will be required and therefore a current of approximately 3.5A.

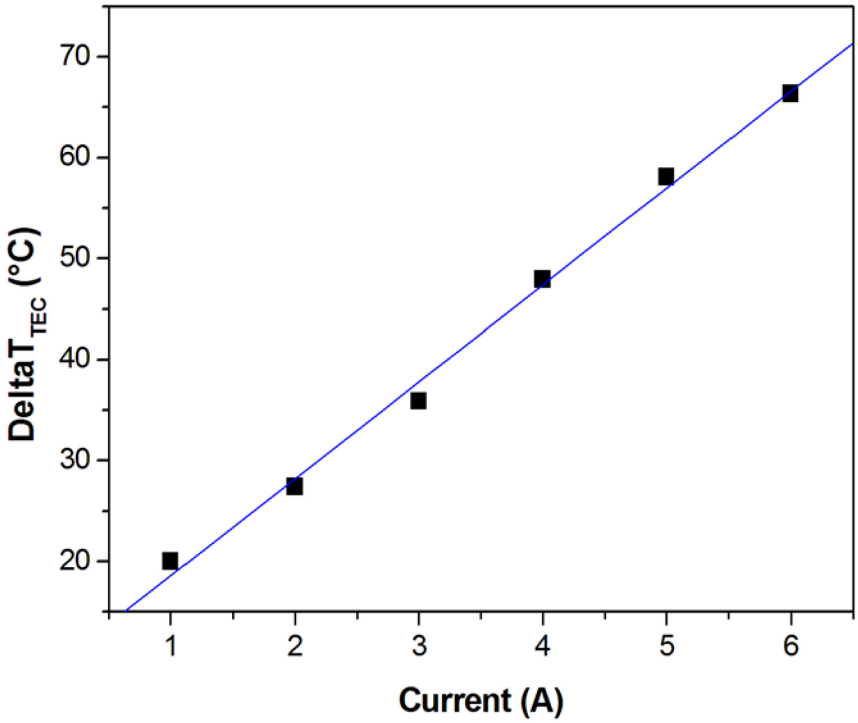

Figure 5.9. Assessment of temperature difference across Peltier with varying current. With a T_C of -10 required, a ΔT_{TEC} of approximately 40°C will be required which is within the capabilities of this Peltier.

Furthermore, it is possible to utilise the final equation to plot the resistance of the heat sink required against the Peltier current (Fig. 5.10). If the Peltier is to function with a current of 3.5A or above, a heat sink with a resistance of 0.3-0.45K/W is required, which

is within the operating range of a fan cooled heat sink and allows further optimisation using its properties[172]. For this reason, other cooling systems for the hotside of the Peltier were not investigated. Aside from thermal performance, aesthetic and functional features may necessitate the consideration of other cooling methods for clinical applications.

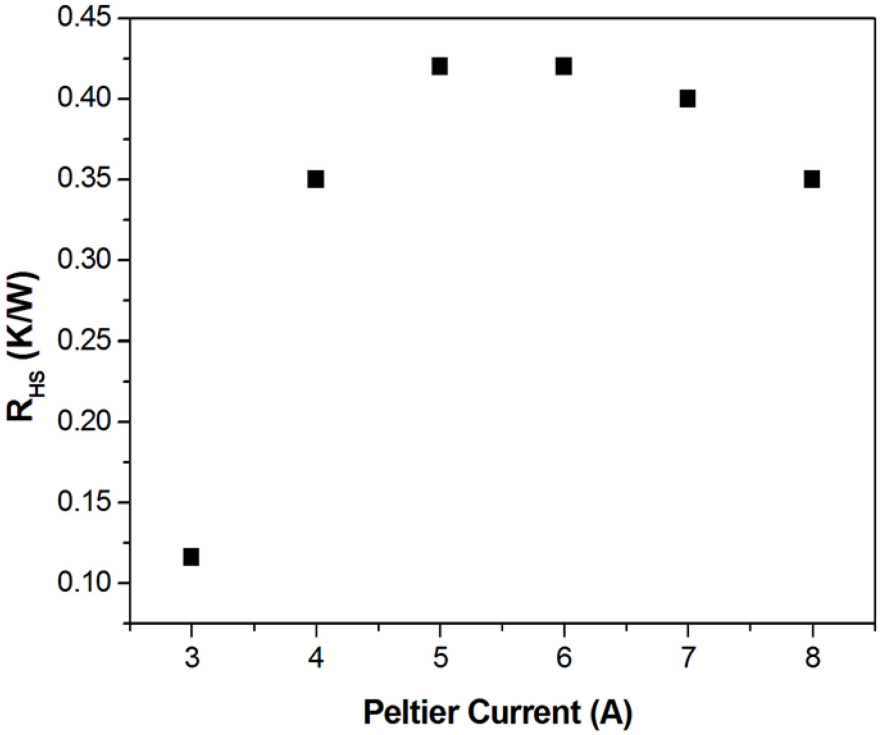

Figure 5.10. Assessment of heat sink resistance with varying current. A heat sink with 0.35-0.45K/W resistance is sufficient if operating at a current of 4A or above.

5.3.4 Experimental Validation

In order to reduce the number of variables and potential for error, experimental validation was carried out using an uncoated probe (Fig. 5.11). The top 3cm of the plant foam brain model was not submerged in the water to prevent splashing on the Peltier element but saturation of the foam and initial temperature of 37°C was checked for each trial.

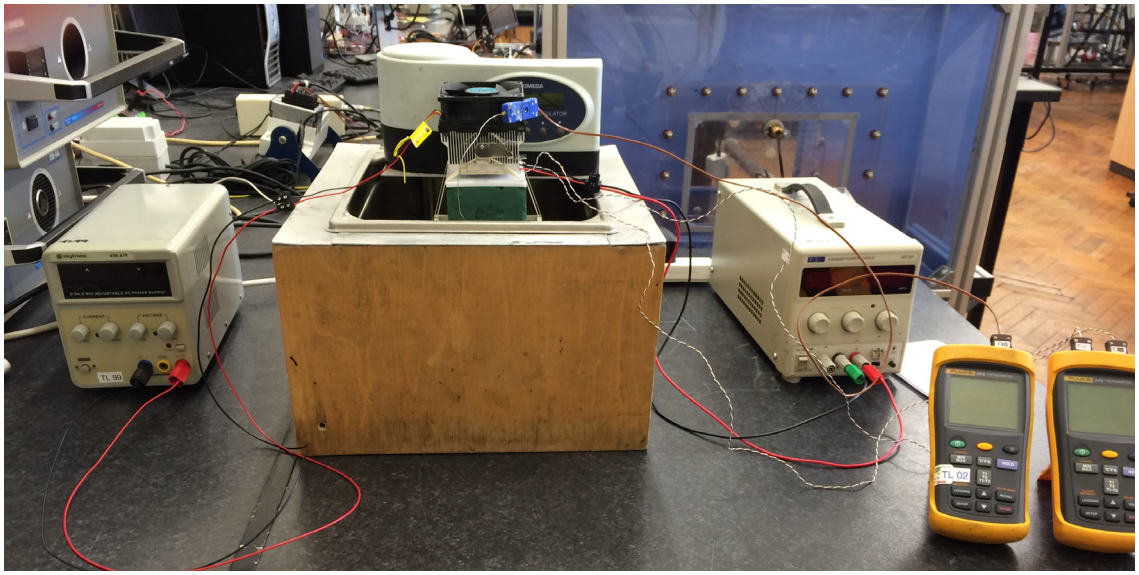

Figure 5.11. Experimental Set up.

Firstly, the calculated cooling potential of the Peltier was plotted against the experimental results and exhibited similar trendlines with the model having a slope of 11.7 vs 10.2 for the observed results. It should be noted that the difference between modelled and measured ΔT_{TEC} increases with increasing current. At 3.5A the difference is 12.5% (Fig. 5.12).

Although the mechanical stiffness of the foam ensured that the cooling probe and the temperature probes were held in place, its dense nature made it difficult to ensure the temperature probes were in direct contact with the cooling probe. For this reason, the temperature probe was finally inserted at the top, beside the cooling probe to different depths, ensuring a consistent gap of 2mm from the cooling probe at all times. In order to compare similar outputs, the Comsol® model was also configured to draw a temperature profile for heat at this distance away from the cooling probe. Figure 5.13 shows how the move away from the probe affects the temperature profile, with up to

10°C temperature drop as the temperature sensor moves away from the surface. This was carried out at 3 different T_C to ensure the validity of the model over a range.

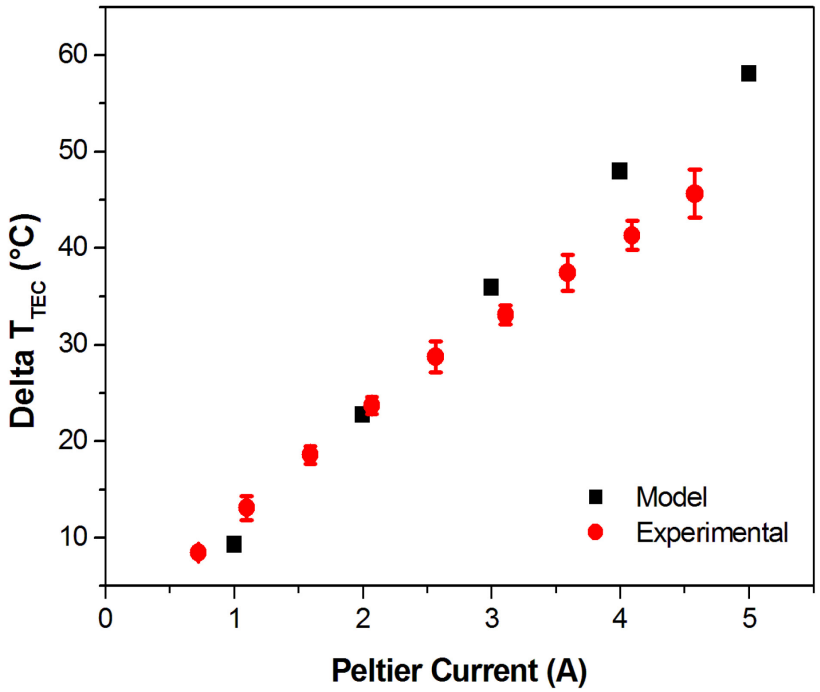

Figure 5.12. Peltier Current vs ΔT_{TEC} predicted vs real results showing good prediction of temperatures with some divergence of values at currents of 4A and higher.

By varying the current through the Peltier chip, the cold side of the Peltier was kept at temperatures comparable to those used in our model. The difference between the model and the experimental results was not significant at a T_C of -10°C (Fig 5.14A). For the models at 10°C and 0°C the temperature deviated from the model by a few degrees at most in the initial length of the probe, with identical temperature profiles for all temperatures after 3cm of probe length (Fig. 5.14B and C).

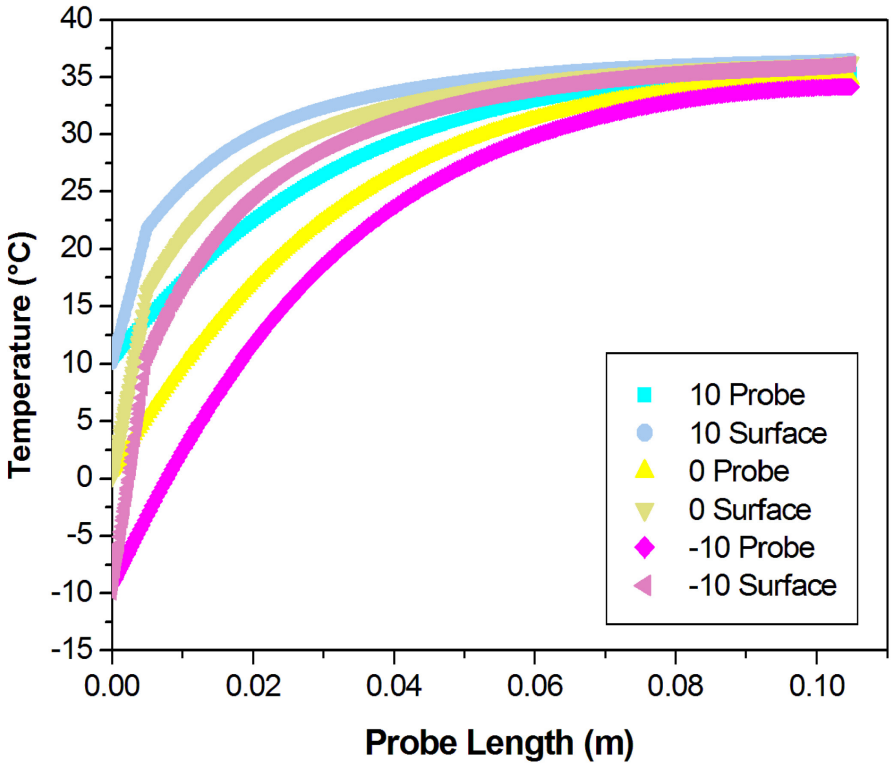

Figure 5.13. Comsol® model of temperature at core vs 2mm away from the surface of probe for initial temperatures of -10°C to 10°C shows a loss of up to 10°C radially at the base of the probe.

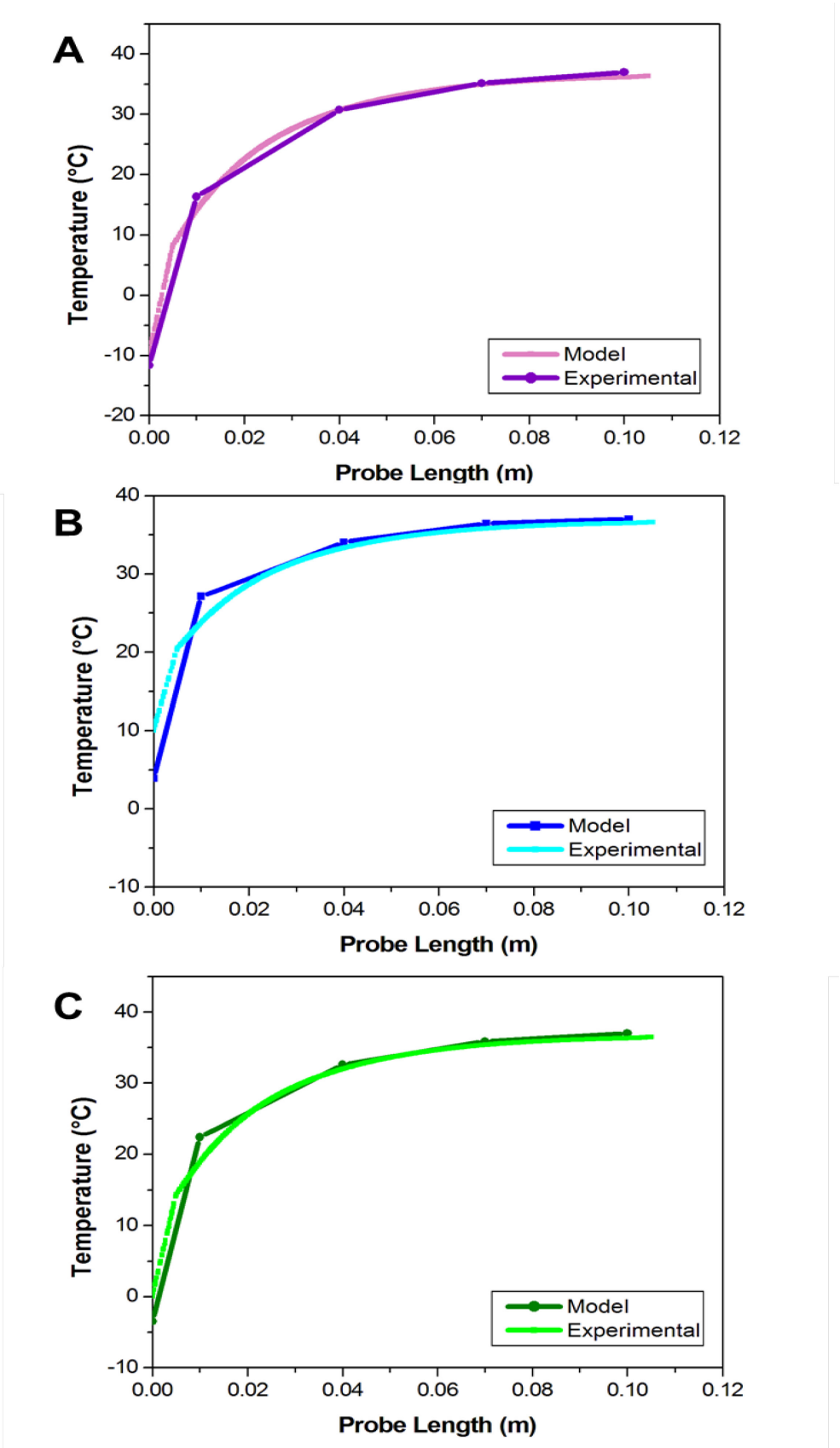

Figure 5.14. Comsol® Model vs experimental results for temperatures 2mm from probe showing similar temperatures profiles.

In order to incorporate the heat sink specifications into the overall probe design, a study was carried out relating the required heat sink resistance to the voltage applied to it. By increasing the voltage applied to the fan cooled heat sink, the heat removed from the hot side of the Peltier was increased, resulting in a lower T_h. This results in a lower heat sink resistance as the heat sink is working more effectively at a higher voltage and the resistance of this heat sink is between 0.34 and 0.42K/W (Fig. 5.15).

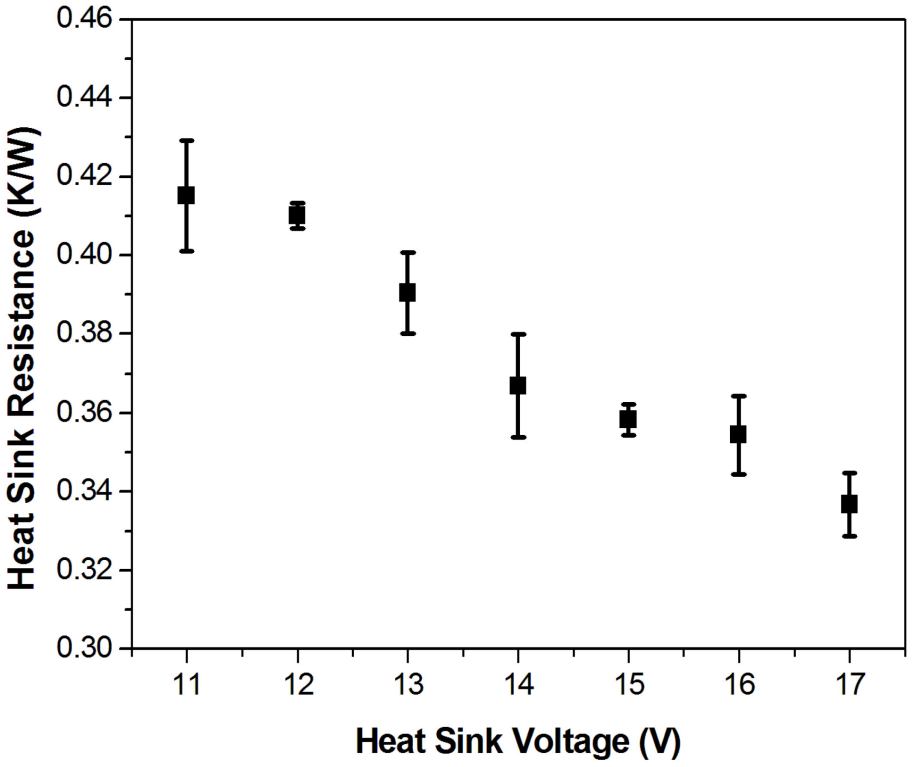

Figure 5.15. Heat sink resistance as a function of voltage. Resistance decreases as voltage increases and heat sink operates at 0.34-0.42K/W. Error bars represent the standard deviation of the average of 5 trials.

5.3.5 Analysis of Model Outputs: Cold Plate Insulation

Another important consideration, which was highlighted in both the model and the experimental validation, was the transfer of heat from the cold plate directly to the brain underneath it. Although PMMA was used as insulation, a thickness of 0.5cm did not

prevent cooling of the brain surface from the cold plate itself. For this reason, both polystyrene and aerogel were modelled as potential surface insulators for a range of probe dimensions and initial temperatures (Fig. 5.16). Both showed similar trends in shape whereby small changes in thickness greatly affect the temperature of the brain until a point beyond which the temperature in the brain is less dependent on the insulation thickness and dependent on T_C. For polystyrene this occurs at 1cm versus 0.3cm for a layer of aerogel.

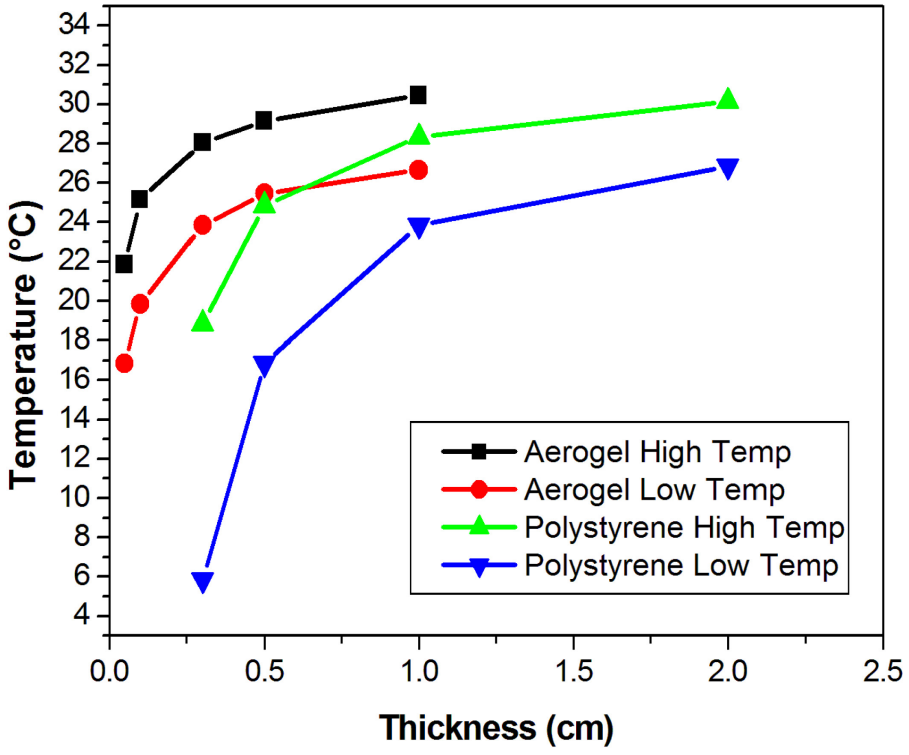

Figure 5.16. Model comparison of temperature of brain surface temperature depending on thicknesses of aerogel and polystyrene insulation with varying initial temperatures showing a strong dependence of brain temperature on insulation thickness until changes in thickness make negligible differences to brain temperature. This occurs at 1cm for polystyrene and 3mm for aerogel.

5.3.6 Analysis of Model Outputs: Thickness to reach therapeutic Temperature

Once the additional cooling driving force from the insulation/brain boundary has been minimised, the required thickness of the coatings for therapeutic effects was re-explored. The initial constraint of 2mm was not achievable given the suggested materials and the desired therapeutic temperature, so a range of diameters up to 6mm were modelled, initially for HA and PDMS (Fig 5.17). Based on the results from Section 5.3.2, an initial ratio of 3:1 for conducting core to insulating material was maintained for all scenarios and each measurement refers to the total thickness of the probe including insulation. Plotting the temperature along the probe as a function of the distance from the Peltier device shows that as the diameter of the probe increases, so does the ΔT_{brain} at the therapeutic tip (Fig. 5.17). It also highlights that the insulating differences between the HA coating and PDMS coating which were minimal when designing a 2mm probe, become more pronounced as the diameter increases. This is due to both an increase in insulation thickness, exposing the differences in insulating capacities and the more effective cooling via conducting core resulting in a larger ΔT_{radial}. As a result, the PDMS coated 5mm probe is indistinguishable from the HA coated 4mm probe offering ΔT_{brain} of 9°C.

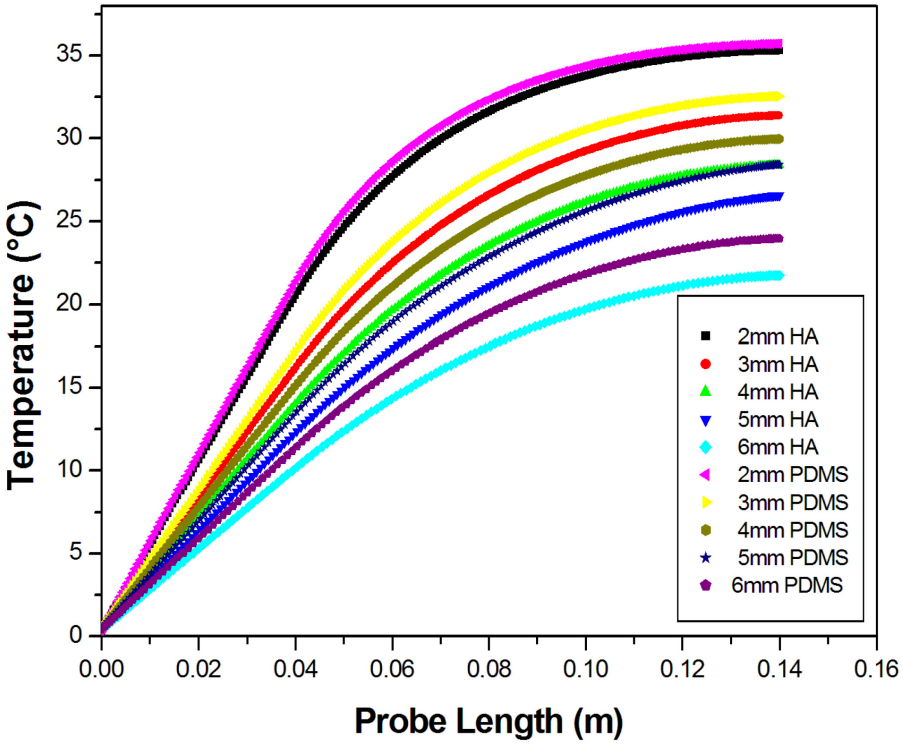

Figure 5.17. Temperature of probes along length with different total diameter but a fixed core: insulation ratio of 3:1. This highlights the increasing differences in performance between HA and PDMS as insulators with increasing thickness.

With optimisation having been carried out for a 2mm probe, the ratios were revisited for larger probes and 3:1, 1:1 and 2:3 ratios were considered (Table 1). Both the conduction along the probe to the probe tip (ΔT_{brain}) and the temperature of the brain tissue adjacent to the probe along its length (ΔT_{radial}) as a result of the insulation were studied, with all models now being run only using HA and a fixed T_C of 0°C(Fig 5.18). For the 3:1 ratio, a 3mm probe gives a therapeutic temperature 28°C with temperatures of 20-30°C along the first 4cm of the probe. A 4mm probe offers a therapeutic temperature of 22°C with temperatures of 20-30°C along the first 5cm of the probe.

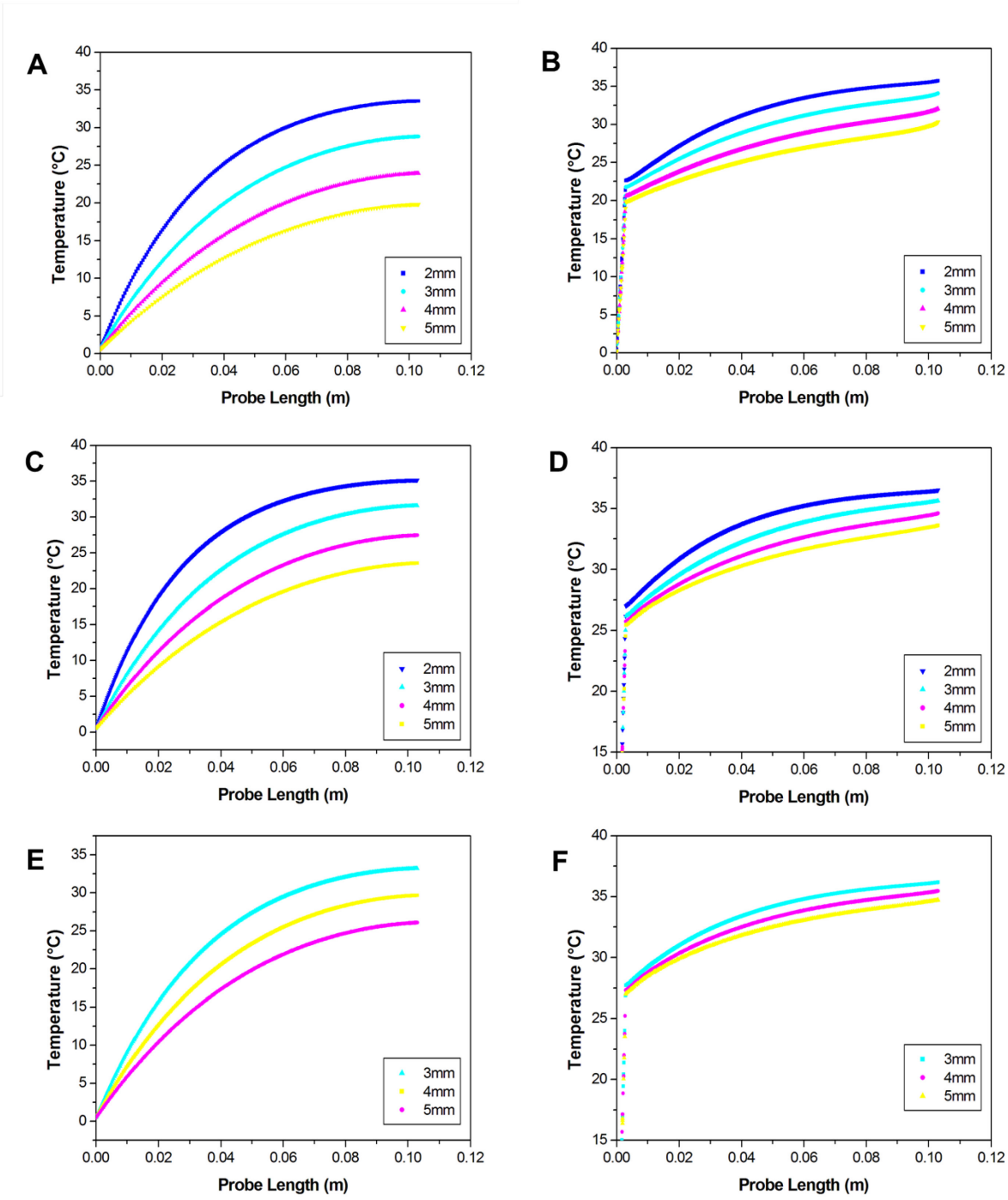

Figure 5.18. Temperature profiles of probe and brain tissue 2mm away probe along the length of probes with different total geometries and ranges of probe:coating. A) 3:1 ratio probe temperature; B) 3:1 ratio brain temperature; C) 1:1 ratio probe temperature; D) 1:1 ratio brain temperature; E) 2:3 ratio probe temperature; B) 2:3 ratio brain temperature.

For the 1:1 ratio a 3mm probe gives a therapeutic temperature of 32°C with temperatures of 26-30°C along the first 2cm of the probe. A 4mm probe offers a therapeutic temperature of 27°C with temperatures of 26-30°C along the first 3cm of the probe. Finally for the 2:3 ratio a 4mm probe gives a therapeutic temperature of 29°C with temperatures of 27-30°C along the first 2cm of the probe. A 5mm probe offers a therapeutic temperature of 26°C also with temperatures of 27-30°C along the first 2cm of the probe. These results indicate that a 1:1 ratio may be best to deliver sufficient cooling at the probe tip without excessive cooling of the brain tissue adjacent to the probe.

5.4 Discussion

Coating a 3D probe raises its own challenges in terms of manufacturability. HA had to be coated onto the silver probes using a simple dip coating method, for ease of experiments but also because of the thicknesses required. Techniques like PLD and ECD discussed in chapter 1 are excellent but can only build layers of nm-µm[123,125–127]. Plasma coating can provide thicker coatings but is not suitable for spraying onto silver due to its relatively low melting point of 962°C[128]. Even dip coating did not allow full sintering of the coatings to achieve surface topographies discussed in chapter 2 as 750°C was the maximum temperature possible without affecting probe integrity. The HA slurry was adapted from a study investigating crack free coatings by increasing solids content to thicken the layers[132]. However, these higher solids ratios, although promising with 1 or 2 coats, developed cracks and became very brittle as additional layers were added, rendering them unusable for thermal testing. PDMS dipcoating methods also proved unsuccessful with large drips solidifying as the polymer cures, something that could perhaps be avoided by rotating the wires in the oven as the PDMS dries. However, the partial curing method with diagonal wrapping proved to coat the probe with an even thickness and strong adherence even on insertion, unlike the horizontally wrapped surface which peeled away upon insertion, and was therefore the method utilised.

Determining the ratio of probe thickness to insulation thickness within the design constraints of a total probe diameter of 2mm involved comparing both conduction down the probe and radially through the insulating coating and into the brain using a Comsol® model. Both the 0.5mm and 1mm silver cores had poor cooling conduction, with 1.5mm and 1.75mm silver cores showing superior cooling, implying that core diameter is the

key driver for better conduction of cooling to the functioning tip. However, as the final temperature delivered at the tip was similar for both 1.5mm and 1.75mm cores, the insulating capabilities of the coating were also taken into consideration. At the midpoint of the probe length, the 1.75mm core was cooling the surrounding tissue by 1.6°C more than the 1.5mm core. As cooling the surrounding tissue needs to be controlled, the 1.5mm core and therefore a ratio of 3:1 conducting core:insulating coating was chosen as a compromise between better cooling conduction and reducing cooling along the entire probe.

In order to validate the Comsol® model experimentally, the potential of a Peltier chip to cool the probe tip sufficiently needed to be assessed. Using a fixed value of T_C, the resultant total heat flux and the Peltier properties, values for current, resistance of the heat sink and ΔT_{TEC} were successfully calculated. The ΔT_{brain} was feasible while operating in the middle of the range of the Peltier's capabilities in terms of current and heat extraction. Operating in the middle of the range of settings was important in case the model and therefore the experimental validation needed adjustment because of any assumptions made while modelling. This also contributed to the choice of a fan cooled heat sink for the system as its resistance can be adjusted using the speed of the fan and the range of resistances required lined up with industrial values for those of fan cooled heat sinks[173].

The first stage of the validation of the entire system involved verifying the Peltier performance had been accurately predicted by the heat transfer equations and the manufacturer's specifications. This showed the model predicts the trend well, particularly in the lower ranges of current. The slight drop in experimental performance

is likely due to heat loss across the heat spreader and into the surroundings. The cold side temperature thermocouple had to be attached to the heat spreader rather than the cold plate directly to prevent a bulky junction with considerable heat loss occurring if the thermocouple were to be in the middle. As the current increases and the temperature differences across the plate increase, the heat losses will also increase, which is why the experimental results show a slight non-linearity and deviate from the predicted values. However, at the relevant current, this deviation is only 12.5%.

In order to validate the model, the temperature at different points along the probe were measured during experiments. As it was difficult to ensure the temperature probe was directly in contact with the cooling probe surface, the probes were inserted alongside each other, ensuring the temperature was being measured at a constant distance of 2mm from the cooling probe surface at all times. The model prediction of this condition was an accurate representation of the temperatures which occurred as voltage was varied to adjust T_c. This implies the model can be used to accurately predict the cooling temperature profile from the Peltier chip through the heat spreader and the probe into the brain, allowing the optimisation of the probe's properties via the model.

As well as this, both the model and the experimental results of the 2mm probe highlighted that the majority of cooling potential is lost within the first few centimetres of the probe whether they are coated or uncoated. The ineffectiveness of the cooling conduction in 2mm probes was further highlighted, as the HA and PDMS coatings only resulted in a ΔT_{brain} of less than 2°C, despite a T_C of 0°C, which is considerably below the temperature drop required to offer therapeutic value. A further concern was that some of the cooling is actually being driven by the incomplete insulation of the cold plate from

the brain itself – resulting in low temperatures in the brain just below the surface. In order to combat this issue, the probe was modelled using polystyrene and aerogel as surface insulators. For polystyrene, a surface insulation thickness of 1cm or more ensured the brain surface temperature was minimally affected by the cold plate temperature. This same was evident for thicknesses of 3mm and above for aerogel. For clinical applications, the size of the external portion of implants should be minimised so far as possible so aerogel was used for all continuing simulations.

Once the cooling from the heat spreader directly into the brain had been reduced to a manageable level, the dimensions required to offer sufficient cooling had to be assessed. In order to offer a therapeutic ΔT_{brain} of approximately 10°C, a 3:1 3mm or 4mm HA coated probe was necessary. However, these both resulted in temperatures alongside the probe of 20-30°C. Some cooling along the length of the probe can be advantageous as it has the potential to reduce the formation of the glial scar by suppressing the reactivity of microglia and astrocytes in response to the implant[102–105]. However, 20°C is clinically categorised as moderate cooling which can seriously interrupt brain function in the vicinity of the probe and is lower than the temperature being offered as therapy at the tip[115]. For this reason a 1:1 ratio of probe to insulation was chosen, with a 4mm probe offering a ΔT_{brain} of 10°C as required along with milder temperatures of 26-30°C for the first 3cm of the brain and reductions of a few degrees thereafter. The 2:3 probes had even smaller temperature drops along the probe but these were not viewed as necessary and required an increased overall diameter to offer the same therapeutic temperature.

Although offering the desired temperature drop, a 4mm probe is still very wide to insert into the brain, double the initial desired design specification. However, the majority of the insertion trauma will be sustained by the brain cortex which has large areas dedicated to different functions and has shown capabilities in reorganising functions in response to an injury[174,175]. Such a large implant may simply cause a migration of any functions interrupted, in contrast to the very precise locations and functions in the small target brain areas of the subthalamic nucleus or hippocampus[174,175]. The cortex also contains large fibre bundles with the task of connecting different segments of the brain which would not be negatively impacted if insertion was carried out along the lengths of these. Professor Shane O'Mara, Professor of Experimental Brain Research at the Institute of Neuroscience TCD, was consulted and indicated that although 4mm was a large diameter for the brain, it was still a clinically viable option, with the immune-suppressive effects of cooling along the length of the probe offering an exciting prospect for the reduction in glial scarring along the probe[176]. The outputs from the Comsol® model for this probe can be used to determine the settings for the Peltier and the heat sink in order to further validate the temperature model experimentally. For this to occur a sophisticated method of coating the probes to ensure a thick crack free HA surface is needed. Once this can be done, *in vivo* trials could assess the effects of the acute injury, of the therapy on induced symptoms and of the mild cooling along the probe length on the formation of a glial scar. Additional applications of a cooling probe could also be explored, for instance for cooling inoperable brain tumours to prevent cell proliferation and therefore growth.

5.5 Conclusions

The previous two chapters dealt with reducing the inflammatory response of brain tissue chronically and in doing so, answered the first four research questions of the thesis. However, in order to design an alternative functional probe, that would negate the need for electrical stimulation, the final two research questions need to be explored. The design of a cooling probe capable of delivering 10°C of cooling to tissue 10cm deep in the brain, while maintaining a clinically viable probe diameter, was achieved by utilising a heat transfer model and integrating its outputs into heat transfer equations in order to test different material thickness configurations which can furthermore be experimentally validated. The key conclusions from this process are outlined below.

Firstly, an FEM model was set up in Comsol® to analyse the conduction of cooling through a probe system into the brain. The temperatures and heat fluxes modelled allowed a feasibility analysis for a given Peltier chip and heat sink system in order to deliver the required cooling deep in the brain via a mathematical model. Both the Peltier and the Comsol® models were shown to be accurate via experimental validation. The study also showed that these models could be utilised with future specifications or materials to predict temperature profiles.

Secondly, the probes were successfully coated in PDMS at the required thickness via a partial curing wrap method with good adherence to the probe. However, the results that emerged from this investigation indicated that thicknesses of 0.5mm coating in HA or PDMS were not sufficient to insulate the brain along the length of the probe and deliver effective cooling at the probe tip. The cooling effects of the heat spreader

through the insulating material into the brain were also highlighted and a 3mm thick aerogel insulating layer on top of the brain is advised.

Thirdly, and following on from this, expanded potential dimensions of a probe to deliver the required 8-10°C cooling were considered and the minimal differences in HA vs PDMS coatings for the 2mm probe were increased with increasing thickness of the device resulting in HA coatings only being considered thereafter. The design tool indicates that in order to deliver the required therapeutic temperature, a 4mm HA coated probe with a probe to insulation ratio of 1:1 is required. This system has the added benefit of ensuring mild cooling along the length of the probe to reduce glial scarring.

In summary, in order to answer research question 5 and optimise the delivery of a therapeutic temperature to the brain, a design tool, incorporating a FEM Comsol® model of a cooling probe and the integration of its outputs into heat transfer equations to specify required Peltier and heat sink capabilities, was developed. This allowed the optimisation of a probe's temperature profile for a desired ΔT_{brain} or ΔT_{radial} as well allowing the feasibility analysis for new conducting core or insulating coatings to be quickly assessed. In answer to research question 6, this tool indicates that to deliver the required therapeutic temperature, a 4mm HA coated probe with a probe to insulation ratio of 1:1 is required. This system has the added benefit of ensuring mild cooling along the length of probe to reduce glial scarring. Indeed, this result renders it unnecessary to combine the two different strategies (as stated in the two hypotheses) developed into one probe, as the reduction in inflammation along the length of the probe is deliverable via the mild cooling or the delivery of anti-inflammatory factors. The next chapter will revisit the findings of Chapter 2, 3, 4 and 5 and summarise the answers to the research

questions outlined previously within the context of the overall aim of the project before drawing final overall conclusions in the final chapter.

6 Overall Discussion

The overall aim of this thesis was to develop an active implantable neural probe system for chronic use. Promising research using Deep Brain Stimulation to alleviate the symptoms of many debilitating neural conditions including epilepsy, Parkinson's and motor neurone disease, resulted in it becoming an FDA approved treatment for dystonia and essential tremor in the US. However, it has become clear that the successful suppression of symptoms seen in the initial months and years steadily deteriorates as a result of the encapsulation of the electrodes in a glial scar. This thesis focuses on how to mitigate this decline in function. Two main tracks of research were investigated – both emerging from a thorough review of the literature and a recognition that the inflammatory response of the brain to insertion, micromotion and long term electrical stimulation impedes chronic applications of the technology.

Firstly, the optimisation of the coating to reduce the formation of the glial scar along the length of the probe was investigated. This involved analysing the response of neural cells to the coating itself, to the material's surface topography and to a functional anti-inflammatory drug release mechanism. This strategy aimed to improve the integration of a probe into the brain to extend its efficacy. Secondly, the introduction of a novel therapeutic method utilising focal cooling rather than electrical stimulation to interrupt the brain signals. Cooling is an alternative mechanism to suppress cell function and therefore prevent symptoms of a neurological condition from occurring, an added benefit being that it does so in a reversible manner. The advantages of this method are two fold in that it not only negates the need for electrical stimulation which is thought to contribute to the formation of the scar itself, but in addition, cooling can have a

neuroprotective effect on the area being cooled, thus reducing the likelihood of a glial scar forming around the functional tip. The thesis postulated that these two strategies could then be integrated to form a probe with reduced inflammatory response both along the probe and at the tip itself. In order to integrate the two strategies, the coating materials for the probes needed careful selection to offer thermal insulation, controllable surface topography, and a potential method for a drug delivery system. For this reason, two very different materials were to be investigated. Polydimethylsiloxane (PDMS) – a thermally insulating material regularly used in neural applications, which can easily contain microfluidic channels and have precisely printed surface structure; and hydroxyapatite (HA) – a thermally insulating well established material for implants elsewhere in the body, which has controllable porosity for the inclusion of anti-inflammatory factors, but has never been utilised in neural applications before.

In order to assess the novel therapeutic method and optimise a coating strategy, six specific research questions were posed. The answers to these questions helped form the basis of a plan to develop prototype probes.

What are the effects of hydroxyapatite (HA) on neural cells and can the control of its topography reduce inflammation?

The HA was non cytotoxic to cells with good survival and attachment of PC12 and primary neuronal cells over a period of a week. By pressing the HA powder at different pressures and sintering it at different temperatures a range of surface topographies were created: a smooth surface 1350S, a moderately rough surface 1350R and a very rough surface 1200R. Of the three surfaces, 1350R showed the best cell attachment and

survival of PC12 cells, closely followed by 1350S, whereas 1200R's cell attachment was comparable to that of the negative control. These results were supported by trials using primary neurons and imply that there is an optimum level of roughness which neuronal cells can thrive on. In these experiments, the moderately rough surface had the best cell attachment and survival of the three HA surfaces across all cell models: this roughness could be further optimised once a coating methodology has been established. As well as looking at the interaction between neurons and HA, experiments were designed to assess how glial cells were affected by the material and its surface features. Human astrocytes were plated both directly onto the HA discs and encapsulated in a gel which was placed on the discs. The direct plating of astrocytes onto the discs showed that the 1200R rough surface had the fewest cells attached to it, which could be viewed as a promising lack of activation of the cells. The cells which were attached, however, looked less healthy than the cells attached to the other two surfaces. This was corroborated by the ELISA data which showed the 1200R surface upregulated the production of inflammatory markers TNF-α and IL-6. In contrast, 1350R and 1350S had lower values and their differences were not statistically significant from each other or from the negative control for IL-6. This supported the finding that very rough HA surfaces are less suitable for neuronal applications than their smoother counterparts. Overall, the HA was found to be suitable for neural applications as it was non cytotoxic and exhibited good PC12 and neuronal cell survival. As well as this, controlling surface roughness did have an effect on both neuronal cells and glial cells with the moderately rough surface 1350R showing the most promise with the best survival and attachment of neuronal cells and the lowest activation of glial cells.

Which cell models are most appropriate for predicting cell immune response to probe coatings for chronic studies?

Five different cell models were utilised: PC12 cells, a mixture of primary neurons and glial cells, purified primary neurons, astrocytes directly plated onto substrates and astrocytes encapsulated in a gel. PC12 cells were a simple test and indicated the surfaces which neurons would attach well to and survive on. The mixture of primary neuronal cells and glial cells was initially thought to be useful as it is more representative of what an implant would encounter in the brain, but when only looking at cell survival and attachment it was impossible to know what proportion of cells was contributing to the total cell count. Ideally this could be supplemented by cell staining, however, this can be difficult to quantify satisfactorily and cell staining and imaging on an opaque surface such as HA is also very challenging. The purification of the primary neurons was also considered as a test model. However, as the cells have to be plated before the Ara-C can be added to prevent the replication and therefore survival of the glial cells, all samples had different initial cell counts on day 0. This proved problematic as the normalisation of the data resulted in very small increases or decreases in cell number seeming significant compared to larger starting values. The purified human astrocytes proved to be the most promising cell model for predicting the brain's immune response to a material as the cell morphology and attachment can be analysed in conjunction with the expression of anti or pro-inflammatory cytokines. The optimisation of the 3D matrix to mimic the ECM brain environment provided a closer representation of *in vivo* conditions, although the 2D and 3D results were comparable in the week long study of HA effects. However, the 3D model is advantageous for chronic studies requiring extended cell

function and testing as the cells can survive weeks rather than days. It is therefore advisable that the inflammatory effects of materials on human astrocytes as a model for the activation of glial cells are investigated in conjunction with simple PC12 testing to give an indication of how neurons will react to a surface which will further contribute to glial response.

How can a coating best deliver anti-inflammatory factors to neural tissue chronically?

Although chapter 3 indicated that the control of surface topography can be utilised to reduce the brain's inflammatory reaction to the surface, this will not mitigate the response entirely, with significant amounts of inflammatory cytokines still being released. In order to reduce this inflammatory response further, a drug delivery system was to be designed, which generated a further two research questions. Firstly, much of the research in the literature indicated that even reductions in acute inflammatory response were not reflected in levels of inflammation chronically. For this reason, the feasibility of a long term drug delivery option was to be investigated. A refillable system could result in not only the long term control of inflammation but also the possibility of administering a precisely changing profile of anti-inflammatory factors to reflect the various stages of inflammation, indeed this could even be patient specific in future.

In order to deliver anti-inflammatory factors to the brain indefinitely, a microfluidic system was investigated. Often the release profiles of drug delivery systems can prove difficult to control and so the idea of a dual-layered microfluidic system was formed. By utilising a hydrogel to contain the microchannels and covering the gel in a porous PDMS membrane, there are two mechanisms by which to control the diffusion co-efficient of

drugs or anti-inflammatory factors – the properties of the hydrogel and the pores of the membrane. The dual layer also opened up further possibilities to reduce the inflammatory response – the mechanical stiffness of the hydrogel is more comparable to brain tissue, reducing the mechanical mismatch at the surface of the probe and the reswelling properties of the hydrogel would allow insertion in a thin dry state before reswelling to improve probe anchorage and reduce micromotion of the probe.

The first step in the process of developing this concept was to create the microchannels in the hydrogel via a sacrificial fibre method. Agarose showed potential as the fibres were easily formed and reduced in size to form smaller microchannels, but suffered issues with breakability, particularly with complex architectures as would be envisaged in a final probe coating. Alginate fibres were difficult to bioprint onto a hydrogel surface and exhibited inconsistencies in fibre diameter. Finally, hair was chosen as the sacrificial fibre, as it is strong with a consistent and small diameter of 80±16μm and could easily be removed from the crosslinked hydrogel even in complex shapes. The hydrogel properties itself had to be optimised to ensure similar mechanical properties to brain tissue, while having sufficient crosslinking to maintain the microchannel architecture chronically and retain its integrity post drying and reswelling. For this reason a 10% GelMA-2% PEG formulation was selected as the pure GelMA hydrogels all suffered from some degree of cracking at the drying stage. The final stage before carrying out diffusion tests involved the addition of the PDMS to slow down diffusion and prevent degradation of the hydrogel over time. In order to ensure the two layers would not separate, the hydrogel was sandwiched in its dry state between two thin layers of PDMS and plasma bonds between these ensured the stability of the coating as a whole. The final step in

the design process involved analysing the release of potential anti-inflammatory drugs and factors from the microfluidic system. By using fluorescent molecule FITC as an isomer and attached to different molecular weights of dextran, diffusion through the whole system into a PBS reservoir over time could be assessed. The molecular weight (MW) of FITC is similar to that of small drug dexamethasone (DEX) whereas FITC-dextran with two different MWs of 20kDa and 40kDa were utilised as a model for larger molecules like cytokines, in particular IL-4 which has a MW of 12-20kDa. The tests indicated that small drug like molecules could be released with minimal burst release and larger cytokine release could be maintained up to 4 days. The optimisation of this system resulted in the successful formation of a dual layered microfluidic system which could be implanted in a thin dry state before swelling and allow the delivery of multiple anti-inflammatory factors in parallel or in series, ensuring minimal burst release and steady release of cytokines for at least 4 days after a single infusion.

Can the long-term delivery of these anti-inflammatory factors reduce the immune response of neural cells in an *in vitro* model?

Once the dual layered coating had been successfully fabricated, its potential to reduce the inflammatory reaction of brain tissue to a probe needed to be assessed. For this, a similar cell encapsulated hydrogel model to the astrocyte one was designed with mechanical properties comparable to those in the brain. The cells utilised at this time were THP-1 monocytes, as they can polarise into M1 pro-inflammatory macrophages or M2 anti-inflammatory macrophages. Microglia have also been shown to have this polarising property and an increase in M2 anti-inflammatory phenotypes would reduce the inflammatory response of the brain tissue and therefore reduce the glial scar. Five

infusion profiles were devised, with each system receiving an initial infusion of DEX or IL-4 and some received repeated infusions of these molecules twice a week based on the results from the diffusion tests. Although there was some cell death between weeks 1 and 2, perhaps due to cells not receiving enough nutrients through the relatively thick 600μm layer of cells, several clear trends in polarisation were still observable.

Firstly, dexamethasone was found to have no effect on polarisation of macrophages. This was surprising as it is a well-established anti-inflammatory drug. However, its mechanisms of action have not been precisely defined and must not affect the polarisation of macrophages. Secondly, the repeated infusion of IL-4 through the system did result in a six-fold increase in M2 macrophages by week 2 versus the negative control and all systems with repeated infusions of IL-4 saw a significant increase in M2 macrophages over the two week period. This implies that the system has successfully delivered a steady supply of IL-4 to the cells over the two week period and that the resulting improvement in M2:M1 macrophage ratio could reduce the inflammation of brain tissue *in vivo*.

These test conditions were repeated with the hydrogel astrocyte system over a period of 3 weeks. The reduced number of cells encapsulated meant there was no significant cell death between weeks and cells were imaged at the end of this period in order to analyse the effects approaching the chronic phase of inflammation. IL-4 had a positive effect once more, ensuring the astrocytes formed a healthy network of astrocytes. The release of TNF-α quantified via ELISA was significantly downregulated with repeated infusions of IL-4, with no difference between initial DEX or IL-4 infusions, indicating that the repeated IL-4 infusions were the primary factor in the down regulation. IL-6 was also

downregulated by the infusion of IL-4 to the system. The consideration of the monocyte and astrocyte studies together strongly indicates that repeated injections of IL-4 could be used to reduce the inflammatory response of brain tissue to a probe over time.

How can a Peltier cooled probe be optimised to maximise focal cooling in the brain?

Parallel to the anti-inflammatory coating design, the feasibility of a Peltier driven cooling probe was being investigated. This first required the development of an FEM model in Comsol® to predict temperatures required at the cold plate for cooling temperatures at the probe tip. Once an initial temperature had been suggested, the potential of a Peltier chip to achieve these temperatures was assessed via heat transfer equations and the Peltier specifications and deemed suitable with the addition of a fan-cooled heat sink. This system could then be built for experimental validation and showed good correlation with the expected temperatures at both sides of the Peltier chip. For the validation of the temperature along the probe, the temperature probe had to be inserted alongside the probe itself. This meant that the temperature was recorded at a distance of 2mm from the probe surface at all times. This was compared to the models outputs for the same location and showed the predictions were reasonably accurate, with variances of only a few degrees for the temperatures at the top of the probe. Both the model and the experimental set-up highlighted the effects of cooling driven by insufficient insulation between the cold plate and the brain and as such polystyrene and aerogel were investigated as superior insulators. The minimum thickness of polystyrene and aerogel to ensure minimal temperature effects on the brain from the plate directly were found to be 1cm or 3mm respectively, so an aerogel layer of 3mm was utilised for all further models as this would be more appropriate in a clinical application.

What probe dimensions are required to deliver therapeutic cooling with an HA/PDMS coating and what are the clinical implications?

Without the driving force of cooling coming directly from the plate as well as the probe, it was clear that initial suggested dimensions of 2mm total diameter of the probe would not be sufficient. Probes of various thicknesses and core to insulation ratios of 3:1, 1:1 and 2:3 were modelled, analysing both therapeutic temperature and temperatures along the length of the probe. The larger ratio of 3:1 offered the best cooling at the tip for a given dimension, however, it resulted in temperatures of 20-30^{o}C along the length of the probe, lower than the therapeutic temperature. Mild cooling along the probe is advantageous to reduce the activation of microglia and astrocytes, but temperatures of 25^{o}C and below may seriously impair all cell functions. For this reason a 4mm probe with a 1:1 ratio was suggested as the optimum solution – offering a 10^{o}C temperature drop at the probe tip for therapeutic purposes and 26-30^{o}C for the first 3cm of the brain and reductions of a few degrees for the remaining 7cm. The effects of the cooling along the probe on the glial scar and the increased acute injury as a result of the larger probe dimensions would have to be assessed *in vivo*. An outcome of this work has also been the development of a systematic design tool for the focused cooling of the brain, including specifications for the probe, the Peltier device and the heat sink for a desired ΔT_{brain} and ΔT_{radial}.

As a result of undertaking the experiments and in the process answering the key research questions, it has become clear that rather than providing one integrated probe developed on the basis of a two-pronged strategy to reduce the inflammatory response, two separate strategies have been developed. Although not integrated into a single

design as was initially intended, they both address the two primary objectives of this work: to reduce the inflammatory response of brain tissue to the probe and to reduce the inflammatory response around the functioning tip. As the cooling side of the project continued, it became evident that there would be some degree of cooling along the whole length of the probe which would be advantageous in reducing the glial response. As the cooling probe needs to have a larger diameter than electrically stimulating probes, adding another coating on top of that would increase the already substantial acute injury to the brain upon insertion and only serve the purpose of attempting to reduce the activation of glial cells, which are already being suppressed by the mild cooling along the length of the probe. This strategy is more novel and requires further work to bring it towards clinical applications.

In addition to this, the dual-layered microfluidic anti-inflammatory coating is now offered as an alternative strategy to coat traditional electrically stimulating electrodes to extend their efficacy. The effect on concentrated drug delivery at the functional tip could also be advantageous. Although limited to current stimulating electrodes, this solution is closer to clinical applications.

If both probes can be shown to reduce glial encapsulation of a probe *in vivo,* this would offer a choice of probes dependent on a patient's condition or other circumstances and suppress the symptoms of the neurological disorder long-term, improving the person's quality of life significantly.

7 Conclusions and Future Work

7.1 Conclusions

Deep Brain Stimulation using neural probes has been shown to alleviate the symptoms of many debilitating neurological conditions, however, the treatment becomes less effective over time due to the formation of a glial scar around the electrode. The overall aim of this research study was to develop a functional neural probe with additional potential to reduce inflammation of brain tissue upon insertion into the brain, a probe that will thus limit the development of a surrounding glial scar, allowing it to function as required for extended periods of time. This overall aim encompassed two broad objectives:

1. *To design a clinically viable cooling probe capable of delivering 10°C of cooling to brain tissue up to depths of 10cm in order to eradicate the need for electrical stimulation during treatment.*
2. *To design a probe coating capable of mitigating the chronic inflammatory response of brain tissue as well as the acute response.*

The study therefore employed a two pronged approach for increasing the chronic efficacy of neural probes with the aim of reducing the brain's immune response at both the functioning tip of a probe and along the length of the probe. The first objective focused on the development of a probe capable of utilising focal cooling rather than electrical stimulation as a therapeutic method to reduce inflammation at the functioning tip. The second objective focused on the development of a microfluidic based drug delivery coating to reduce inflammation along the length of the probe. The intention

was to then integrate the two systems into one probe. A summary of the research study's key findings and future directions for research are outlined below.

Chapter 2 examined a wide-ranging academic literature on neural probes used for chronic implantation. It indicated that there were a number of significant knowledge gaps, which both highlighted the opportunity for further research and gave rise to a two pronged hypothesis that closely reflected the two broad objectives set out above as well as six research questions which provided the focus for the remainder of the research.

The results of initial experimental work on hydroxyapatite (HA) set out in Chapter 3 answered *research question 1:* HA is non cytotoxic to neural cells and manipulation of its surface topography can promote neuronal survival and attachment and reduce glial cell activation, with a moderately rough surface performing best in all trials. However, more chronic biocompatibility tests would be advantageous as well as a method to ensure coatings that are both crack free and stable. A 3D gelatin methacryloyl (GelMA) encapsulated astrocyte cell model was developed which can be utilised to assess the activation of astrocytes for chronic trials of at least three weeks. The utilisation of this method in conjunction with assessment of PC12 cell attachment and survival is advised for predicting brain tissue immune response *in vitro* and provides an answer to *research question 2*.

Chapter 4 addressed *research question 3*. The findings summarised in this chapter highlighted the study's success in developing a dual layered microfluidic drug delivery system for use as a coating for neural probes. This system consists of an 80±16µm microchannel created by a sacrificial fibre in a thin GelMA-PEG composite hydrogel

covered by a PDMS membrane. It has a total thickness of 350±20µm in its dry state and reswells to protect the brain from damage caused by micromotion of the probe once inserted. The system can easily be infused with a range of anti-inflammatory factors at body temperature for a period of at least three weeks without degradation and this profile of factors has the potential to specifically target specific phases of the brain's immune reaction. Cytokine-like molecules can be released steadily for at least four days and there is minimal burst release of small drug-like molecules. Hydrogels encapsulated with monocytes were developed as a brain-like model for studying cell response and these hydrogels were able to last in an *in vivo* mimicking environment for a minimum of 2 weeks. *Research question 4* was also answered in this chapter: the repeated infusion of IL-4 caused both an upregulation in M2 anti-inflammatory macrophages over 2 weeks and a downregulation of two pro-inflammatory markers TNF-α and IL-6 in astrocytes over a 3 week period. Dexamethasone infusion had no effect on either of these inflammatory markers. These improvements in anti-inflammatory effects *in vitro* imply that repeated infusions of anti-inflammatory factors like IL-4 could be utilised in the future to reduce the formation of a glial scar around neural implants and increase their efficacy long–term.

Finally, in chapter 5, a prototype of a Peltier chip driven cooling neural probe was designed and an FEM model was set up in Comsol® in order to allow *research question 5* to be answered. This can predict the temperature required at the cold side of the Peltier to deliver specific therapeutic cooling temperatures at the probe tip and total heat flux from the probe. A separate programme, based on heat transfer equations, can successfully predict the current required by the Peltier and voltage required by a fan

cooled heat sink to deliver these temperatures. The Peltier and probe models were shown to be accurate via experimental validation and in their integrated form represent a comprehensive design tool for the development of focused cooling neural probes for future researchers. It can be utilised as a design tool to target specific temperatures in the brain, both at the tip and along the length of the probe, and predict the required Peltier and heat sink settings for any dimensions or materials investigated in the future. This design tool helped to answer *research question 6* by predicting the potential dimensions of a probe to deliver the required tip temperature for therapeutic cooling 10cm deep into the brain. Different ratios of conducting core to insulation coating were analysed and small differences in insulation between HA and PDMS for small probes were amplified at larger probe dimensions, making HA the preferred coating material. As a consequence of delivering the target low temperatures at the tip of the probe, some mild cooling along the length of the probe has been observed despite the insulation. Given the anticipated level of cooling, it is reasonable to assume that this will reduce the inflammatory response of the brain to the probe along its length and therefore reduce the formation of a glial scar. In order to deliver the maximum therapeutic temperature at the tip while ensuring mild cooling along the length of probe to reduce glial scarring, a 4mm HA coated probe with a probe to insulation ratio of 1:1 is suggested.

These findings, guided by addressing the six research questions that emerged from the review of the academic literature, corroborated the original hypotheses: highly thermally insulating materials were effective in allowing the production of a viable cooling prototype and the sustained release of anti-inflammatory factors was shown to downregulate the immune response of brain cells compared to a negative control which

would imply it could reduce cell response similarly *in vivo.* The two broad objectives of the study were also achieved. Principally, a clinically viable cooling probe delivering 10°C of cooling to tissue 10cm deep in the brain capable of eradicating the need for electrical stimulation was designed and a suitable dual layered microfluidic coating capable of mitigating the chronic inflammatory response of brain tissue as well as the acute response was created.

Prior to this work, some limited research had been carried out using focal cooling to supress brain activity but principally focused on surface cooling and small mammal applications. This study has taken these findings forward. Its research findings on cooling probes have shown that, despite the challenges associated with maintaining low temperatures to a significant depth in the human brain, this method of symptom suppression in humans is possible, allowing further system optimisation utilising the design tool to achieve these goals. The additional benefit of inflammation reduction along the length of the probe is also very promising and strengthens the advantages of this method. Due to the innovative nature of this solution, there will be more work required to get it to a clinical setting, work that is outlined in the next section.

Previous research has also been successful in reducing inflammatory response to neural probes in the acute stage of inflammation. The dual layered microfluidic system developed in this thesis is a significant step in the design of a clinically relevant coating that delivers anti-inflammatory factors to the brain long term to address the chronic inflammation of tissue as well as at the acute stage. This system could also deliver a patient-specific profile of anti-inflammatory factors targeting specific stages of the inflammatory mechanism. This coating can be applied to current electrically stimulating

electrodes on the market and therefore has the potential to become clinically useful in the near future, subject to successful trials *in vivo*.

The above two paragraphs demonstrate that not only were the two broad objectives of the thesis achieved, but that the closely related two pronged hypothesis underpinning the research was also substantiated. However, the further hypothesis that integrating the two approaches would bring about a probe capable of further reducing inflammatory response was rejected as the cooling probe already encompassed both target areas by reducing the chances of glial scarring along the length of the probe via an unforeseen mild cooling effect – rendering the integration of the two strategies unnecessary. The final section of this thesis will outline the limitations of the work carried out and use these as a basis for prescribing further work to develop these two strategies in the future.

7.2 Limitations

As with all experimental, leading edge research, there are a number of limitations to the studies carried out which need to be considered when evaluating the results of the component parts of the study and specifying the directions for future work aimed at advancing both the functional cooling probe and the drug delivery microfluidic coating towards *in vivo* and clinical trials.

Firstly, there are several key issues that need to be examined regarding the use of hydroxyapatite in neural applications. Although shown to be non-cytotoxic to neuronal cells, the effect of calcium ion release to the brain was not investigated as part of this study - any risk of calcification and loss of function of areas of the brain surrounding the implant need to be assessed before moving forward with its usage in neural applications.

Secondly – a suitable process for applying a thick crack-free coating to a 3D probe below the melting point of the probe itself was outside the scope of this study. Consequently, the thermal conductivity of porous HA used in the thermal analysis of a cooling probe is currently an estimate from the literature.

Thirdly, the stability of the coating itself must be considered as it would need to fully adhere to the conducting core without chipping or cracking during or post implantation, something that can only be assessed once the coating process is established.

In addition to the hydroxyapatite related limitations set out above, there were also a number of limitations implicit in the Comsol® model. For although this model was experimentally validated, a number of key assumptions that underpinned the model may reduce the validity of the results. Firstly, the assumption that the thermal

conductivity of brain tissue can be estimated on the basis that it is very similar to that of water due to the high water content of the brain. This value is often used in scientific studies but is an average for the tissue. In reality, it may vary between different locations in the brain and heat may be conducted away more quickly in close proximity to capillaries. This needs to be taken into account when assessing the volume of tissue that may be being cooled *in vivo*. Secondly, the experimental validation itself was only carried out with uncoated probes which may reduce the model's accuracy when expanding it to include various coatings as extra variables are being introduced. However, despite these limitations, the model is still a useful tool, particularly for comparing different potential ratios of coating pre-optimisation.

Finally, with regards to the cooling probe, the current thickness of the probe is still a cause for concern, although discussions with experts in the field indicated that the advantages of mild cooling along the length of the probe may outweigh the effects of the initial injury caused by such a large probe. In addition, the design of the probe was limited by the size of the brain and the temperature required to offer therapeutic cooling. With current materials available, these larger thicknesses are required in order to ensure sufficient conduction and insulation to the probe tip.

The size related limitations must also be considered when looking at the microfluidic drug delivery coating. For example, a 350µm thick coating applied to a cylindrical probe will increase the total thickness by 700µm if wrapped around the entirety of the probe, which is a significant increase as current probes are approximately 1.3mm in diameter. As an alternative, such a coating could also be applied on only one side to reduce the effects of such an increased thickness upon the initial insertion caused injury. If further

miniaturisation of the system is carried out, the diffusion profiles of various anti-inflammatory factors would also need reassessed as they will be traversing a smaller distance or alternatively, an accurate scaling method would need to be investigated.

This study showed that repeated infusions of IL-4 to brain-like tissue models significantly downregulated the immune response of monocytes and astrocytes over a period of 3 weeks. This in itself is a very promising discovery. However, the acute phase of inflammation is defined as ending anywhere between 2 and 12 weeks depending upon the study so undertaking extended trials past the 12 week period would be advantageous. These trials, however, may need to be done *in vivo* as even the 3D cell models may not remain viable at this stage.

The cell models are an excellent tool for predicting how the brain will respond to materials or external stimuli. However, these cells often interact with the other cells around them in a slightly different way than when used alone. Even when harvesting a mixture of glial cells it is important to note that these cells are already effectively being put under stress during the harvesting process. The collation of results from many cell types (PC12, neurons, astrocytes etc.) helps give robustness to the conclusions from these cell studies, but it cannot be assumed that they will behave in exactly the same manner during *in vivo* trials as was found in these studies. However, it must also be recognised that the more cell types are introduced simultaneously to a study, the more difficult it becomes to accurately predict outcomes because of the potential intermingling of differential cause-effect relationships.

Despite these limitations, this thesis makes a significant contribution to the research field by:

- Developing a drug-eluting microfluidic system capable of delivering anti-inflammatory factors chronically to the brain
- Ascertaining that repeated infusions of IL-4 can reduce the brain's inflammatory response long-term
- Designing a clinically viable cooling probe as an alternative solution to electrically stimulating probes
- Providing a useful design tool for the design of cooling probes in future which allows the direction input of materials and their thicknesses into the simulation, returning estimated temperatures along the probe

These are the first key steps to bringing these two designs to clinical applications in future and the limitations highlighted above direct the future research required to bring these two strategies towards the clinical trial stage and this is outlined in the next section.

7.3 Future Work

This thesis set out to develop a neural probe that would reduce the inflammation of brain tissue upon insertion into the brain, allowing it to alleviate the symptoms of chronic neurological disorders for extended periods of time unlike those currently available on the market which are effective for much shorter periods of time. It has developed two separate strategies for doing so, thereby realising the two main objectives of the thesis. However, the conclusions and limitations of the studies previously discussed in this chapter have highlighted several key areas for future productive research in order to bring those two solutions towards prototypes for testing *in vivo* and in clinical trials.

Cell lines

Firstly, there is work to be done regarding the reliability of *in vitro* cell studies in predicting immune response *in vivo*. Particularly at the early screening stage, a repeatable easy method of assessing the response of neural cells would be advantageous. This thesis suggested the best methods when using individual cell types, however, a co-culture hydrogel system of PC12 cells, monocytes and astrocytes could be designed in order to create a standardised cell line based brain model for predicting glial scarring *in vitro* as an alternative to brain slice cultures or in vivo work, allowing greater confidence in, and easy comparison of, results. This would also allow potential solutions to be carried out on a 2D plane for chronic time-points before a 3D or miniaturised model is required.

HA Coating

Secondly, although hydroxyapatite has been highlighted as an effective thermal insulator for a cooling probe at clinically viable dimensions, the manufacturability and long-term stability of such a coating needs to be determined. An effective method for coating HA onto neural probes crack free at temperatures of under 900°C at thicknesses of over 1mm needs to be devised, in order to allow the insulation to work effectively and prevent chipping of the coating upon insertion into the brain. A full range of mechanical tests are also required to assess the interface strength of the HA coating with the conducting core to ensure adhesion. The long term stability of the coating in a brain model would also need assessed – in case the release of ions affects its integrity or triggers calcification of surrounding neural tissue or, indeed, if motion of the brain within the skull has a detrimental effect on coating cohesion. A full investigation into the porosities and surface roughnesses achievable through the selected coating methodology would also need carried out, in order to precisely determine the optimal thermal properties of HA in such a system and ensure inflammatory reaction of neural cells is minimised. This would result in the development of an optimised prototype to further validate the Comsol® model before being used *in vivo* trials.

Design Tool

Thirdly, the design tool itself could be utilised to further optimise the properties of a cooling probe. This study focused on selecting materials and thicknesses of the conducting core and insulating coating. However, there are many alternative properties that could be adjusted and optimised, such as the effective conduction of heat from the Peltier chip, through the heat spreader and to the probe itself. The geometry of the

probe tip could also increase or decrease heat conduction and experimenting with this could affect the volume of tissue cooled in the desired region of the brain. Determination of this volume cooled is also an important parameter for design of a functional probe. The optimisation of all heat conduction parameters is important to ensuring the least invasive cooling prototype is designed.

Cooling Probe Design

Fourthly, given that the dimensions of the cooling probe have been highlighted as a concern, an alternative method of cooling tissue deep in the brain could also be investigated. The larger dimensions required are a result of trying to transmit a much greater degree of cooling from the surface of the brain to a location deep within its structure. An alternative mechanism via circulation of cool fluid through a microfluidic system could also be investigated. This would involve the mechanical design of the system, calculation of circulation rates and assessment of the heat transfer required in order to deliver a therapeutic temperature. The overall dimensions of the system could be reduced with this technology and its clinical potential assessed by comparing its performance with the Peltier chip driven system devised by this thesis.

Drug-delivery Coating

Fifthly, the dual-layered microfluidic drug-eluting system can be utilised to test alternative anti-inflammatory drug and cytokines. Combinations of these can also be tested and designed to target and inhibit specific occurrences in the brain's inflammatory process. The properties of the PDMS membrane could also be exploited to further control the diffusion rate of selected factors through the system. The optimum architecture of the microchannels through the gel for a 3D probe should also

be considered with special attention given to the system's potential to preferentially release anti-inflammatory factors around the functioning tip. As with the HA coating, the coating methodology and adherence to the system would need to be tested. Some miniaturisation of the hydrogel thickness via more precise control of the microchannel placement will allow a prototype probe to be created. Once this prototype has been created, extended trials of longer than 12 weeks should be carried out, in order to determine if the improvement in reduction of inflammatory response can be maintained throughout the glial scar development phase and confirm that the advantageous affects will be seen chronically.

Wider Applications

Finally, the potential uses of all strategies and their translational application in other areas of bioengineering should be considered. The chronic drug delivery coating could be utilised on implants elsewhere in the body or used to control delivery of nutrients into an *in vitro* cell system. The cooling probe could be tested as a mechanism to slow down the proliferation of cells in an inoperable brain tumour or reduce inflammation and further damage after a spinal cord injury or during surgery to temporarily inactivate specific areas of the central nervous system. With the results of this work showing that the integration of these two strategies is no longer needed as it would be a duplication of purpose, *in vivo* trials comparing the two systems would be provide useful indications of future research priorities. Firstly, they would allow the comparison of the effects and mechanisms of the two different therapeutic strategies of cooling and electrical stimulation. Secondly, they would allow the comparison of the effectiveness of mild

cooling versus strategic chronic drug delivery as mechanisms to reduce glial scarring around probes and highlight the more promising direction for future work.

The overall conclusion to the thesis was structured on the basis of the objectives, hypotheses and emerging research questions and reminded the reader of the key findings of a study that focused on reducing the brain's inflammatory response to neural probes in order to prevent loss of functionality over time. It is hoped that the findings from this research have made a small but significant contribution to progressing two key strategies for reducing glial scarring around probes: firstly, by creating a microfluidic drug eluting coating capable of administering anti-inflammatory factors to the brain chronically and indicating that chronic infusions of IL-4 will have a positive effect in reducing chronic inflammation and, secondly, by designing an alternative cooling probe that negates the need to use electrical stimulation – something that is also thought to contribute to glial scarring – and allows anti-inflammatory mild cooling along the length of the probe. By carrying out the further work outlined in the preceding paragraphs, prototypes of both strategies that are suitable for usage in *in vivo* and clinical trials could be produced. Successful results from these trials would then facilitate the approval of these methods in the future for use in patients with debilitating neurological conditions, greatly improving the quality of life offered to them in the longer term.

Bibliography

1. MD Health Website. www.mdhealth.com. Accessed April 2, 2016.
2. Polikov VS, Tresco P a, Reichert WM. Response of brain tissue to chronically implanted neural electrodes. *J Neurosci Methods*. 2005;148(1):1-18. doi:10.1016/j.jneumeth.2005.08.015.
3. Medtronic. Lead kit for deep brain stimulation. 1998.
4. Mayfield Clinic Website. https://www.mayfieldclinic.com/PE-SurgPD.html. Accessed May 9, 2016.
5. Bellamkonda R V., Pai SB, Renaud P. Materials for neural interfaces. *MRS Bull*. 2012;37(06):557-561. doi:10.1557/mrs.2012.122.
6. NHS Website. http://www.nhs.uk/conditions/Epilepsy/Pages/Introduction.aspx. Accessed August 20, 2012.
7. Parkinson's UK Website. https://www.parkinsons.org.uk/content/facts-journalists. Accessed August 22, 2012.
8. He W, McConnell GC, Schneider TM, Bellamkonda RV. A Novel Anti-inflammatory Surface for Neural Electrodes. *Adv Mater*. 2007;19(21):3529-3533. doi:10.1002/adma.200700943.
9. Lu Y, Wang D, Li T, et al. Poly(vinyl alcohol)/poly(acrylic acid) hydrogel coatings for improving electrode-neural tissue interface. *Biomaterials*. 2009;30(25):4143-4151. doi:10.1016/j.biomaterials.2009.04.030.
10. Rao L, Zhou H, Li T, Li C, Duan YY. Polyethylene glycol-containing polyurethane hydrogel coatings for improving the biocompatibility of neural electrodes. *Acta Biomater*. 2012;8(6):2233-2242. doi:10.1016/j.actbio.2012.03.001.
11. Yue Z, Moulton SE, Cook M, O'Leary S, Wallace GG. Controlled delivery for neuro-bionic devices. *Adv Drug Deliv Rev*. 2012;65(4):559-569. doi:10.1016/j.addr.2012.06.002.
12. Caparros-Lefebvre D, Blond S, Vermersch P, Pecheux N, Guieu JD, Petit H. Chronic thalamic stimulation improves tremor and levodopa induced dyskinesias in Parkinson's disease. *J Neurol Neurosurg Psychiatry*. 1993;56(3):268-273. doi:10.1136/jnnp.56.3.268.
13. Chen S, Allen MG. Extracellular matrix-based materials for neural interfacing. *MRS Bull*. 2012;37(06):606-613. doi:10.1557/mrs.2012.120.
14. Hochberg LR, Bacher D, Jarosiewicz B, et al. Reach and grasp by people with tetraplegia using a neurally controlled robotic arm. *Nature*. 2012;485(7398):372-375. doi:10.1038/nature11076.
15. Thompson BC, Moulton SE, Richardson RT, Wallace GG. Effect of the dopant

anion in polypyrrole on nerve growth and release of a neurotrophic protein. *Biomaterials*. 2011;32(15):3822-3831. doi:10.1016/j.biomaterials.2011.01.053.

16. Gray H. *Gray's Anatomy*. 20th Editi. (Lewis W, ed.). Bartleby; 1918.

17. Fawcett JW, Asher R. The glial scar and central nervous system repair. *Brain Res Bull*. 1999;49(6):377-391. doi:10.1016/S0361-9230(99)00072-6.

18. Polazzi E, Monti B. Microglia and neuroprotection: from in vitro studies to therapeutic applications. *Prog Neurobiol*. 2010;92(3):293-315. doi:10.1016/j.pneurobio.2010.06.009.

19. Liu W, Tang Y, Feng J. Cross talk between activation of microglia and astrocytes in pathological conditions in the central nervous system. *Life Sci*. 2011;89(5-6):141-146. doi:10.1016/j.lfs.2011.05.011.

20. Sironi VA. Origin and evolution of deep brain stimulation. *Front Integr Neurosci*. 2011;5(August):42. doi:10.3389/fnint.2011.00042.

21. Miles J. Electrical Stimulation for the Relief of Pain. *Ann R Coll Surg Engl*. 1984;66:108-112.

22. Cerletti U. L'elettroshock. *Ist Psichiatr di S Lazzaro*. 1940.

23. Sarem-Aslani A, Mullett K. Industrial perspective on deep brain stimulation: history, current state, and future developments. *Front Integr Neurosci*. 2011;5(September):46. doi:10.3389/fnint.2011.00046.

24. Gardner J. A history of deep brain stimulation: Technological innovation and the role of clinical assessment tools. *Soc Stud Sci*. 2013;43:707-728. doi:10.1177/0306312713483678.

25. Miocinovic S, Somayajula S, Chitnis S, Vitek JL. History, applications, and mechanisms of deep brain stimulation. *JAMA Neurol*. 2013;70(2):163-171. doi:10.1001/2013.jamaneurol.45.

26. Udupa K, Chen R. The mechanisms of action of deep brain stimulation and ideas for the future development. *Prog Neurobiol*. 2015;133:27-49. doi:10.1016/j.pneurobio.2015.08.001.

27. Medtronic Website. http://www.medtronicdbs.com/. Accessed September 17, 2012.

28. York MK, Wilde EA, Simpson R, Jankovic J. Relationship between neuropsychological outcome and DBS surgical trajectory and electrode location. *J Neurol Sci*. 2009;287(1-2):159-171. doi:10.1016/j.jns.2009.08.003.

29. Parvareshrizi M, Alijani B, Fereshtehnejad S. Anatomical situation of the subthalamic nucleus (STN) from mid- commissural point (MCP) in Parkinson ' s disease patients underwent deep brain stimulation (DBS): an MRI targeting study. 2010;24(1):35-42.

30. Medical SJ. Constant-Current DBS Stimulation Improves Movement Disorder. :1-8.

31. Boston Scietific Website. https://www.bostonscientific.com/en-US/products.html. Accessed December 12, 2014.

32. Martin JL, Murphy E, Crowe J a, Norris BJ. Capturing User Requirements in Medical Device Development : The Role of Ergonomics The published version of this paper can be found as : Martin , J ., Murphy E . A ., Crowe , J . A . and Norris B . (2006) Capturing User Requirements in Medical Device De. *Physiol Meas*. 2006;27(8):49.

33. Pilitsis JG, Metman L V, Toleikis JR, Hughes LE, Sani SB, Bakay RAE. Factors involved in long-term efficacy of deep brain stimulation of the thalamus for essential tremor: Clinical article. *J Neurosurg*. 2008;109(4):640-646. doi:http://dx.doi.org/10.3171/JNS/2008/109/10/0640.

34. Zhang K, Bhatia S, Oh MY, Cohen D, Angle C, Whiting D. Long-term results of thalamic deep brain stimulation for essential tremor. *J Neurosurg*. 2010;112(6):1271-1276. doi:10.3171/2009.10.JNS09371.

35. Rousche PJ, Normann R a. Chronic intracortical microstimulation (ICMS) of cat sensory cortex using the Utah Intracortical Electrode Array. *IEEE Trans Rehabil Eng*. 1999;7(1):56-68. http://www.ncbi.nlm.nih.gov/pubmed/10188608.

36. Branner A, Stein RB, Fernandez E, Aoyagi Y, Normann R a. Long-term stimulation and recording with a penetrating microelectrode array in cat sciatic nerve. *IEEE Trans Biomed Eng*. 2004;51(1):146-157. doi:10.1109/TBME.2003.820321.

37. Nicolelis M a L, Dimitrov D, Carmena JM, et al. Chronic, multisite, multielectrode recordings in macaque monkeys. *Proc Natl Acad Sci U S A*. 2003;100(19):11041-11046. doi:10.1073/pnas.1934665100.

38. Rousche PJ, Normann R a. Chronic recording capability of the Utah Intracortical Electrode Array in cat sensory cortex. *J Neurosci Methods*. 1998;82(1):1-15. http://www.ncbi.nlm.nih.gov/pubmed/10223510.

39. Massia SP, Holecko MM, Ehteshami GR. In vitro assessment of bioactive coatings for neural implant applications. *J Biomed Mater Res A*. 2004;68(1):177-186. doi:10.1002/jbm.a.20009.

40. Szarowski DH, Andersen MD, Retterer S, et al. Brain responses to micro-machined silicon devices. *Brain Res*. 2003;983(1-2):23-35.

41. McCreery DB, Agnew WF, Yuen TG, Bullara L. Charge density and charge per phase as cofactors in neural injury induced by electrical stimulation. *IEEE Trans Biomed Eng*. 1990;37(10):996-1001. http://www.ncbi.nlm.nih.gov/pubmed/2249872.

42. Liu H, Zhu L, Sheng S, et al. Post stimulus effects of high frequency biphasic electrical current on a fibre's conductibility in isolated frog nerves. *J Neural Eng*.

2013;10(3):036024. doi:10.1088/1741-2560/10/3/036024.

43. McConnell GC, Rees HD, Levey AI, Gutekunst C-A, Gross RE, Bellamkonda R V. Implanted neural electrodes cause chronic, local inflammation that is correlated with local neurodegeneration. *J Neural Eng*. 2009;6(5):056003. doi:10.1088/1741-2560/6/5/056003.

44. Rao SS, Winter JO. Adhesion molecule-modified biomaterials for neural tissue engineering. *Front Neuroeng*. 2009;2(June):6. doi:10.3389/neuro.16.006.2009.

45. Hersel U, Dahmen C, Kessler H. RGD modified polymers: biomaterials for stimulated cell adhesion and beyond. *Biomaterials*. 2003;24(24):4385-4415. doi:10.1016/S0142-9612(03)00343-0.

46. Yu LMY, Leipzig ND, Shoichet MS. Promoting neuron adhesion and growth. *materialstoday*. 2008;11(5):36-43.

47. Cui X, Wiler J, Dzaman M, Altschuler RA, Martin DC. In vivo studies of polypyrrole / peptide coated neural probes. *Biomaterials*. 2003;24:777-787.

48. Kim D-H, Abidian M, Martin DC. Conducting polymers grown in hydrogel scaffolds coated on neural prosthetic devices. *J Biomed Mater Res A*. 2004;71(4):577-585. doi:10.1002/jbm.a.30124.

49. Cogan SF. Neural stimulation and recording electrodes. *Annu Rev Biomed Eng*. 2008;10:275-309. doi:10.1146/annurev.bioeng.10.061807.160518.

50. Ludwig K a, Uram JD, Yang J, Martin DC, Kipke DR. Chronic neural recordings using silicon microelectrode arrays electrochemically deposited with a poly(3,4-ethylenedioxythiophene) (PEDOT) film. *J Neural Eng*. 2006;3(1):59-70. doi:10.1088/1741-2560/3/1/007.

51. Green R a, Lovell NH, Poole-Warren L a. Cell attachment functionality of bioactive conducting polymers for neural interfaces. *Biomaterials*. 2009;30(22):3637-3644. doi:10.1016/j.biomaterials.2009.03.043.

52. Green R a., Hassarati RT, Bouchinet L, et al. Substrate dependent stability of conducting polymer coatings on medical electrodes. *Biomaterials*. 2012;33(25):5875-5886. doi:10.1016/j.biomaterials.2012.05.017.

53. Luo X, Weaver CL, Zhou DD, Greenberg R, Cui XT. Highly stable carbon nanotube doped poly(3,4-ethylenedioxythiophene) for chronic neural stimulation. *Biomaterials*. 2011;32(24):5551-5557. doi:10.1016/j.biomaterials.2011.04.051.

54. Lee K, Singh A, He J, Massia S, Kim B, Raupp G. Polyimide based neural implants with stiffness improvement. *Sensors Actuators B Chem*. 2004;102(1):67-72. doi:10.1016/j.snb.2003.10.018.

55. Castagnola V, Descamps E, Lecestre a., et al. Parylene-based flexible neural probes with pedot coated surface for brain stimulation and recording. *Biosens Bioelectron*. September 2014. doi:10.1016/j.bios.2014.09.004.

56. Peixoto AC, Goncalves SB, Pinho F, Silva AF, Dias NS, Correia JH. Flexible three-dimensional microelectrode array for neural applications. *Sensors Actuators, A Phys*. 2014;217:21-28. doi:10.1016/j.sna.2014.06.020.

57. Huang SH, Lin SP, Chen JJJ. In vitro and in vivo characterization of SU-8 flexible neuroprobe: From mechanical properties to electrophysiological recording. *Sensors Actuators, A Phys*. 2014;216:257-265. doi:10.1016/j.sna.2014.06.005.

58. Yang SY, O'Cearbhaill ED, Sisk GC, et al. A bio-inspired swellable microneedle adhesive for mechanical interlocking with tissue. *Nat Commun*. 2013;4:1702. doi:10.1038/ncomms2715.

59. Ereifej ES, Cheng MM-C, Mao G, Vandevord PJ. Examining the inflammatory response to nanopatterned polydimethylsiloxane using organotypic brain slice methods. *J Neurosci Methods*. 2013;217(1-2):17-25. doi:10.1016/j.jneumeth.2013.04.023.

60. Chen S, Jones J a, Xu Y, Low H-Y, Anderson JM, Leong KW. Characterization of topographical effects on macrophage behavior in a foreign body response model. *Biomaterials*. 2010;31(13):3479-3491. doi:10.1016/j.biomaterials.2010.01.074.

61. Grill WM, Norman SE, Bellamkonda R V. Implanted neural interfaces: biochallenges and engineered solutions. *Annu Rev Biomed Eng*. 2009;11:1-24. doi:10.1146/annurev-bioeng-061008-124927.

62. Bjornsson CS, Oh SJ, Al-Kofahi Y a, et al. Effects of insertion conditions on tissue strain and vascular damage during neuroprosthetic device insertion. *J Neural Eng*. 2006;3(3):196-207. doi:10.1088/1741-2560/3/3/002.

63. Polikov VS, Su EC, Ball M a, Hong J-S, Reichert WM. Control protocol for robust in vitro glial scar formation around microwires: essential roles of bFGF and serum in gliosis. *J Neurosci Methods*. 2009;181(2):170-177. doi:10.1016/j.jneumeth.2009.05.002.

64. Karumbaiah L, Saxena T, Carlson D, et al. Relationship between intracortical electrode design and chronic recording function. *Biomaterials*. 2013;34(33):8061-8074. doi:10.1016/j.biomaterials.2013.07.016.

65. Biran R, Martin DC, Tresco PA. The brain tissue response to implanted silicon microelectrode arrays is increased when the device is tethered to the skull. *J Biomed Mater Res A*. 2007:169-178. doi:10.1002/jbm.a.

66. Rennaker RL, Street S, Ruyle M, Sloan M. A comparison of chronic multi-channel cortical implantation techniques: manual versus mechanical insertion. *J Neurosci Methods*. 2005;142(2):169-176. doi:10.1016/j.jneumeth.2004.08.009.

67. Musallam S, Bak MJ, Troyk PR, Andersen R a. A floating metal microelectrode array for chronic implantation. *J Neurosci Methods*. 2007;160(1):122-127. doi:10.1016/j.jneumeth.2006.09.005.

68. Jaroch DB, Ward MP, Chow EY, Rickus JL, Irazoqui PP. Magnetic insertion system for flexible electrode implantation. *J Neurosci Methods*. 2009;183(2):213-222. doi:10.1016/j.jneumeth.2009.07.001.

69. Ben Yakir-Blumkin M, Loboda Y, Schächter L, Finberg JPM. Neuroprotective effect of weak static magnetic fields in primary neuronal cultures. *Neuroscience*. 2014;(September). doi:10.1016/j.neuroscience.2014.08.029.

70. Eliades SJ, Wang X. Chronic multi-electrode neural recording in free-roaming monkeys. *J Neurosci Methods*. 2009;172(2):201-214. doi:10.1016/j.jneumeth.2008.04.029.Chronic.

71. Manzano M, Vallet-Regí M. Revisiting bioceramics: Bone regenerative and local drug delivery systems. *Prog Solid State Chem*. 2012;40(3):17-30. doi:10.1016/j.progsolidstchem.2012.05.001.

72. Willerth SM, Sakiyama-Elbert SE. Approaches to neural tissue engineering using scaffolds for drug delivery. *Adv Drug Deliv Rev*. 2007;59(4-5):325-338. doi:10.1016/j.addr.2007.03.014.

73. Yu X, Bellamkonda R V. Tissue-engineered scaffolds are effective alternatives to autografts for bridging peripheral nerve gaps. *Tissue Eng*. 2003;9(3):421-430. doi:10.1089/107632703322066606.

74. Burdick JA, Ward M, Liang E, Young MJ, Langer R. Stimulation of neurite outgrowth by neurotrophins delivered from degradable hydrogels. *Biomaterials*. 2006;27(3):452-459. doi:10.1016/j.biomaterials.2005.06.034.

75. Winter JO, Cogan SF, Iii JFR. Neurotrophin-Eluting Hydrogel Coatings for Neural Stimulating Electrodes. *J Biomed Mater Res Part B Appl Biomater*. 2007;81B:551-563. doi:10.1002/jbmb.

76. Potter K a, Jorfi M, Householder KT, Foster EJ, Weder C, Capadona JR. Curcumin-releasing mechanically adaptive intracortical implants improve the proximal neuronal density and blood-brain barrier stability. *Acta Biomater*. 2014;10(5):2209-2222. doi:10.1016/j.actbio.2014.01.018.

77. Ahsan F, Rivas IP, Khan MA, Torres Su??rez AI. Targeting to macrophages: Role of physicochemical properties of particulate carriers - Liposomes and microspheres - On the phagocytosis by macrophages. *J Control Release*. 2002;79(1-3):29-40. doi:10.1016/S0168-3659(01)00549-1.

78. Bartneck M, Scheyda KM, Warzecha KT, et al. Fluorescent cell-traceable dexamethasone-loaded liposomes for the treatment of inflammatory liver diseases. *Biomaterials*. 2015;37:367-382. doi:10.1016/j.biomaterials.2014.10.030.

79. Xie Y, Ye L, Zhang X, et al. Transport of nerve growth factor encapsulated into liposomes across the blood-brain barrier: in vitro and in vivo studies. *J Control Release*. 2005;105(1-2):106-119. doi:10.1016/j.jconrel.2005.03.005.

80. Bridges AW, García AJ. Anti-inflammatory polymeric coatings for implantable biomaterials and devices. *J diabetes Sci Technol*. 2008;2(6):984-994.

81. Chen L, Apte RN, Cohen S. Characterization of PLGA microspheres for the controlled delivery of IL-1?? for tumor immunotherapy. *J Control Release*. 1997;43(2-3):261-272. doi:10.1016/S0168-3659(96)01496-4.

82. Kim D-H, Martin DC. Sustained release of dexamethasone from hydrophilic matrices using PLGA nanoparticles for neural drug delivery. *Biomaterials*. 2006;27(15):3031-3037. doi:10.1016/j.biomaterials.2005.12.021.

83. Hickey T, Kreutzer D, Burgess DJ, Moussy F. Dexamethasone/PLGA microspheres for continuous delivery of an anti-inflammatory drug for implantable medical devices. *Biomaterials*. 2002;23(7):1649-1656. doi:10.1016/S0142-9612(01)00291-5.

84. Zhong Y, Bellamkonda R V. Controlled release of anti-inflammatory agent alpha-MSH from neural implants. *J Control Release*. 2005;106(3):309-318. doi:10.1016/j.jconrel.2005.05.012.

85. Papageorgiou DP, Shore SE, Bledsoe SC, Wise KD. A Shuttered Neural Probe With On-Chip Flowmeters for Chronic In Vivo Drug Delivery. *J microelectromechanical Syst*. 2006;15(4):1025-1033.

86. Gao K, Li G, Liao L, Cheng J, Zhao J, Xu Y. Fabrication of flexible microelectrode arrays integrated with microfluidic channels for stable neural interfaces. *Sensors Actuators A Phys*. 2013;197:9-14. doi:10.1016/j.sna.2013.04.005.

87. Netz DJ, Sepulveda P, Pandolfelli VC, et al. Potential use of gelcasting hydroxyapatite porous ceramic as an implantable drug delivery system. *Int J Pharm*. 2001;213(1-2):117-125. http://www.ncbi.nlm.nih.gov/pubmed/11165099.

88. Habraken WJEM, Wolke JGC, Jansen J a. Ceramic composites as matrices and scaffolds for drug delivery in tissue engineering. *Adv Drug Deliv Rev*. 2007;59(4-5):234-248. doi:10.1016/j.addr.2007.03.011.

89. Byrne RS, Deasy PB. Use of commercial porous ceramic particles for sustained drug delivery. *Int J Pharm*. 2002;246:61-73.

90. Ito T, Fraser IP, Yeo Y, Highley CB, Bellas E, Kohane DS. Anti-inflammatory function of an in situ cross-linkable conjugate hydrogel of hyaluronic acid and dexamethasone. *Biomaterials*. 2007;28(10):1778-1786. doi:10.1016/j.biomaterials.2006.12.012.

91. Zhong Y, Bellamkonda R V. Dexamethasone-coated neural probes elicit attenuated inflammatory response and neuronal loss compared to uncoated neural probes. *Brain Res*. 2007;1148:15-27. doi:10.1016/j.brainres.2007.02.024.

92. Bas E, Bohorquez J, Goncalves S, et al. Electrode array-eluted dexamethasone protects against electrode insertion trauma induced hearing and hair cell losses,

damage to neural elements, increases in impedance and fibrosis: A dose response study. *Hear Res*. 2016;337:12-24. doi:10.1016/j.heares.2016.02.003.

93. Mosser DM, Edwards JP. Exploring the full spectrum of macrophage activation. *Genetics*. 2009;8(12):958-969. doi:10.1038/nri2448.

94. McWhorter FY, Wang T, Nguyen P, Chung T, Liu WF. Modulation of macrophage phenotype by cell shape. *Proc Natl Acad Sci U S A*. 2013;110(43):17253-17258. doi:10.1073/pnas.1308887110.

95. Vishwakarma A, Bhise NS, Evangelista MB, et al. Engineering Immunomodulatory Biomaterials To Tune the Inflammatory Response. *Trends Biotechnol*. 2016;34(6):470-482. doi:10.1016/j.tibtech.2016.03.009.

96. Michelucci A, Heurtaux T, Grandbarbe L, Morga E, Heuschling P. Characterization of the microglial phenotype under specific pro-inflammatory and anti-inflammatory conditions: Effects of oligomeric and fibrillar amyloid-?? *J Neuroimmunol*. 2009;210(1-2):3-12. doi:10.1016/j.jneuroim.2009.02.003.

97. Gao S, Zhou J, Liu N, et al. Curcumin induces M2 macrophage polarization by secretion IL-4 and/or IL-13. *J Mol Cell Cardiol*. 2015;85:131-139. doi:10.1016/j.yjmcc.2015.04.025.

98. Stein M, Keshav S, Harris N, Gordon S. Interleukin 4 potently enhances murine macrophage mannose receptor activity: a marker of alternative immunologic macrophage activation. *J Exp Med*. 1992;176(1):287-292. doi:10.1084/jem.176.1.287.

99. Vishwakarma A, Bhise NS, Evangelista MB, et al. Engineering Immunomodulatory Biomaterials To Tune the Inflammatory Response. *Trends Biotechnol*. 2016;34(6):470-482. doi:10.1016/j.tibtech.2016.03.009.

100. Jurga M, Dainiak MB, Sarnowska A, et al. The performance of laminin-containing cryogel scaffolds in neural tissue regeneration. *Biomaterials*. 2011;32(13):3423-3434. doi:10.1016/j.biomaterials.2011.01.049.

101. Koutsopoulos S, Zhang S. Long-term three-dimensional neural tissue cultures in functionalized self-assembling peptide hydrogels, matrigel and collagen I. *Acta Biomater*. 2013;9(2):5162-5169. doi:10.1016/j.actbio.2012.09.010.

102. Wang GJ, Deng HY, Maier CM, Sun GH, Yenari MA. Mild hypothermia reduces ICAM-1 expression, neutrophil infiltration and microglia/monocyte accumulation following experimental stroke. *Neuroscience*. 2002;114(4):1081-1090.

103. Kataoka K, Yanase H. Mild hypothermia - A revived countermeasure against ischemic neuronal damages. *Neurosci Res*. 1998;32(2):103-117. doi:10.1016/S0168-0102(98)00076-5.

104. Tamames I, King C, Bas E, Dietrich WD, Telischi F, Rajguru SM. A cool approach to reducing electrode-induced trauma: localized therapeutic hypothermia

conserves residual hearing in cochlear implantation. *Hear Res*. 2016. doi:10.1016/j.heares.2016.05.015.

105. Yenari MA, Han HS. Neuroprotective mechanisms of hypothermia in brain ischaemia. *Nat Rev Neurosci*. 2012;13(4):267-278. doi:10.1038/nrn3174.

106. Tokiwa T, Inoue T, Fujii M, et al. Penicillin-induced epileptiform activity elevates focal brain temperature in anesthetized rats. *Neurosci Res*. 2013;76(4):257-260. doi:10.1016/j.neures.2013.05.001.

107. Brooks V. Study of Brain Function by Local , Reversible Cooling. *Rev Physiol Biochem Pharmacol*. 1983;95.

108. Lomber SG, Payne BR, Horel J a. The cryoloop: an adaptable reversible cooling deactivation method for behavioral or electrophysiological assessment of neural function. *J Neurosci Methods*. 1999;86(2):179-194.

109. Bakken HE, Kawasaki H, Oya H, Greenlee JDW, Howard M a. A device for cooling localized regions of human cerebral cortex. Technical note. *J Neurosurg*. 2003;99(3):604-608.

110. Oku T, Fujii M, Tanaka N, Imoto H, Uchiyama J, Oka F, Kunitsugu I, Fujioka H, Nomura S, Kajiwara K, Fujisawa H, Kato S, Saito T SM. The influence of focal brain cooling on neurophysiopathology: validation for clinical application. *J Neurosurg*. 2009;110 (6):1209-1217.

111. Cooke DF, Goldring a. B, Yamayoshi I, et al. Fabrication of an inexpensive, implantable cooling device for reversible brain deactivation in animals ranging from rodents to primates. *J Neurophysiol*. 2012;107(March):3543-3558. doi:10.1152/jn.01101.2011.

112. Rothman S, Yang X-F. Local Cooling : A Therapy for. *Epilepsy Curr*. 2003;3(5):153-156.

113. Imoto H, Fujii M, Uchiyama J, et al. Use of a Peltier chip with a newly devised local brain-cooling system for neocortical seizures in the rat. Technical note. *J Neurosurg*. 2006;104(1):150-156. doi:10.3171/jns.2006.104.1.150.

114. Imoto H, Fujii M, Uchiyama J, et al. Use of a Peltier chip with a newly devised local brain-cooling system for neocortical seizures in the rat. Technical note. *J Neurosurg*. 2006;104(1):150-156. doi:10.3171/jns.2006.104.1.150.

115. Tanaka N, Fujii M, Imoto H, et al. Effective suppression of hippocampal seizures in rats by direct hippocampal cooling with a Peltier chip. *J Neurosurg*. 2008;108(4):791-797. doi:10.3171/JNS/2008/108/4/0791.

116. Lukins TR, Tisch S, Jonker B. The latest evidence on target selection in deep brain stimulation for Parkinson's disease. *J Clin Neurosci*. 2014;21(1):22-27. doi:10.1016/j.jocn.2013.05.011.

117. Wei Q, Mukaida M, Kirihara K, Naitoh Y, Ishida T. Recent progress on PEDOT-

based thermoelectric materials. *Materials (Basel)*. 2015;8(2):732-750. doi:10.3390/ma8020732.

118. Sparavigna AC. Polypyrrole Coated PET Fabrics for Thermal Applications. *Mater Sci Appl*. 2010;1(4):252-258. doi:10.4236/msa.2010.14037.

119. Sih SS, Barlow JW. Measurement and prediction of the thermal conductivity of powders at high temperatures. *Solid Free 400 Fabr Symp Proc*. 1992:321-329.

120. Živcová Z, Gregorová E, Pabst W, Smith DS, Michot A, Poulier C. Thermal conductivity of porous alumina ceramics prepared using starch as a pore-forming agent. *J Eur Ceram Soc*. 2009;29(3):347-353. doi:10.1016/j.jeurceramsoc.2008.06.018.

121. Chen C-Y, Chang C-L, Chien T-F, Luo C-H. Flexible PDMS electrode for one-point wearable wireless bio-potential acquisition. *Sensors Actuators A Phys*. 2013;203:20-28. doi:10.1016/j.sna.2013.08.010.

122. Bhattacharya S, Datta A, Berg JM, Gangopadhyay S. Studies on surface wettability of poly(dimethyl) siloxane (PDMS) and glass under oxygen-plasma treatment and correlation with bond strength. *J Microelectromechanical Syst*. 2005;14(3):590-597. doi:10.1109/JMEMS.2005.844746.

123. Wang H, Eliaz N, Xiang Z, Hsu H-P, Spector M, Hobbs LW. Early bone apposition in vivo on plasma-sprayed and electrochemically deposited hydroxyapatite coatings on titanium alloy. *Biomaterials*. 2006;27(23):4192-4203. doi:10.1016/j.biomaterials.2006.03.034.

124. Moskalewicz T, Seuss S, Boccaccini AR. Microstructure and properties of composite polyetheretherketone/Bioglass® coatings deposited on Ti–6Al–7Nb alloy for medical applications. *Appl Surf Sci*. 2013;273:62-67. doi:10.1016/j.apsusc.2013.01.174.

125. Eliaz N, Sridhar TM, Kamachi Mudali U, Raj B. Electrochemical and electrophoretic deposition of hydroxyapatite for orthopaedic applications. *Surf Eng*. 2005;21(3):238-242. doi:10.1179/174329405X50091.

126. Carradò A. Nano-crystalline pulsed laser deposition hydroxyapatite thin films on Ti substrate for biomedical application. *J Coatings Technol Res*. 2011;8(6):749-755. doi:10.1007/s11998-011-9355-9.

127. Fernandez-Prada JM. Hydroxyapatite coatings grown by pulsed laser deposition with a beam of 355 nm wavelength. *J Mater Res*. 1999;14(12):4715-4719.

128. Tucker BE, Cottell CM, Auyeung RC, Spector M, Nancollas GH. Pre-conditioning and dual constant composition dissolution kinetics of pulsed laser deposited hydroxyapatite thin films on silicon substrates. *Biomaterials*. 1996;17(6):631-637. http://www.ncbi.nlm.nih.gov/pubmed/8652782.

129. Yang Y, Kim K-H, Ong JL. A review on calcium phosphate coatings produced using a sputtering process--an alternative to plasma spraying. *Biomaterials*.

2005;26(3):327-337. doi:10.1016/j.biomaterials.2004.02.029.

130. Mohseni E, Zalnezhad E, Bushroa a. R. Comparative investigation on the adhesion of hydroxyapatite coating on Ti–6Al–4V implant: A review paper. *Int J Adhes Adhes*. 2014;48:238-257. doi:10.1016/j.ijadhadh.2013.09.030.

131. Wheeler DL, Campbell AA, Graff GL, Miller GJ. Technical Note Histological and biomechanical evaluation of calcium phosphate coatings applied through surface-induced mineralization to porous titanium implants. *Biomed Mater Res*. 1997;34:539-543.

132. Mavis B, Cu A. Dip Coating of Calcium Hydroxyapatite on Ti-6Al-4V Substrates. *J Am Ceram Soc*. 2000;91:989-991.

133. Aronov D, Fee MS. Analyzing the dynamics of brain circuits with temperature: design and implementation of a miniature thermoelectric device. *J Neurosci Methods*. 2011;197(1):32-47. doi:10.1016/j.jneumeth.2011.01.024.

134. Elwassif MM, Kong Q, Vazquez M, Bikson M. Bio-heat transfer model of deep brain stimulation induced temperature changes. *Annu Int Conf IEEE Eng Med Biol - Proc*. 2006;3:3580-3583. doi:10.1109/IEMBS.2006.259425.

135. Yao L, Damodaran G, Nikolskaya N, Gorman AM, Windebank A, Pandit A. The effect of laminin peptide gradient in enzymatically cross-linked collagen scaffolds on neurite growth. *J Biomed Mater Res A*. 2010;92(2):484-492. doi:10.1002/jbm.a.32359.

136. Yao L, Wang S, Cui W, et al. Effect of functionalized micropatterned PLGA on guided neurite growth. *Acta Biomater*. 2009;5(2):580-588. doi:10.1016/j.actbio.2008.09.002.

137. Kajiwara K, Kamamoto M, Ogata S, Tanihara M. A synthetic peptide corresponding to residues 301-320 of human Wnt-1 promotes PC12 cell adhesion and hippocampal neural stem cell differentiation. *Peptides*. 2008;29(9):1479-1485. doi:10.1016/j.peptides.2008.05.013.

138. Losciuto S, Dorban G, Gabel S, et al. An efficient method to limit microglia-dependent effects in astroglial cultures. *J Neurosci Methods*. 2012;207(1):59-71. doi:10.1016/j.jneumeth.2012.03.010.

139. Wilcock DM. A changing perspective on the role of neuroinflammation in Alzheimer's disease. *Int J Alzheimers Dis*. 2012;2012:495243. doi:10.1155/2012/495243.

140. Sawyer AJ, Tian W, Saucier-Sawyer JK, et al. The effect of inflammatory cell-derived MCP-1 loss on neuronal survival during chronic neuroinflammation. *Biomaterials*. 2014;35(25):6698-6706. doi:10.1016/j.biomaterials.2014.05.008.

141. Placone AL, McGuiggan PM, Bergles DE, Guerrero-Cazares H, Quiñones-Hinojosa A, Searson PC. Human astrocytes develop physiological morphology and remain quiescent in a novel 3D matrix. *Biomaterials*. 2015;42:134-143.

doi:10.1016/j.biomaterials.2014.11.046.

142. Cheng X, Li T, Zhou H, et al. Cortical electrical stimulation with varied low frequencies promotes functional recovery and brain remodeling in a rat model of ischemia. *Brain Res Bull*. 2012;89(3-4):124-132. doi:10.1016/j.brainresbull.2012.07.009.

143. Winslow BD, Christensen MB, Yang W-K, Solzbacher F, Tresco P a. A comparison of the tissue response to chronically implanted Parylene-C-coated and uncoated planar silicon microelectrode arrays in rat cortex. *Biomaterials*. 2010;31(35):9163-9172. doi:10.1016/j.biomaterials.2010.05.050.

144. Kolarcik CL, Bourbeau D, Azemi E, et al. In vivo effects of L1 coating on inflammation and neuronal health at the electrode–tissue interface in rat spinal cord and dorsal root ganglion. *Acta Biomater*. 2012;8(10):3561-3575. doi:10.1016/j.actbio.2012.06.034.

145. Seymour JP, Kipke DR. Neural probe design for reduced tissue encapsulation in CNS. *Biomaterials*. 2007;28(25):3594-3607. doi:10.1016/j.biomaterials.2007.03.024.

146. Ereifej ES, Khan S, Newaz G, Zhang J, Auner GW, Vandevord PJ. Characterization of astrocyte reactivity and gene expression on biomaterials for neural electrodes. *J Biomed Mater Res - Part A*. 2011;99 A(1):141-150. doi:10.1002/jbm.a.33170.

147. Erickson D, Sinton D, Li D. Joule heating and heat transfer in poly(dimethylsiloxane) microfluidic systems. *Lab Chip*. 2003;3(3):141-149. doi:10.1039/b306158b.

148. Lin YH, Kang SW, Wu TY. Fabrication of polydimethylsiloxane (PDMS) pulsating heat pipe. *Appl Therm Eng*. 2009;29(2-3):573-580. doi:10.1016/j.applthermaleng.2008.03.028.

149. Yi P, Awang R a, Rowe WST, Kalantar-Zadeh K, Khoshmanesh K. PDMS nanocomposites for heat transfer enhancement in microfluidic platforms. *Lab Chip*. 2014;14(17):3419-3426. doi:10.1039/c4lc00615a.

150. Berkovitch Y, Yelin D, Seliktar D. *Photo-Patterning PEG-Based Hydrogels for Neuronal Engineering*. Vol 72. Elsevier Ltd; 2015. doi:10.1016/j.eurpolymj.2015.07.014.

151. Mealy J, O'Kelly K. Cell response to hydroxyapatite surface topography modulated by sintering temperature. *J Biomed Mater Res - Part A*. 2015;103(11):3533-3538. doi:10.1002/jbm.a.35487.

152. Rhodes KE, Moon LDF, Fawcett JW. Inhibiting cell proliferation during formation of the glial scar: Effects on axon regeneration in the CNS. *Neuroscience*. 2003;120(1):41-56. doi:10.1016/S0306-4522(03)00285-9.

153. Placone AL, McGuiggan PM, Bergles DE, Guerrero-Cazares H, Quiñones-Hinojosa

A, Searson PC. Human astrocytes develop physiological morphology and remain quiescent in a novel 3D matrix. *Biomaterials*. 2015;42:134-143. doi:10.1016/j.biomaterials.2014.11.046.

154. Falkenburger BH, Schulz JB. Limitations of cellular models in Parkinson's disease research. *J Neural Transm*. 2006;(February):261-268.

155. O'Connor SM, Stenger DA, Shaffer KM, Ma W. Survival and neurite outgrowth of rat cortical neurons in three-dimensional agarose and collagen gel matrices. *Neurosci Lett*. 2001;304(3):189-193. doi:10.1016/S0304-3940(01)01769-4.

156. Yue Z, Moulton SE, Cook M, O'Leary S, Wallace GG. Controlled delivery for neuro-bionic devices. *Adv Drug Deliv Rev*. 2013;65(4):559-569. doi:10.1016/j.addr.2012.06.002.

157. Spataro L, Dilgen J, Retterer S, et al. Dexamethasone treatment reduces astroglia responses to inserted neuroprosthetic devices in rat neocortex. *Exp Neurol*. 2005;194(2):289-300. doi:10.1016/j.expneurol.2004.08.037.

158. Abràmoff MD, Magalhães PJ, Ram SJ. Image processing with imageJ. *Biophotonics Int*. 2004;11(7):36-41. doi:10.1117/1.3589100.

159. Nichol JW, Koshy ST, Bae H, Hwang CM, Yamanlar S, Khademhosseini A. Cell-laden microengineered gelatin methacrylate hydrogels. *Biomaterials*. 2010;31(21):5536-5544. doi:10.1016/j.biomaterials.2010.03.064.

160. Yue K, Trujillo-de Santiago G, Alvarez MM, Tamayol A, Annabi N, Khademhosseini A. Synthesis, properties, and biomedical applications of gelatin methacryloyl (GelMA) hydrogels. *Biomaterials*. 2015;73:254-271. doi:10.1016/j.biomaterials.2015.08.045.

161. Coimbra P, Gil MH, Figueiredo M. Tailoring the properties of gelatin films for drug delivery applications: influence of the chemical cross-linking method. *Int J Biol Macromol*. 2014;70:10-19. doi:10.1016/j.ijbiomac.2014.06.021.

162. Joint C, Nandi D, Parkin S, Gregory R, Aziz T. Hardware-related problems of deep brain stimulation. *Mov Disord*. 2002;17(SUPPL. 3). doi:10.1002/mds.10161.

163. Coimbra P, Gil MH, Figueiredo M. Tailoring the properties of gelatin films for drug delivery applications: influence of the chemical cross-linking method. *Int J Biol Macromol*. 2014;70:10-19. doi:10.1016/j.ijbiomac.2014.06.021.

164. Simmons A, Padsalgikar AD, Ferris LM, Poole-Warren LA. Biostability and biological performance of a PDMS-based polyurethane for controlled drug release. *Biomaterials*. 2008;29(20):2987-2995. doi:10.1016/j.biomaterials.2008.04.007.

165. Agarwal A, Goss JA, Cho A, McCain ML, Parker KK. Microfluidic heart on a chip for higher throughput pharmacological studies. *Lab Chip*. 2013;13(18):3599-3608. doi:10.1039/c3lc50350j.

166. Budday S, Nay R, de Rooij R, et al. Mechanical properties of gray and white matter brain tissue by indentation. *J Mech Behav Biomed Mater*. 2015;46:318-330. doi:10.1016/j.jmbbm.2015.02.024.

167. Shkilnyy A, Proulx P, Sharp J, Lepage M, Vermette P. Colloids and Surfaces B : Biointerfaces Diffusion of rhodamine B and bovine serum albumin in fibrin gels seeded with primary endothelial cells. *Colloids Surfaces B Biointerfaces*. 2012;93:202-207. doi:10.1016/j.colsurfb.2012.01.005.

168. Bergey GK. Neurostimulation in the treatment of epilepsy. *Exp Neurol*. 2013;244:87-95. doi:10.1016/j.expneurol.2013.04.004.

169. Rothman SM, Smyth MD, Yang XF, Peterson GP. Focal cooling for epilepsy: An alternative therapy that might actually work. *Epilepsy Behav*. 2005;7(2):214-221. doi:10.1016/j.yebeh.2005.05.021.

170. Zhang HY. A general approach in evaluating and optimizing thermoelectric coolers. *Int J Refrig*. 2010;33(6):1187-1196. doi:10.1016/j.ijrefrig.2010.04.007.

171. Rhee SK. Porosity-Thermal conductivity correlations for ceramic materials. *Mater Sci Eng*. 1975;20(C):89-93. doi:10.1016/0025-5416(75)90134-2.

172. Staats WL, Brisson JG. Active heat transfer enhancement in air cooled heat sinks using integrated centrifugal fans. *Int J Heat Mass Transf*. 2015;82:189-205. doi:10.1016/j.ijheatmasstransfer.2014.10.075.

173. Staats WL, Brisson JG. Active heat transfer enhancement in air cooled heat sinks using integrated centrifugal fans. *Int J Heat Mass Transf*. 2015;82:189-205. doi:10.1016/j.ijheatmasstransfer.2014.10.075.

174. Buonomano D V, Merzenich MM. Cortical plasticity: from synapses to maps. *Annu Rev Neurosci*. 1998;21(149):149-186. doi:10.1146/annurev.neuro.21.1.149.

175. Castellanos NP, Leyva I, Buld JM, et al. Principles of recovery from traumatic brain injury: Reorganization of functional networks. *Neuroimage*. 2011;55(3):1189-1199. doi:10.1016/j.neuroimage.2010.12.046.

176. O'Mara SM. Interview with Professor Shane O'Mara. 2016.

Appendices

Appendix A:

As well as simply studying metabolic activity of primary neuronal and glial cells, an attempt was made to stain the cells according to their individual cell type in order to analyse the percentage of cell types using confocal microscopy. Images were taken on day 1 and day 7 of each mixture, with GFAP alexa 488 (green) staining for astrocytes (cytoplasmic), NeuN alexa 633 (red) staining for neurons as well as DAPI (blue) staining for nuclei, meaning all cells stained blue without green or red are assumed to be other glial cells such as microglia or oligodendrocytes. Individual images were taken of the whole scaffold and then stitched together which sometimes resulted in an excess of background staining around tile boundaries (Fig. A1). Cell staining was patchy and not clear, indicating that perhaps some of the staining solution was absorbed into the porous scaffold structure rather than staining the cells on the surface properly or that the staining was background staining from incomplete washing of discs. As well as this, only DAPI was picked up with no clear staining of GFAP or NeuN, rendering it impossible to differentiate between cell types. For this reason, only the metabolic activity of the cells was assessed and it was decided that using individual cell types at this stage would be a more useful indication of cell behaviour.

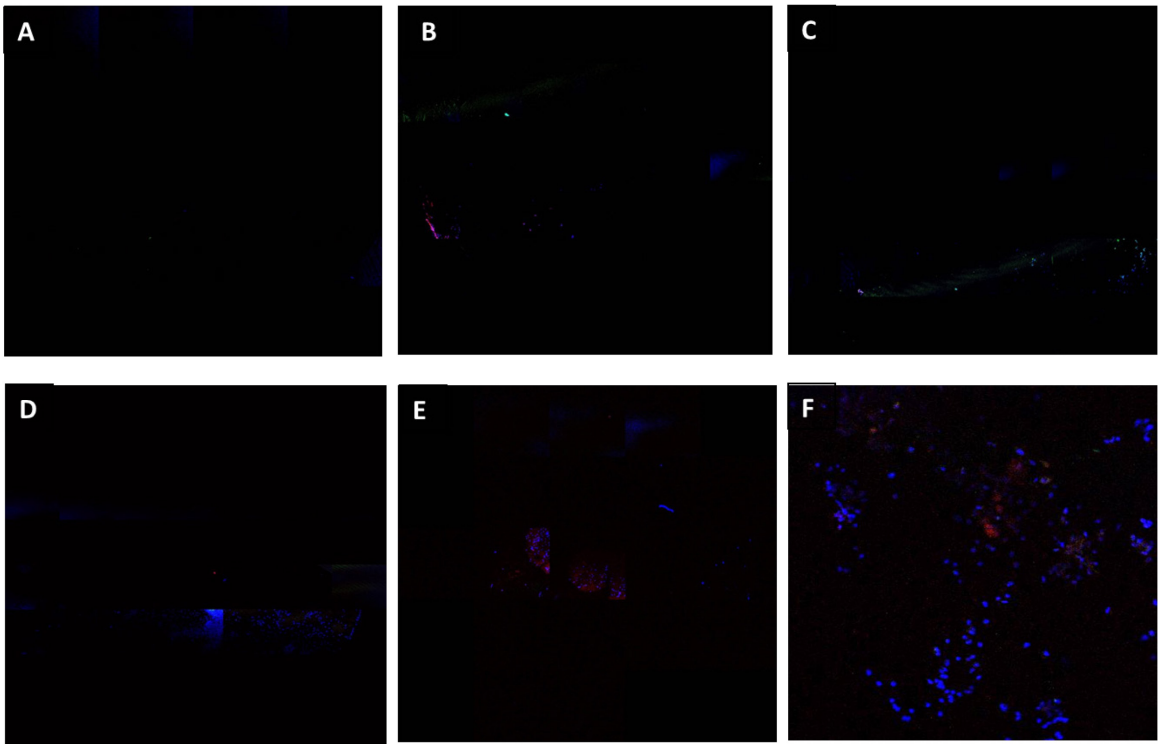

Figure A1. Confocal images of scaffolds stained with GFAP (green), DAPI (blue) and NeuN (red): 1200 Day 7(A); 1350S Day 7 (B); Negative Control Day 7 (C); Positive Control Day 7 (D); 1350R Day 1 (E); 1350R Day 7 (F).

Appendix B:

As an additional measure of the inflammation of astrocytic cells in response to different drug delivery profiles, cells were stained with GFAP with the hope of quantifying the results using Image J software. However, limited cell staining was visible under the confocal microscope. In order to improve this, a combination of different GFAP sources and secondary antibodies were tested to assess if one of these were causing the reduced staining as a standard immunochemistry protocol was being used (Fig. A2.). The results below show that the best staining was visible with GFAP B and secondary A. However, the staining was still not picking up all cells – which it should have as the cells were all astrocytes. For this reason, it was deemed an unreliable supplementary quantification and all further studies relied solely on the cell structure indications as well as the ELISA data.

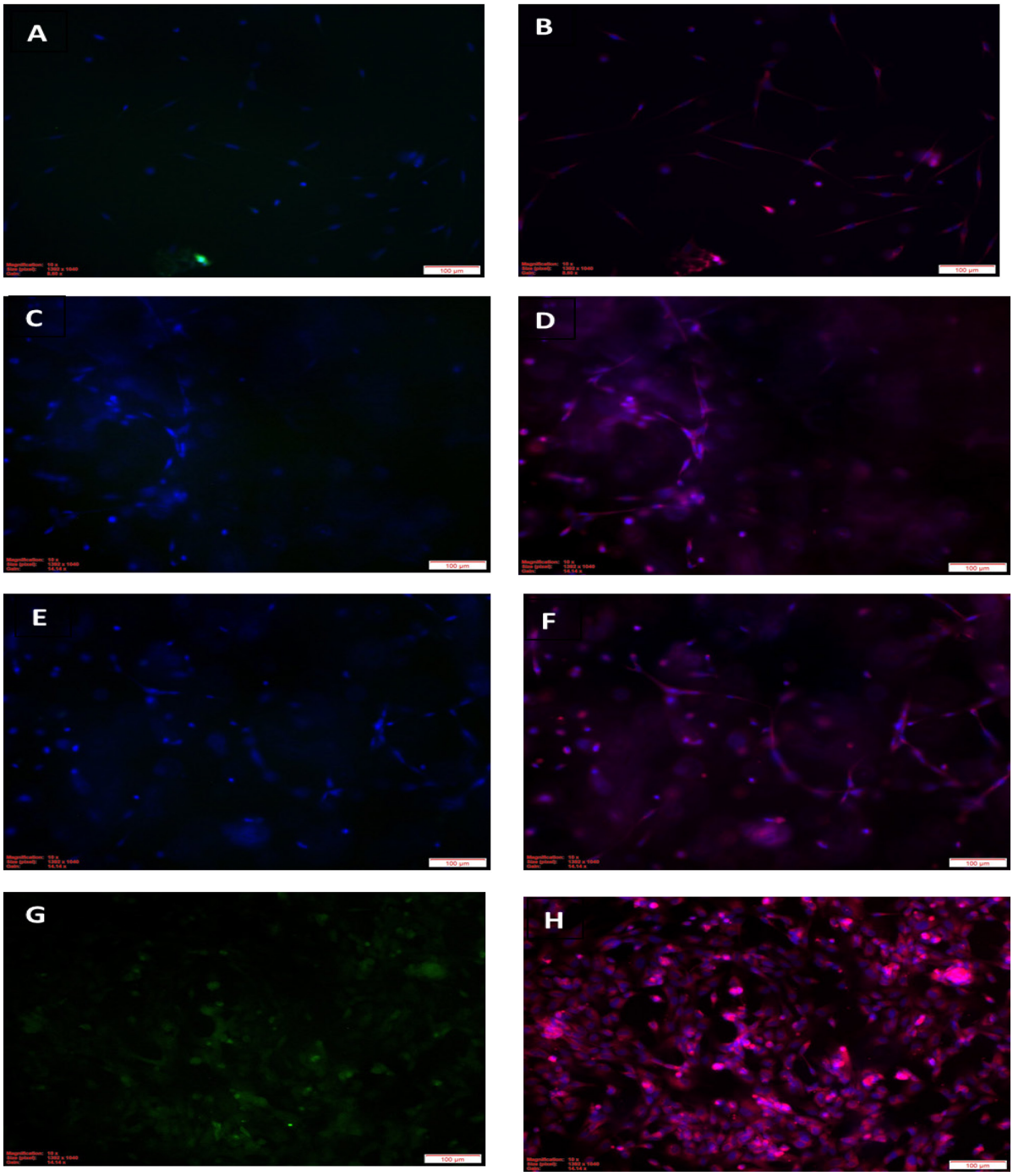

Figure A2. Confocal images of unsuccessful astrocyte GFAP staining after 1 week of culture in a 5% GelMA hydrogel**.** DAPI staining (blue) for nuclei and either GFAP staining (green) for intermediate filaments (left column) or Cell Mask 649 (red) for cell structure (right column) for different combinations of GFAP and secondary antibody. A+B) GFAP A-Secondary A; C+D) GFAP A-Secondary B; E+F) GFAP B-Secondary A; G+H) GFAP B-Secondary B.